University of Alberta

PROBING THE FUNCTION OF LFA-1 USING FLUORESCENT PROTEINS THAT TARGET THE BETA-2 INTEGRIN TRANSMEMBRANE DOMAIN

by

Njuacha George Ebesoh

A thesis submitted to the Faculty of Graduate Studies and Research
in partial fulfillment of the requirements for the degree of

Master of Science

Department of Chemistry

Spring 2011
Edmonton, Alberta

DEDICATION

To God Almighty, for the abounding miracles in my life.

To my parents Mr/Mrs Foretia Richard and my siblings, for their unconditional love and support.

ABSTRACT

The lymphocyte functional antigen-1 (LFA-1) is a type I heterodimeric transmembrane (TM) proteins involved in cell adhesion, and mediates a number of cellular and physiological processes. In this work, we used recombinant fluorescently-tagged proteins derived from the TM domain of the β_2 integrin to disrupt the function of LFA-1 on Jurkat cells. Four variants of the proteins were made including: one with a short cytoplasmic tail (EGFPβ_2TM+CD), without the cytoplasmic tail (EGFPβ_2TM-CD), truncation of five amino acids (EGFPβ_2TM-5B) and truncation of ten amino acid (EGFPβ_2TM-10B). These proteins were able to label Jurkat cells *in vitro* in a protein binding assay with affinity, K_d as high as 280 ± 80 nM (EGFPβ_2TM-5B). We used fluosphere beads conjugated to different mAb to study the effect of binding on the epitopes of LFA-1. The proteins had an overall activation effect on MEM148 and an inhibitory effect on MEM48 epitope of LFA-1 receptor.

ACKNOWLEDGEMENT

I would like to acknowledge all those who in one way or another assisted me throughout my graduate studies here at the University of Alberta either emotionally, academically, spiritually, financially or socially. I want to say I love you all and thank you all for being there.

I would first want to thank my supervisor, Dr. Christopher W. Cairo for his unrestrained support throughout my studies. His academically and professional critics and guidance has been the driving force for my realisation of this work and for preparing me through a scientific career. I equally want to thank the other members of my supervisory committee: Dr. Robert E. Campbell and Dr. James Stafford for their time, comments and suggestions in putting up this work. I want to thank Dr. Campbell for his advice, guidance, comments and suggestions during my studies. I am equally grateful to Dr Stafford for his useful suggestions and comments on the use of the flow cytometer especially for granting me access to the instrument and to other accessories of his lab. I am equally indebted to all the past and present members of the Cairo's lab for their moral and academic support. They were always there when I needed them. A big thank you to Chris Sadek, Dr. Mahendra Sandhbor, Dr. Caisung Li, for all your tremendous support. To Leah Martins, Dr. Sandra Marcus, Garrett Lambkin, Ruixiang Zheng for teaching me most of the techniques I used for my research, and all the people I worked with in and out of the department of Chemistry, I say thank you.

Again I would like to thank my uncles and wives Mr/Mrs Anu Martin, Mr/Mrs Nyochembeng Sylvester, Mr/Mrs John Foretia, Mr/Mrs Benedict Foretia, for their financial, material and emotional support. I equally greatly appreciate the support of Prof. Tazoacha Asonganyi, the families of Dr/Mrs Asongalem Emmanuel, Mr/Mrs Asongamin David (Nkwetta Forwedndah), Mr/Mrs Anu Micheal, Dr/Mrs Sulayman Oladepo, Mr/Mrs Atemkeng Frankline, Mr/Mrs Feulefac Joseph, and Mr/Mrs Lambiv Gideon, Mrs Fontem Rose for all their relentless academic, financial, emotional and material support.

I am indebted to my parents and siblings most especially Akamin, Nkeng Atabong, Divine, Nguasong, Ngulefac and baby Ebesoh for all their love and unflinching support. To you Mang Ngembus, Leke Lynn, Enow Richard, Atabong Pamela, Fobellah Asonganyi and all my friends at the Chemistry department, I must say you all are wonderful. A special thank you to Yimnai Justine, at times I wonder what I would have done if you were not there to give me a pat on my back. Those words “Nju you can do it” were just too much to re-energize me. At all times you were there to comfort and strengthen me. Thank you very much for all, very few sisters like you exist and may God guide you through all your endeavours.

TABLE OF CONTENTS

LIST OF TABLES

LIST OF FIGURES

LIST OF EQUATIONS

LIST OF ABBREVIATIONS

a.a.	amino acid
Ab	Antibody
ABC	ATP binding cassette
ACN	Acetonitrile
ADAMS	A disintegrin and metalloprotease
ADP	Adenosine diphosphate
amp	Ampicillin
AR	Adrenergic receptor
ATP	Adenosine triphosphate
Avg	Average
bp	Base pairs
BP	Band pass
B-PER	Bacterial protein extraction reagent
BSA	Bovine serum albumin
CAM	Cellular adhesion molecule
CAT	Chloramphenicol acetyltransferase
CD 54	Cluster of differentiation 54
CD	Circular dichroism
cDNA	complementary DNA
CHAMP	Computed helical anti-membrane protein
conc.	Concentration
CR	Cadherin-specific repeats
Cyto D	Cytochalasin D
DMSO	Dimethyl sulfoxide
DNA	Deoxyribonucleic acid
DTT	Dithiothreitol
EC_{50}	Concentration to cause 50% saturation
ECM	Extracellular matrix

EDTA	Ethylene diaminetetraacetate
EGF	Epidermal growth factor
EGFP	Enhanced green fluorescent protein
Endo H_f	Endo-β-N-acetylglucosaminidase H (fusion)
ErbB	Epidermal growth factor receptor (EGFR)
EV	Electronic volume
FACS	Flourescence activated cell sorting
FC	Flow cytometry
FBS	Fetal bovine serum
FRET	Fluorescence resonance energy transfer
G -	Gram negative bacteria
GpA	Glycophorin A
GPCR	G-protein coupled receptor
GST	Glutathione-S-transferase
HEPES	(4-(2-hydroxyethyl)-1-piperazineethanesulfonic acid)
HIV	Human immunideficiency virus
h	Hour
HSPGS	Heparan sulfate proteoglycans
ICAM-1	Intercellular adhesion molecule I
Ig	Immunoglobulin
IgCAM	Immunoglobulin-like domain containing CAM
IPTG	Isopropyl-1-thio-β-galactopyranoside
K_d	Binding constant
KSI	Ketosteroid isomerase
LAD	Leukocyte adhesion deficiency
LB	Luria-Bertani
LC MS/MS	Liquid chromatography mass spectroscopy
LCF	Lymphocyte chemotatic factor
LFA-1	Leukocyte function associated-antigen 1

mAb	Monoclonal antibody
MALDI-TOF	Matrix-assisted laser desorption ionization time of flight
MBP	Maltose binding protein
MHC	Major histocompartibility complex
m	Minutes
MS	Mass spectroscopy
MWCO	Molecular weight cut off
NEU	Neuraminidase
Ni-NTA	Nickel nitrilotriacetic acid
NMR	Nuclear magnetic resonance
NrCAM	Neuronal CAM
OD_{600}	Optical density at wavelength of 600 nm
PBS	Phosphate buffered saline
PCR	Polymerase chain reaction
PEG	Polyethyleneglycol
PFA	Paraformaldehyde
P-gp	P-glycoprotein
pIgG	Polyclonal immunoglobulin G
PKC	Protein kinase C
PMA	Phorbol-12-myristate-13-acetate
PNGase F	peptide-N^4-(*N*-acetyl-β-D-glucosaminyl)- asparagine aminidase
PTP	Protein tyrosine phosphatise
RNA	Ribonucleic acid
rpm	revolutions per minute
SA	Sinapinic acid
SD	Standard deviation
SDS PAGE	Sodium dodecylsulfate Polyacrylamide gel electrophoresis
sICAM	secretory ICAM
SPPS	Solid phase peptide synthesis
SS	Side scattering

ST6Gal-1	β-galactosamide-α-2-6-sialytransferase-1
TCR	T cell receptor
TFA	Trifluoroacetic acid
TM	Transmembrane domain
UV	Ultra violet
WT	Wild type
YG	Yellow- green

CHAPTER ONE

INTEGRINS IN CELL ADHESION: PROBING THE TRANSMEMBRANE DOMAINS

1.1. INTRODUCTION

Cell adhesion is an important physiological phenomenon that involves a cell binding to another cell, surface, or an extracellular matrix (ECM) (1-2). Cell adhesion usually features a number of different cell adhesion molecules (CAM) interacting with their receptors in either homophilic binding (interactions between two identical molecules) or heterophilic binding (an interaction between two different CAM or two structurally different molecules) (3). CAMs function as cell adhesion and signalling receptors, transducing signals from an extracellular source to an intracellular network resulting in a number of physiological processes including cell proliferation, cell migration, cell differentiation, and therefore have implications in many diseases. Selective disruption of CAM-associations or interactions can be used to better understand the role of these molecules and the pathways involved in disease processes. Successful strategies may also form the basis of new chemotherapeutic strategies**.**

1.2. CELL ADHESION MOLECULES

The major groups of CAMs are the immunoglobulin-like domain containing cell adhesion molecules (IgCAMs), integrins, selectins and cadherins (4-9). Other adhesion molecules include cell surface heparin sulphate proteoglycans (HSPG), ADAMS (a disintegrin and metalloprotease), adherens junctions, and protein tyrosine phosphatase (PTP) (10-14). Focal adhesions and focal complexes, desmosomes and hemidesmosomes have also been ascribed as cell adhesion and signalling molecules (15-21). Most CAMs belong to the

transmembrane family of proteins in which an extracellular signal binding domain transduce signal via a transmembrane spanning region unto a cytoplasmic domain which is involved in different signalling pathways or networks (4).

Selectins are adhesion molecules which bind to carbohydrates on the cell surfaces in a Ca^{2+}- dependent manner (22-23). Selectins have a common structure with an *N*-terminal calcium-dependent lectin domain adjacent to an epidermal growth factor (EGF)-like motif, followed by a series of short consensus repeats, a transmembrane domain and finally a cytoplasmic tail (5). There are three types of selectins: L-selectin, P-selectin, and E-selectin which are involved in interactions between leukocytes, plateletes, endothelial cells and other blood cells with the endothelial membrane leading to leukocyte trafficking (5, 22, 24-27). Leukocyte trafficking is a multistep process including tethering of leukocytes to the endothelial membrane, rolling of the cells along the vessel walls, firm adhesion, and finally transendothelial migration (5, 25, 28-32). The cytoplasmic domain of P and E-selectins are not essential for leukocyte adhesion (33).

IgCAMs are part of the immunoglobulin super-family of protein, another class of CAM involved in signal transduction and cell adhesion through a Ca^{2+}-independent pathway (34). IgCAMs are involved in the regulation of a number of embryonic and adult developmental processes involving cell-cell and cell-ECM interactions (4). Generally, IgCAMs are structurally similar containing one or more Ig-like domains that are usually combined with other protein motifs such as FNIII-like repeats. IgCAMs are highly expressed at neuron-neuron, neuron-glia,

and neuron-ECM junctions resulting in neurite induction, extension and outgrowth where neuronal CAM (NrCAM) receptors on neurofasin are involved (35-42). Interactions of IgCAMs can either be *trans*, in which IgCAMs on opposing cells bind together, or *cis*, in which there is interaction between lateral molecules on the same cell. IgCAMs have been implicated in a number of disorders including neurodegenerative disorders, migration of malignant glioma and melanoma (43-45).

Another group of Ca^{2+}-dependent CAMs are the cadherins, a family of proteins strongly correlated with the complexity of organisation in multicellular organisms (46). The role of cadherins in the brain has been suggested for the pattern of selection and connectivity of neurons in the central nervous system. Their function in cell adhesion and signalling has been proposed to include cell proliferation, migration, differentiation, invasiveness, morphogenesis and apoptosis. Structurally, the family has a common feature which is the presence of multiple cadherin-specific repeats (CR) which vary from four to over thirty in the different member of the cadherin family.

1.3. THE INTEGRIN SUPERFAMILY OF CELL ADHESION MOLECULES

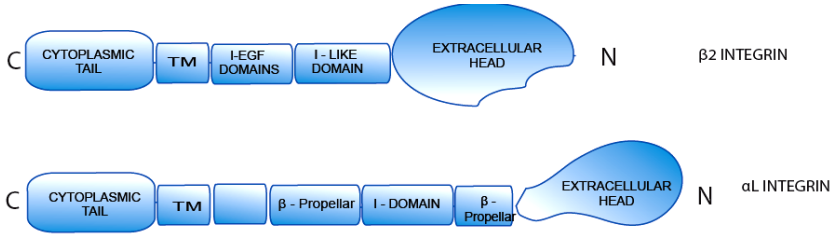

Figure 1.1: Structure of the $\alpha_L\beta_2$ integrin complex.

Integrins are cell adhesion molecules in a heterodimeric association which generally consists of a cytoplasmic tail, a transmembrane domain, and an extracellular ligand-binding head domain.

Integrins are type-I heterodimeric transmembrane cell adhesion molecules that mediate a series of biochemical processes (47-52). Integrins are confined to members of the kingdom Animalia, with no homologs identified in the Plantae, Protista, Fungi, or Monera kingdoms (53-56). Integrins generally consist of two sub-units; the α- and β- glycoproteins each containing an extracellular head region (ectodomain), which binds extracellular matrices (ligands); a transmembrane domain which is the transducer of signals relayed from the cytoplasmic domains to the distal ligand binding site, and the cytoplasmic tail which is thought to function in integrin-mediated adhesion. About half of the α-subunits have an insertion, termed the I-domain. Integrins are formed through non-covalent association of an α- and β- subunit (56-60). In humans, about eighteen α and eight β sub-units have been identified from which twenty-four

different functional integrin combinations are known. Apart from their role in cell adhesion, integrins, through their connection with the cell cytoskeleton-mediate a number of intracellular pathways that lead to leukocyte trafficking, development, haemostasis, immune response, auto-immune and genetic diseases, and cancer (61-62). These have been detected through mutation and knock-out studies of the genes for these integrins (63-68). Targeting integrins could be an effective way for treating such diseases. In fact, monoclonal antibodies which block integrins are already used clinically to treat psoriasis and inflammation (hu1124 against CD11a) (195)

Most integrins are expressed on cell surfaces as inactive forms which can be regulated through changes in clustering, lateral diffusion, or conformation to generate their active forms (110,112). Accordingly, two models have been proposed to explain the function of integrins based on microscopic, mutational, functional and structural analysis. In the 'switchblade model', integrins are in a 'bent' conformation with their head region facing down. Following the binding of regulatory molecules (such as talin), the cytoplasmic and transmembrane regions dissociate leading to dislocation of the β-stalk which results in an upward extension of the head region in switchblade-like motion (69-75). In the 'deadbolt' model, the activated integrin is in a 'bent' conformation which upon binding of regulatory molecules, causes sliding of the stalks which disrupt the interaction between the head region and the β-stalk (76-78). Integrin activation ultimately

leads to a conformational change in the ligand binding pocket of the head region that increases its affinity for the ligand.

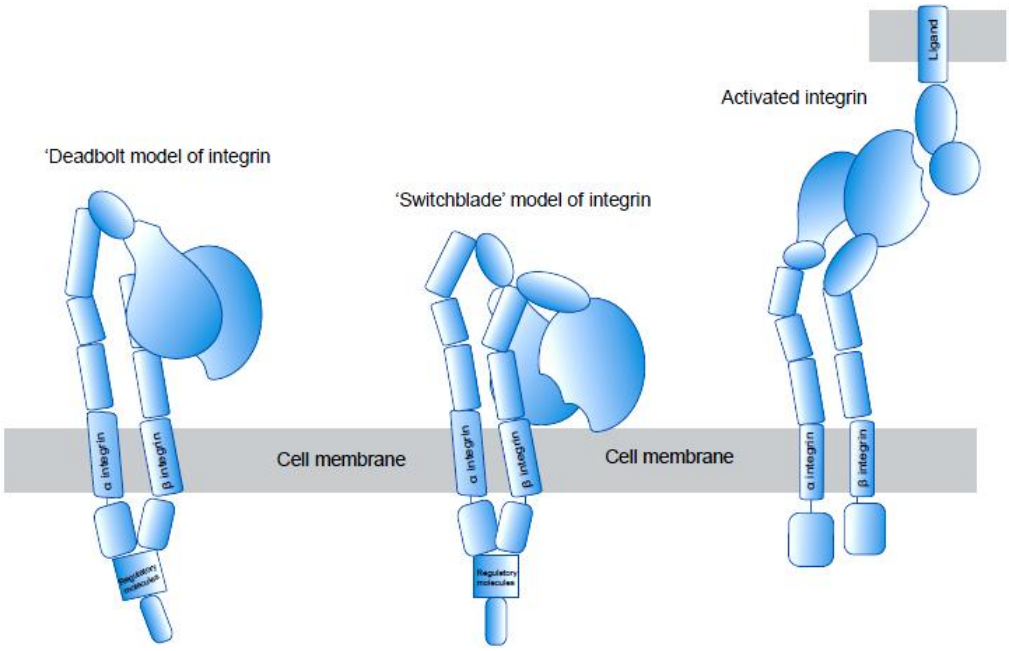

Figure 1.2. The 'Deadbolt' and 'Switchblade' models for integrin activation.

Two models of integrin activation has been proposed: the 'deadbolt' and 'switchblade' models. In the 'deadbolt' model, the activated integrin is in a 'bent' conformation which upon binding of regulatory molecules, causes sliding of the stalks which disrupt the interaction between the head region and the β-stalk (76-78). In the 'switchblade' model, integrins are in a 'bent' conformation with their head region facing down. Following the binding of regulatory molecules (such as talin), the cytoplasmic and transmembrane regions dissociate leading to dislocation of the β-stalk which results in an upward extension of the head region in switchblade-like motion (69-75).

Integrin bidirectional signalling across the plasma membrane has been described in two categories; ‘outside-in signalling’ and ‘inside-out signalling’ (50). In outside-in signalling, integrin-mediated binding to ECM results in transduction of signal from the extracellular domain via the transmembrane domain to the cytoplasmic tail initiates biochemical processes in the cytosol. Inside-out signalling involves binding of a regulatory molecule to the cytoplasmic tail which leads to transduction of signals via the transmembrane domain to the ectoplasmic ligand-binding site. Inside-out signalling has been shown in platelet formation of haemostatic plug involving the cytoplasmic domains of the integrin $\alpha_{IIb}\beta_3$ which is responsible for platelet aggregation to the plasma protein fibrinogen. This supports the fact that resting platelets are unable to bind fibrinogen despite the presence of the $\alpha_{IIb}\beta_3$ integrin on their surfaces until they are activated.(79-82).

The integrin transmembrane domain is the means through which signals are transmitted from the cytoplasmic tail to the ectodomain. In the resting or low affinity state, transmembrane domains (TMs) are thought to interact with each other forming heterodimers. Binding of cytosolic molecules to the cytoplasmic tail would trigger re-orientation or separation of the TMs, which in turn induces a structural change in the ectodomain. The disruption of the TM interface alone has been shown to promote the activation of $\alpha_{IIb}\beta_3$ (133,137).

1.3.1. The $\alpha_L\beta_2$ (CD11a, CD18) Integrin, LFA-1

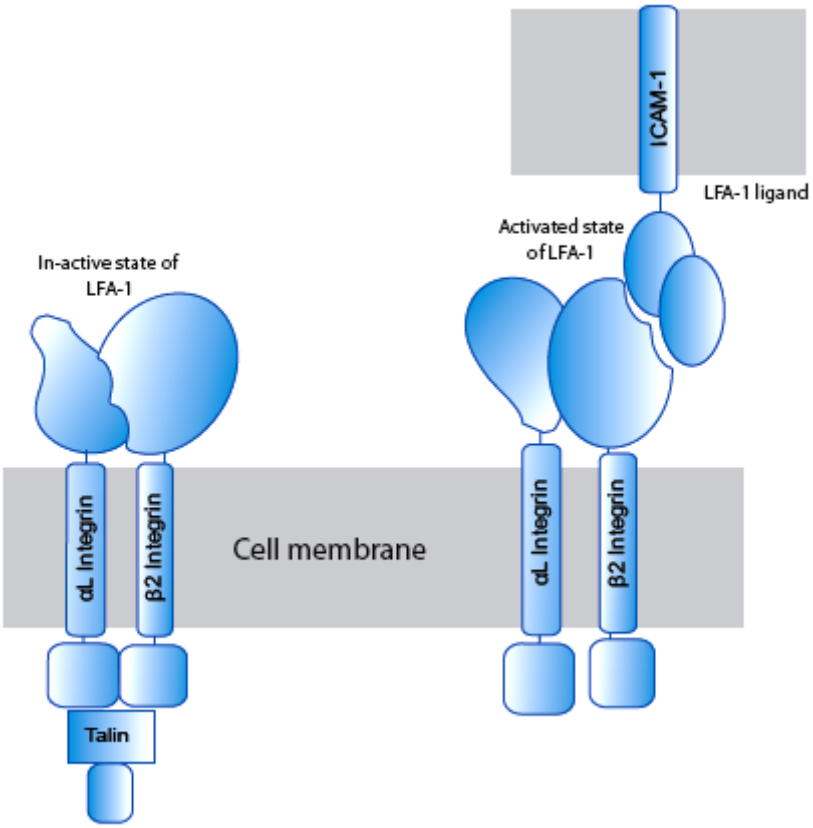

Figure 1.3: In-active and active forms of LFA-1 molecules on cell surface.

The majority of the LFA-1 molecules on the cell surface are in the inactive form, with their ectoplasmic domain facing the cell membrane. Binding of regulatory proteins, such as talin, lead to an activation of the receptor exposing the ectoplasmic domain for binding to its counter-receptor, such as ICAM-1.

The $\alpha_L\beta_2$ integrin, also known as lymphocyte function associated antigen-1 (LFA-1), is expressed solely on the surface of T lymphocytes. LFA-1 is a leukocyte-specific receptor that is involved in cell-cell interactions in the immune system (83-87). The intercellular adhesion molecules (ICAM) 1-3, which belong

to the Ig super family of proteins, are the major ligands that bind to LFA-1 (88-95). The β_2 integrin is expressed exclusively on the surface of cells in the haematopoietic system. The β_2 integrin associates with different I-like domain containing α-integrins sub-units forming heterodimers ($\alpha_L\beta_2$, $\alpha_X\beta_2$, $\alpha_D\beta_2$, $\alpha_M\beta_2$) which enables their interactions with numerous counter receptors on the surface of activated endothelial cells. Leukocytes adhesion deficiency, LAD (types I, II, and III) is an autosomal-recessive immunodeficiency associated with β_2 malfunctioning or deficiency (65, 96-99). This disease is associated with an inability of leukocytes to firmly adhere to blood vessels, with subsequent persistent leukocytosis, dramatically reduced accumulation of neutrophils and monocytes at extra-vascular sites, impairment of tissue remodelling and a recurring life-threatening bacterial infection (100-102).

1.3.2. Affinity states of LFA-1

LFA-1 has been shown to exist in three distinct conformations corresponding to three different states with different binding affinity for the ligands ICAM-1 and secretory ICAM-1 (sICAM-1). These conformations are the open, intermediate (open-close) and closed; corresponding to high, medium, and low affinities for its ligand (69, 75, 103-108). Continuous regulation of these conformations is crucial for maintaining the LFA-1 receptors on circulating lymphocytes. Interaction of ICAM-1 and LFA-1 mediates a number of immunological processes including leukocyte extravasation, antigen presentation, and effector functions (92, 109-112). LFA-1 regulation is important in

maintaining the number of circulating leukocytes in the body. In the low affinity form, the receptor has its β and α sub-units bending downward thereby bringing its binding site to 5 nm of the cell surface. On the other hand, the open conformation which corresponds to the high affinity state has its extracellular domain extended, bringing the binding site approximately 20 nm from the cell surface (105-106). In the intermediate conformation, the α_L and β_2 sub-units are partially bent (108). Some of these conformations can be recognised by the binding of specific mAbs. Antibody clone HI 111 recognises and binds the closed conformation, while TS1/18 will bind the open-close conformation (103-104, 113). The open conformation is recognised by binding of Ab clone MEM148 which recognizes an activating epitope for β_2 integrin (114). The active form of LFA-1 can be detected using mAb 24, and is known as an LFA-1 activation reporter (115-119). On resting leukocytes, about 80% of LFA-1 is maintained in an inactive form, while about 20% is in the high affinity state (120). The conformational state of LFA-1 is important in regulating the adhesiveness of LFA-1 on circulating leukocytes to their ligands, thereby preventing adherence of leukocytes to different cells or ECM (112). During an infection or an immunological response requiring leukocyte trafficking, LFA-1 receptors are activated to the high affinity form. Regulation of LFA-1 can either be through changes in the affinity of the receptor or through rearrangement of the cell surface receptor (130, 196).

The high affinity state of LFA-1 can be induced through binding of its ligand at cell-cell contact sites, in what is termed a ligand-induced conformational change (81, 118). Induction of the high affinity forms can be caused by agonist, such as phorbol-12-myristate-13-acetate (PMA), divalent cations (Mg^{2+} or Mn^{2+}), or phosphorylation of the β_2 integrin (121-129). Cross-linking of receptors can also lead to an increase adhesiveness of the LFA-1 receptors to its ligands. The high affinity form is enhanced through cell spreading and clustering of receptors (110). Whereas Mg^{2+} ions concentrations of over 1 mM causes high expression of the mAb 24 binding epitope, phorbol esters does not. Thus, the avidity of T cell LFA-1 to its ligands is dependent on its binding affinity, receptor and ligand density, rearrangement of surface ligands and receptors and mechanisms of cytoskeletal movements including disruption of cytoplasmic domains of the individual integrins (112, 130-134). The receptors are confined to the cytoskeleton through their cytoplasmic tail (135). Regulation of LFA-1 affinity is not dependent on T cell activation as surface levels do not change following T cell activation (112, 136).

Rearrangement of the cytoskeleton results in a shift from the low affinity to a high affinity conformation of integrin (137). This has been shown in the platelet integrin $\alpha_{IIb}\beta_3$ molecule to involve separation of the TM and cytoplasmic domains of the two sub-units (138-140). In the low-affinity state, the integrin TM and cytoplasmic tails are in close proximity. Any process that can lead to separation of the homomeric association between the TM domains causes

rearrangement of the integrin leading to clustering, and finally increased binding affinity. Mutations at the sites on the α and β sub-units responsible for this homomeric association have been shown to disrupt this association, leading to activation of the integrin (130, 141-142).

1.4. INTEGRINS AS TRANSMEMBRANE PROTEINS

Transmembrane proteins (TM) constitute over 30% of the genome and form the target for over 60% of currently marketed small molecule therapeutics (143-144). TMs play a crucial role in cellular processes, including communication between cells, between organelles and the cytosol, ion channels and nutrient transports, anchors proteins to cell cytoskeleton and links to ECM. Most viral and bacterial receptors are TM proteins. TMs are implicated in diseases such as diabetes, hypertension, arthritis, depression among others.

1.4.1. Structure of transmembrane proteins

In general, TM proteins are found embedded within the hydrophobic membrane bilayer. Thus, these proteins consist of mostly non-polar hydrophobic amino acid (a.a.) side chains that fold in a manner to satisfy the polypeptide H-bond site chain with its a.a. side chains facing outward into the lipids. TM domains often assume one of either α-helix or β-barrel conformation. More than 90% of structurally characterized TM proteins assume an α-helix conformation which could either be a single bitopic helix or a polytopic helix bundle (145). In the α-helix, the amino acids fold in a way that favours the formation of a H-bonded backbone with the hydrophobic side chains facing outward towards the

acyl chains of the lipid. Examples of α-helix membrane proteins include: human growth hormone receptor, HGHR, insulin receptor, ATP binding cassette family, P-glycoproteins (such as ABC transporters), and G protein-coupled receptors (GPCR). TM β-barrel structures consist of β sheets that satisfy the formation of H-backbone between strands, wrapping the sheets into a barrel shapes with the a.a. hydrophobic side chains facing outward in the acyl lipid chains. The β-barrel sheets are observed in the outer membranes of Gram negative (G –) bacteria and some membrane acting toxins (such as porins). The structure of TM proteins is determined in part by the phospholipids in the membrane bilayer (146-147). The structure of the β_3 integrin and glycophorin A (GpA) in phospholipid bicelles (for example glycerophosphatidylcholine-based lipids) and detergent micelles (for example dodecylphosphocholine) has shown a preference for the integrin to immerse in the hydrophobic bicelle core in a manner typical of α-helical proteins in the membrane (148-150). These proteins are able to form heterooligomers or homooligomers in micelles and bacteria membranes (151-153).

TM α-helices of integrin glycoproteins contain a GXXXG motif that participates in the formation of homo and heterodimers (151). This sequence of a.a. has been shown on GpA using NMR studies and also in the $\alpha_{IIb}\beta_3$ integrin using mutational and NMR analyses (154). Formation of integrin homodimers within the TM region is crucial in regulating integrin function. Activation of integrin has been induced by modulating the helix association of the integrin TM. Disruption of TM helix association can lead to activation, as in the case of

activation of the platelet $\alpha_{IIb}\beta_3$ integrin by an exogenous peptide that corresponds to the TM of α_{IIb} integrin (133). Disruption of TM association can result in inhibition of receptor function, as in the case of an exogenous peptide mimicking TM domain of GPCR or the P-glycoprotein, an ABC transporter (155-156). Disruption of integrin function can also be brought about through mutation in an a.a. in the region essential for homodimerization (84).

1.4.2. Transmembrane protein association

The GXXXG motif in TM proteins, commonly referred to as the glycine zipper, is crucial for the formation of homomers and heteromers observed in TM domain association seen in lipid bicelles and bacterial membranes (157). Homomers are products formed through non-covalent association of a single type of integrin subunit whereas heteromers are formed between non-covalent associations between different subunits of integrins. The small size of the glycine residue can allow two TM helices to come into close proximity while the random a.a. residues further add specificity in the formation of a distinct binding cleft. Homomeric and heteromeric associations observed in integrin TM domains are important in regulating integrin function. In the inactive form, the TM domains of the α and β glycoprotein sub-units are in a heteromeric association. Disruption of this association results in activation of the integrin which can lead to a simultaneous homomerization of the individual sub-unit. These associations have been described using TM domains expressed in different bacterial reporter systems (158-160).

1.4.2.1. Homo-oligomeric and Hetero-oligomeric association of TM proteins

Heteromeric associations observed in integrins are usually strong enough to maintain the integrin in its inactive conformation, but weak enough to be easily disrupted during integrin activation. Integrins as heterodimers form an ideal system for understanding these associations. Heteromeric and homomeric associations have been described using the platelet $\alpha_{IIb}\beta_3$ integrin receptor, the dimerization of GpA TM and the ErbB1 and ErbB2 (also known as epidermal growth factor receptors) using the TOXCAT and GALLEX bacterial reporter systems (151, 158-159, 161). The TOXCAT assay makes use of the *N*-terminal DNA binding domain of ToxR in a chimeric fusion with a periplasmic maltose binding protein (MBP). In between the ToxR and MBP is a transmembrane (TM) protein of interest. Association of the TM protein leads to activation of a chloramphenicol acetyltransferase (CAT) gene which can be measured by the level of CAT expression (159). The GALLEX system on the other hand makes use of two LexA DNA binding domains of different specificity coupled separately to two TM proteins. Association of these TM proteins will lead to the repression of β-galactosidase synthesis (158).

In the TOXCAT assay, the TM domain of interest is expressed as a chimeric protein between an *N*-terminal binding domain of ToxR (a dimerization-dependent transcriptional activator) and a *C*-terminal monomeric periplasmic anchor MBP (159). This is done by inserting the cDNA encoding the TM domain of interest in a plasmid between the *MalE* and the *ToxR* transcription activator

genes (ToxR-TM-MalE construct) (160). The resulting plasmid is expressed in *E. coli* cells and grown on M9 medium/agar containing maltose as the only source of carbon. In the TOXCAT reporter system, association of the TMs results in activation of the ToxR transcription factor which encodes a CAT reporter. CAT expressional level as a measure of β-galactosidase activity is then quantified, and is directly proportional to the strength of dimerization observed in the TM. The orientation of the chimeric protein in the membrane was determined by the ability of transformed MBP-deficient bacteria strain with the plasmid to grow in medium containing maltose as the only carbon source. Only cells that expressed periplasmic maltose were able to grow under such conditions.

The introduction of a TM protein such as GpA, α_{IIb}, ErbB1 in the membrane that mediates dimerization will lead to the dimerization of the ToxR cytoplasmic tails resulting in activation of the CAT gene under the ctx promoter with a subsequent resistance to chloramphenicol (CAM) being acquired. The extent of dimerization can be quantified in two ways: by measuring *in vitro* the amount of CAM acetylation by CAT or by *in vivo* acquisition of resistance to CAM. Using this system, Gerber *et al*. showed that two motifs on the TM domains of ErbB1 and ErbB2 are responsible for homodimerization and heterodimerization. The ErbB is a family of receptors that are involved in cancer proliferation and differentiation (162). In ErbB1, only site I motifs (*N*-terminal) are involved in homodimerization whereas in ErbB2 both sites I and II (*C*-terminal) are involved (163). To detect any heterodimerization, an exogeneous

peptide is added to the system, and the CAT activity measured (164-165). In this case the addition of a synthetic peptide corresponding to ErbB1 (with just the site I motif) to the ErbB2 system resulted in a decrease in the β-galactosidase reporter gene signal (163). Control peptides used were by introducing mutations within the GXXXG motif including a M81V and G83I.

Homomeric and heteromeric association of the platelet integrin $\alpha_{IIb}\beta_3$ has been examined using the TOXCAT system (151). In this study, Zhu *et al*. were able to determine the a.a. residues responsible for heterodimer and homodimer formation through a number of mutational studies. Residues involved in homodimer interactions are widely dispersed, whereas those involved in heterodimer association are comprised of interdigitated a.a. residues. Mutation of most of these residues results in destabilization of these interactions with some favouring homodimerization. Although homomeric associations between the β_3 TM are substantially weaker compared to those of α_{IIb}, heteromeric associations between the two integrins are strong enough to maintain the $\alpha_{IIb}\beta_3$ association of the platelet integrin. Unlike the G652I mutation in the ErbB1 system that showed a significant reduction in heterodimer formation, mutations in the GXXXG motif in α_{IIb} makes it more glycine zipper-like thereby mediating homomeric interactions similar to that observed in GpA (141, 166). Mutations along the GXXXG face of the α_{IIb} disrupt heterodimer formation as this result in residues which are unable to pack into the grooves formed by the β_3 face. Mutations along the full length β_3 integrin was activating in contrast to the TOXCAT assay which

could either enhance or disrupt homomeric activity. They further tested the effects of these mutations in the full length integrin by observing their binding ability to fibrinogen. Some mutations that had a disruptive effect on the TOXCAT assay did not induce fibrinogen binding. There is a remarkable difference in the essential residues involved in each type of association. The *N*-terminal L697, M701 and I704 of β_3 pack closely against the GXXXG motif of the α_{IIb}. The G708 of β_3 is also involved in a complementary interaction with residues on the α_{IIb}, whereas it is less important for homooligomeric interaction as assessed by mutation of G708A(L).

The GALLEX reporter system functions in a similar way except that it is based on the repression of a reporter gene activity by two LexA DNA binding domains with different DNA specificities (158, 167). LexA is a transcriptional factor whose dimerization is required to efficiently repress transcription (168). LexA has been employed in the development of a system to study heterodimerization of soluble proteins in *E. coli* (169). Schneider *et al*. were able to use the GALLEX reporter system in analysing the interaction between the α_4 and β_7 integrin TM helices. They showed that these TM domains both form weak homo- and hetero- oligomers. The gene encoding the TM of interest was inserted between the MalE and LexA genes in a plasmid forming an *N*-terminal cytoplasmic LexA and a *C*-terminal periplasmic MBP protein (LexA-TM-MBP). Like in the TOXCAT system, introduction of a TM protein that drives dimerization will lead to binding of the two different variants of *C*-terminal LexA

domains to different DNA sequences that are adjacent to one another. This will result in binding to an operator region leading to repression of the β-galactosidase activity. The correct orientation and insertion of the chimeric protein was ascertained by growing *E. coli* cells transformed with the plasmid in M9 medium containing 0.4% maltose as the only source of carbon. Cells that expressed maltose in their periplasm were able to grow under such conditions. Homodimerization was done in *E. coli* SU101 cells in which the lacZ gene is under the WT LexA recognition sequence (op+) whereas heterodimerization was done in the *E. coli* SU102 cells with its lacZ reporter gene placed under the control of op480/op+ hybrid operator (half WT plus an alter half LexA DNA).

1.4.3. Probing transmembrane protein interactions

Studies of TM proteins have been lagging behind that of their water-soluble counterparts due mainly to their hydrophobic nature. Due to their vast role in cellular processes and their therapeutic propensities, understanding TM protein is an important target. The development of agents that target protein-protein interaction in the membrane is crucial to elucidating their functions. Major advances in understanding membrane protein-protein interactions through the development of agents that selectively, and specifically, target protein TM domains are in progress. Current techniques being employed include, but are not limited to: the use of computer designed peptides, the use of exogenous peptides mimicking TM domains of receptors, mutation of essential amino acid involved in TM associations and the use of fluorescent and genetic screens. These methods

have been reviewed by Zhao *et al*., Slivka *et al*. and Hang Yin (144, 170-171). Here we will discuss work that involves the use of synthetic peptides to probe the function of a TM interaction.

1.4.3.1. Use of computationally designed anti-TM peptides

Computational protein chemistry has been used to study water-soluble proteins, but their application in membrane proteins has not been widely investigated (172-176). In their resting state, the TM domains of integrins are in a heterodimeric association which becomes disrupted when integrin is activated (142, 177-179). Yin *et al*. have developed a computational approach to designing anti-membrane proteins that specifically binds to the TM of α_{IIb} and α_v integrins. This approach is termed computed helical anti-membrane protein (CHAMP) (180-181). The first step in the design of CHAMP peptides involves selection of a backbone peptide-target complex. This is preceded by a selection of the peptide amino acid sequence. A database containing membrane-protein structures is used for selecting the backbone peptides to serve as potential templates. Since most TM helix-helix pairs have a well defined structural motif, it was possible to predict preferred interactions between target TM helices. In the case of integrins, their TM helices have a GXXXG sequence motif which can form a parallel right-handed glycine-alanine-serine (GAS_{Right}) motif with approaching helices. With the identification of the preferred mode of interaction, the helical pairs from known protein structures could serve as a backbone for designing CHAMP peptides. The helical pairs selected are referred to as template pairs, with the

individual helices being the template helix. Following the identification of the template helices, the sequence of the target TM helix (α_{IIb} and α_v integrins) was threaded onto one of the two template helices. This was realized by matching the GXXXG motifs of both the target and templates together. Once this was achieved, the amino acid sequence of the CHAMP peptide was selected using a side chain repacking algorithm which optimized the rotamers of the CHAMP helix.

Using CHAMP, Yin and co-workers were able to design anti-α_{IIb} and anti-α_v peptides that specifically target the TM of α_{IIb} and α_v, respectively both *in vivo* and *in vitro*. The templates used in the design of CHAMP were taken from polytopic proteins which had no structural or functional relation with integrins. They used the glycerol-3-phosphate transporter (1PW4) as a template for the anti-α_v peptide and the photosystem I reaction center (1JB0) for the anti-α_{IIb}. These peptides were then synthesized using solid phase peptide synthesis (SPPS) with their solubility enhanced by introduction of polar groups at their *C*- and *N*-termini. FRET analysis was used to evaluate the association of CHAMP peptides with their targets in micelles. Both SDS PAGE and analytical ultracentrifugation indicated the presence of homodimers and heterodimers with their respective targets. Using the dominant-negative TOXCAT assay, they showed that both anti-α_{IIb} and anti-α_v formed homodimers in bacterial membranes and that they were highly specific for their targets, as opposed to other TM domains. The TM of α_2, α_v, β_1, or β_3 did not interact with the anti-α_{IIb} and in a similar manner; the TM domains of α_2, α_{IIb}, β_1 or β_3 failed to associate with anti-α_v.

CHAMP peptides induced platelet aggregation and adhesion *in vivo*. Platelet aggregation is brought about by binding of the $\alpha_{IIb}\beta_3$ through an ADP mediated interaction of its extracellular head with its divalent ligand, fibrinogen. Platelet adhesion to osteopontin is mediated via $\alpha_v\beta_3$ integrins. Incubation of platelets with 0.5 µM anti-α_{IIb} caused an increase in aggregation to fibrinogen, an indication that anti-α_{IIb} CHAMP peptide recognises and specifically binds to its target α_{IIb} *in vivo,* even in the presence of closely related integrins. Binding of the anti-α_{IIb} to its target resulted in destabilisation of the $\alpha_{IIb}\beta_3$ integrin heterodimer which leads to activation of the integrin causing the increase in aggregation observed. Aggregation was not significantly altered with inhibitors of platelets such as inhibitors of glycoproteins PG IIb/IIIa receptor such as abciximab, tirofiban, integrilin and aspirin. On the other hand, 10 µM of anti-α_v peptide equally induced an increase in adhesion of platelet cells to the matrix protein osteopontin.

In conclusion, the action of CHAMP peptides was consistent with the push-pull mechanism of integrin activation where any process that causes a disruption of the integrin association (such as mutation in the region involve in helix-helix formation) resulted in activation of the integrin. In this case, CHAMP peptides bind to a site on the α-TM helix that is involved in heterodimerization with the β-TM, thereby preventing the formation of the heterodimer. CHAMP peptides can thus be applied in a similar way to the use of antibodies in blocking water soluble proteins.

1.4.3.2. Use of synthetic peptide mimics

The use of synthetic peptides in targeting TM domains of protein receptors is challenging. TM protein sequences are generally highly hydrophobic, resulting in sequences that are prone to aggregation of the peptide. Hence the design of synthetic peptides that mimic TM domains must take into consideration several parameters, among which are the inclusion of terminal anionic amino acids to confer solubility for easy delivery, hydrophobic residues to facilitate binding and insertion of peptide, and anchoring residues to ensure proper orientation of the peptide in the membrane.

1.4.3.2.1. Inhibition of dimerization and activation of β_2 adrenergic receptor

Hebert *et al*. used a synthetic peptide derived from the β_2-AR TM to inhibit dimerization and activation of the receptor *in vivo* (182). β_2-AR is a member of the GPCR family of proteins that mediates a number of neurological processes in the body. Activation of the receptor is seen in its effector molecule, adenylyl cyclase being activated. Here, the investigators were able to show the importance of dimerization to the functioning of the receptor by inhibiting the receptor with a peptide derived from the TM domain. β_2-AR forms oligomers which are readily visible on SDS-PAGE, and are resistant to treatment of the receptors with reducing and denaturing agents such as β-mercaptoethanol, dithiothreitol, urea, guanidinium hydrochloride. It has been shown that there is a motif in the TM domain of GpA which was responsible for dimer formation. Analysis of β_2-AR also revealed the presence of a similar motif at the cytoplasmic

end of the sixth TM domain consisting of leucine and glycine residues (LXXXG) positioned with a similar spacing as was observed in GpA.

It has been suggested that TM VI was the most exposed TM segment and the leucine and glycine residues appear on the external face of the helix (183). To test this hypothesis, a 20 a.a. peptide was synthesized that corresponded to the TM VI. The results showed that addition of the TM VI peptide significantly reduced the amount of dimmers formed in a time-dependent manner with up to 69% reduction observed in 30 m. A control peptide derived from the TM VII of the D2 dopamine receptor had no effect even at maximal concentration. Another control peptide derived from TM VI of β_2-AR with mutations of G276, G280 and L284 to alanine slightly decreased dimer formation, but in effect, did not cause any appreciable decrease in dimer formation compared to the TM VI peptide. Treatment of cells with 0.15 µg/µL of TM VI peptide significantly inhibited receptor stimulated adenylyl cyclase activity from inhibition of receptor dimerization.

1.4.3.2.2. Inhibition of GPCRs

Building upon the above findings, Michejda and co-workers used synthetic peptides that mimic TMs of GPCRs to inhibit receptor function by disruption of TM interactions (155). GPCR serves as a therapeutic target for most diseases. The general strategy for targeting GPCR has been the design of antagonists that target the external binding site. Michejda and co-workers sought to target GPCRs by disruption of the TM interaction. They synthesized peptides

corresponding to the TM of all seven proposed TM domains of the GPCR to test their hypothesis. The synthetic peptides corresponding to TM domain of GPCR did indeed disrupt receptor function by interfering with TM associations. This could be evaluated by measuring the amount of intracellular Ca^{2+} released in cell lines expressing CXCR4.

Michejda and co-workers found that a 24 a.a. peptide, CXCR4-2-2 corresponding to TM2 of the CXC chemokine receptor 4 (CXCR4) was the most potent antagonist, completely blocking the transduction of signal at a concentration of 0.2 μM. Introduction of terminal anionic amino acid residues to the peptides enhanced the potency of the antagonist by facilitating penetration of the cellular membrane. They further identified antagonists from the remaining TM domains. The selectivity of the antagonist to its specific TM domain was supported by the fact that all peptides derived from the CXCR4 receptor had no influence on signalling via the CC chemokine receptor 5 (CCR5), a chemokine involved in HIV-1 entry. A peptide derived from TM2 of CCR5 (CCR5-2-1) completely abolished RANTES-induced CCR5 signalling in U87 cells at 0.5 μM but had no influence on CXCR4 signalling. Combination of CXCR4-6-1 and CXCR4-7-3 antagonists together had a higher inhibitory effect on the CXCR4 receptor compared to the individual antagonists.

In a similar manner, Michejda and coworkers extended their findings to the rat chemokine CCKAR where they showed that peptides derived from the first and second TM (CCKAR-1-1 and CCKAR-2-1) were able to inhibit ligand

binding and signalling in CHO cells transfected with rat CCKAR. These same antagonists had no effect on CXCR4 and CCR5, illustrating the selectivity and specificity of the antagonists to the target TM. Coupling of GPCRs to adenylate cyclase and G-protein has also been inhibited using a similar approach in an attempt to understand the molecular basis of receptor function (184-185).

A direct application of these findings was extended to a drug candidate for use in inhibiting HIV-1 replication in a cell-based cytoprotection *in vitro*. CXCR4 and CCR5 are chemokine receptors involved in HIV-1 entry. Michejda *et al.* showed that CXCR4-4-2 was the most potent peptide for inhibition of HIV-1 infection at concentrations of 1 μM with an IC_{50} of approximately 300 nM (155). The peptides CXCR4-2-2 and CXCR4-7-3 also inhibited infections at 2-3 μM concentrations. They also observed that none of the CCKAR peptides inhibited HIV-1 infection and none of these peptides caused cell toxicity. The inhibition of receptor function can be explained by antagonist peptide insertion in the cell membrane, and competition with the intra-membrane helices, thereby disrupting the cytoskeleton.

1.4.3.2.3. Inhibition of P-glycoprotein (P-gp)

ABC transporters, such as P-glycoprotein, modulate numerous cellular functions through their action as pumps for various compounds across the cytoplasm and organelles. These proteins utilize ATP as an energy source for their pumping functions. ABC transporters have been shown to be highly involved in rendering cancer cells resistant to chemotherapy, and as such development of

specific inhibitors against them can form a target for oncology (186-188). ABC transporters consist of twelve helical TM segments forming two membrane domains with two nucleotide binding domains at their cytoplasmic surfaces. The TM domains form part of the substrate binding site and undergo reorganization during the pumping process. There is a high homology between the primary and tertiary structures of the nucleotide binding domain while the TM domain shows a structural variation in the amino acid sequence in the tertiary protein (189-190).

Michejda *et al*. extended their inhibition of GPCRs to the ABC transporter by synthesizing derivatives of all 12 TM helices of P-gp and testing their ability to inhibit the function of the transporter (156). Based on the predicted TM domains, they were able to generate, using different computer programs, TM domains corresponding to the 12 TM. Due to limitations of the SPPS, the maximum number of amino acid residues synthesized was 26. Substitution of terminal a.a. with anionic a.a. residues enhanced the potency of the peptides. The effect of adding aspartates at the *C*-terminus of the peptides was clearly seen in the increase in potency for peptides having the aspartates as opposed to those without the *C*-terminal aspartate (MDR1-5-4 compared to MDR1-5-2, MDR1-7-3 compared to MDR1-7-2, and MDR1-4-2 compared to MDR1-4-1). Apart from the TM 10 that formed high aggregates and could not serve as inhibitor, TM of all other helices could form active inhibitors though with varied potency. The length of the peptides also contributed to potency with some shorter peptides showing

high potency compared to the longer variants. In most cases however, decreasing peptide length was associated with a corresponding decrease in potency.

The activity of these inhibitors was measured by FC analysis of cells incubated with rhodamine 123 which confirmed the inhibitory activity of the peptides. Laser scanning confocal microscopy further revealed much higher fluorescence of the cells following treatment with peptide inhibitors. The inhibitory ability of these peptides inhibitors was found to be selective as the CXCR4 derived peptides had no effects on the efflux of fluorescent substrates of P-gp. Other derived peptides from ABC G2 transporter had no influence on P-gp and vice versa. Finally, they tested the ability of the most soluble MDR1-2-2 peptides to sensitize highly resistant colon cancer cell lines expressing MDR1 to doxorubicin. They observed several-fold increase in toxicity of doxorubicin in the presence of the peptide. Due to solubility constrains in culture medium, the other peptides could not be tested.

1.5. OBJECTIVES

The goal of this project was to make exogeneous protein probes with fluorescent tags that can specifically and selectively bind and insert to cell lines expressing LFA-1 as the only β_2 integrin containing receptor. These proteins would be engineered using molecular biology techniques and the proteins tested *in vitro* on Jurkat cells (clone E6.1). Insertion of these chimeric proteins would result to disruption of the receptor function. We can then quantify the extent of this disruption by an *in vitro* adhesion assays with ICAM-1 or by measuring the

change in binding of mAbs directed against specific epitopes on the LFA-1 individual integrins.

1.6. RATIONALE

Synthetic peptide mimics have been successfully used to inhibit receptor function of the GPCRs, ABC transporter, and the inhibition of TM dimerization. We hypothesize that peptides which specifically bind to integrin TM could be used to specifically disrupt the function of LFA-1. Furthermore, we considered that if the peptides specifically bind to LFA-1, they could be used as a labelling strategy if a fluorophore were incorporated. We designed chimeric peptides having an *N*-terminal EGFP tag linked to a *C*-terminal β_2 integrin TM variant. Unlike SPPS, we used a bacterial expression system to make our proteins. The solubility of the fusion protein was enhanced by adding several amino acids of the cytoplasmic tail of β_2 integrin to the construct.

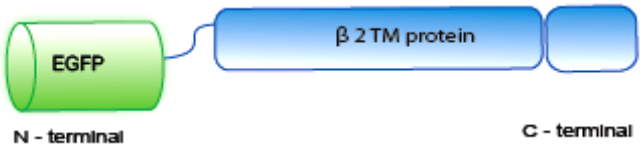

Figure 1.4: Design of β_2 TM proteins

Designed proteins for this study had an *N*-terminal EGFP fused to the β_2-TM protein variant via a 9-mer linker.

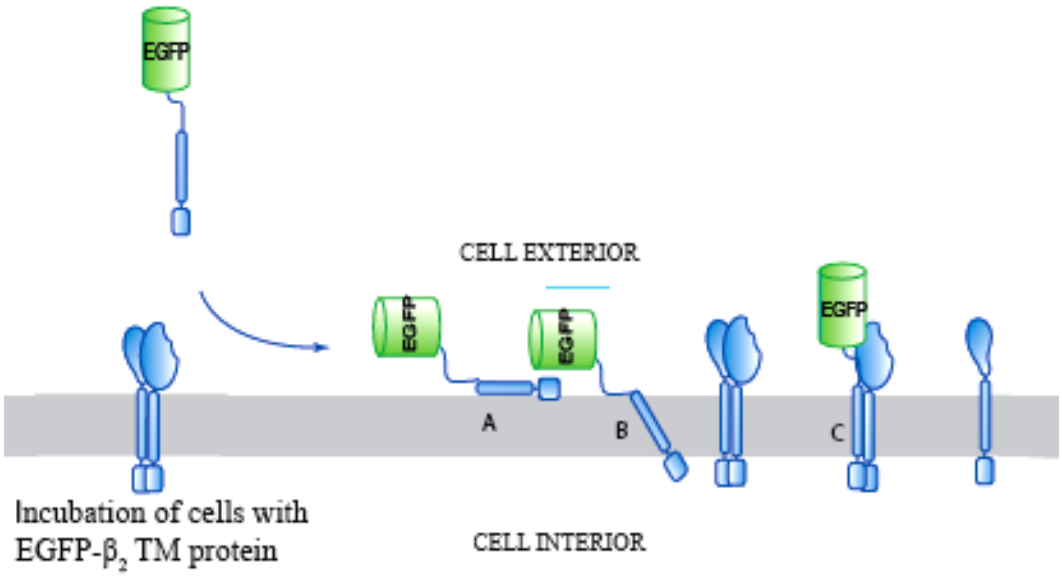

Figure 1.4: Schematic representation of binding and disruption of LFA-1 receptor by β_2 fusion proteins.

The binding and disruption of β_2 integrin proposed to occur in three steps (166, 191-194). **A**: Binding of the TM to the lipid bilayer. **B**: Bound TM inserts into the membrane and assumes the desired orientation for interaction with the integrin of interest. **C**: TM associates with the WT TM domain of the target integrin.

We hypothesized that if cells are incubated with such peptides, they will assume an orientation that will favour the insertion of small, mostly hydrophobic, *C*-terminus-attached β_2 TM domain into the cell membrane. The presence of hydrophilic residues will facilitate binding on the membrane. The hydrophobic residues can then orient the recombinant proteins in a conformation that favours insertion. Once inserted, the protein can move in the membrane and bind to the target TM rearranging the target integrin receptor and displacing the β_2 integrin. This displacement can either lead to activation or inhibition of the LFA-1 receptor

to binding of its ligand. This disruption should have a substantial effect on the binding of mAb to epitopes located on the β_2 integrin.

In this thesis, Chapter 2 will discuss the engineering of the recombinant EGFP-β_2TM proteins and characterize the binding of these proteins to cells. Four variants of the EGFP-β_2TM proteins were expressed in a bacterial system and characterised using SDS-PAGE, CD spectroscopy, and mass spectroscopy. Jurkat cells (clone E6.1) were treated with these recombinant proteins, and their binding was evaluated using flow cytometry (FC) and fluorescence microscopy. The results obtained showed that the recombinant proteins bind to cells and caused labelling of the cells. EGFP protein was used as a control protein, and did not show any binding to cells.

In Chapter 3, we report on the use of the β_2-TM proteins in interfering with the structure of LFA-1 heterodimers. Jurkat cells were treated with these recombinant proteins, and their ability to bind to fluorsphere beads conjugated with specific mAb to LFA-1 epitopes was determined. The results showed that some recombinant proteins enhanced binding of MEM48 and MEM148 mAbs against the β_2 integrin. Further analysis with PMA, a T-cell activator showed a greater than 2-fold increase in binding of LFA-1 to mAb, whereas, cyto D, an inhibitor of cytoskeletal disruption caused a decrease. The effect of glycosidases on LFA-1 was also determined since very little work has been done in determining the role of glycosylation on LFA-1 receptor.

1.7. REFERENCES

1. Buckley, C. D., Rainger, G. E., Bradfield, P. F., Nash, G. B., and Simmons, D. L. (1998) Cell adhesion: more than just glue (review), *Mol Membr Biol 15*, 167-176.
2. Gumbiner, B. M. (1996) Cell adhesion: the molecular basis of tissue architecture and morphogenesis, *Cell 84*, 345-357.
3. Prakasam, A. K., Maruthamuthu, V., and Leckband, D. E. (2006) Similarities between heterophilic and homophilic cadherin adhesion, *Proc Natl Acad Sci U S A 103*, 15434-15439.
4. Brummendorf, T., and Rathjen, F. G. (1995) Cell adhesion molecules 1: immunoglobulin superfamily, *Protein Profile 2*, 963-1108.
5. Kansas, G. S. (1996) Selectins and their ligands: current concepts and controversies, *Blood 88*, 3259-3287.
6. Rojas, A. I., and Ahmed, A. R. (1999) Adhesion receptors in health and disease, *Crit Rev Oral Biol Med 10*, 337-358.
7. Hynes, R. O. (1999) Cell adhesion: old and new questions, *Trends Cell Biol 9*, M33-37.
8. Joseph-Silverstein, J., and Silverstein, R. L. (1998) Cell adhesion molecules: an overview, *Cancer Invest 16*, 176-182.
9. Gonzalez-Amaro, R., and Sanchez-Madrid, F. (1999) Cell adhesion molecules: selectins and integrins, *Crit Rev Immunol 19*, 389-429.
10. Yanagishita, M., and Hascall, V. C. (1992) Cell surface heparan sulfate proteoglycans, *J Biol Chem 267*, 9451-9454.
11. Bernfield, M., Gotte, M., Park, P. W., Reizes, O., Fitzgerald, M. L., Lincecum, J., and Zako, M. (1999) Functions of cell surface heparan sulfate proteoglycans, *Annu Rev Biochem 68*, 729-777.
12. Wolfsberg, T. G., Straight, P. D., Gerena, R. L., Huovila, A. P., Primakoff, P., Myles, D. G., and White, J. M. (1995) ADAM, a widely distributed and developmentally regulated gene family encoding membrane proteins with a disintegrin and metalloprotease domain, *Dev Biol 169*, 378-383.
13. Hooft van Huijsduijnen, R. (1998) Protein tyrosine phosphatases: counting the trees in the forest, *Gene 225*, 1-8.
14. Fannon, A. M., Sherman, D. L., Ilyina-Gragerova, G., Brophy, P. J., Friedrich, V. L., Jr., and Colman, D. R. (1995) Novel E-cadherin-mediated adhesion in peripheral nerve: Schwann cell architecture is stabilized by autotypic adherens junctions, *J Cell Biol 129*, 189-202.
15. Abercrombie, M., Heaysman, J. E., and Pegrum, S. M. (1971) The locomotion of fibroblasts in culture. IV. Electron microscopy of the leading lamella, *Exp Cell Res 67*, 359-367.
16. Nobes, C. D., and Hall, A. (1995) Rho, rac, and cdc42 GTPases regulate the assembly of multimolecular focal complexes associated with actin stress fibers, lamellipodia, and filopodia, *Cell 81*, 53-62.

17. Izzard, C. S., and Lochner, L. R. (1976) Cell-to-substrate contacts in living fibroblasts: an interference reflexion study with an evaluation of the technique, *J Cell Sci 21*, 129-159.
18. Garrod, D. R. (1993) Desmosomes and hemidesmosomes, *Curr Opin Cell Biol 5*, 30-40.
19. Green, K. J., and Jones, J. C. (1996) Desmosomes and hemidesmosomes: structure and function of molecular components, *FASEB J 10*, 871-881.
20. Schwarz, M. A., Owaribe, K., Kartenbeck, J., and Franke, W. W. (1990) Desmosomes and hemidesmosomes: constitutive molecular components, *Annu Rev Cell Biol 6*, 461-491.
21. Borradori, L., and Sonnenberg, A. (1999) Structure and function of hemidesmosomes: more than simple adhesion complexes, *J Invest Dermatol 112*, 411-418.
22. McEver, R. P., Moore, K. L., and Cummings, R. D. (1995) Leukocyte trafficking mediated by selectin-carbohydrate interactions, *J Biol Chem 270*, 11025-11028.
23. Brackenbury, R., Rutishauser, U., and Edelman, G. M. (1981) Distinct calcium-independent and calcium-dependent adhesion systems of chicken embryo cells, *Proc Natl Acad Sci U S A 78*, 387-391.
24. Butcher, E. C., and Picker, L. J. (1996) Lymphocyte homing and homeostasis, *Science 272*, 60-66.
25. Lorant, D. E., McEver, R. P., McIntyre, T. M., Moore, K. L., Prescott, S. M., and Zimmerman, G. A. (1995) Activation of polymorphonuclear leukocytes reduces their adhesion to P-selectin and causes redistribution of ligands for P-selectin on their surfaces, *J Clin Invest 96*, 171-182.
26. McEver, R. P. (1995) Regulation of function and expression of P-selectin, *Agents Actions Suppl 47*, 117-119.
27. Moore, K. L., Patel, K. D., Bruehl, R. E., Li, F., Johnson, D. A., Lichenstein, H. S., Cummings, R. D., Bainton, D. F., and McEver, R. P. (1995) P-selectin glycoprotein ligand-1 mediates rolling of human neutrophils on P-selectin, *J Cell Biol 128*, 661-671.
28. Springer, T. A. (1994) Traffic signals for lymphocyte recirculation and leukocyte emigration: the multistep paradigm, *Cell 76*, 301-314.
29. Norman, K. E., Moore, K. L., McEver, R. P., and Ley, K. (1995) Leukocyte rolling in vivo is mediated by P-selectin glycoprotein ligand-1, *Blood 86*, 4417-4421.
30. Weyrich, A. S., McIntyre, T. M., McEver, R. P., Prescott, S. M., and Zimmerman, G. A. (1995) Monocyte tethering by P-selectin regulates monocyte chemotactic protein-1 and tumor necrosis factor-alpha secretion. Signal integration and NF-kappa B translocation, *J Clin Invest 95*, 2297-2303.

31. Elstad, M. R., La Pine, T. R., Cowley, F. S., McEver, R. P., McIntyre, T. M., Prescott, S. M., and Zimmerman, G. A. (1995) P-selectin regulates platelet-activating factor synthesis and phagocytosis by monocytes, *J Immunol 155*, 2109-2122.
32. Patel, K. D., Moore, K. L., Nollert, M. U., and McEver, R. P. (1995) Neutrophils use both shared and distinct mechanisms to adhere to selectins under static and flow conditions, *J Clin Invest 96*, 1887-1896.
33. Kansas, G. S., and Pavalko, F. M. (1996) The cytoplasmic domains of E- and P-selectin do not constitutively interact with alpha-actinin and are not essential for leukocyte adhesion, *J Immunol 157*, 321-325.
34. Takeichi, M. (1977) Functional correlation between cell adhesive properties and some cell surface proteins, *J Cell Biol 75*, 464-474.
35. Lemmon, V., Farr, K. L., and Lagenaur, C. (1989) L1-mediated axon outgrowth occurs via a homophilic binding mechanism, *Neuron 2*, 1597-1603.
36. Williams, E. J., Doherty, P., Turner, G., Reid, R. A., Hemperly, J. J., and Walsh, F. S. (1992) Calcium influx into neurons can solely account for cell contact-dependent neurite outgrowth stimulated by transfected L1, *J Cell Biol 119*, 883-892.
37. Peles, E., Schlessinger, J., and Grumet, M. (1998) Multi-ligand interactions with receptor-like protein tyrosine phosphatase beta: implications for intercellular signaling, *Trends Biochem Sci 23*, 121-124.
38. Peles, E., Nativ, M., Campbell, P. L., Sakurai, T., Martinez, R., Lev, S., Clary, D. O., Schilling, J., Barnea, G., Plowman, G. D., Grumet, M., and Schlessinger, J. (1995) The carbonic anhydrase domain of receptor tyrosine phosphatase beta is a functional ligand for the axonal cell recognition molecule contactin, *Cell 82*, 251-260.
39. Morales, G., Hubert, M., Brummendorf, T., Treubert, U., Tarnok, A., Schwarz, U., and Rathjen, F. G. (1993) Induction of axonal growth by heterophilic interactions between the cell surface recognition proteins F11 and Nr-CAM/Bravo, *Neuron 11*, 1113-1122.
40. Volkmer, H., Leuschner, R., Zacharias, U., and Rathjen, F. G. (1996) Neurofascin induces neurites by heterophilic interactions with axonal NrCAM while NrCAM requires F11 on the axonal surface to extend neurites, *J Cell Biol 135*, 1059-1069.
41. Volkmer, H., Zacharias, U., Norenberg, U., and Rathjen, F. G. (1998) Dissection of complex molecular interactions of neurofascin with axonin-1, F11, and tenascin-R, which promote attachment and neurite formation of tectal cells, *J Cell Biol 142*, 1083-1093.
42. Lustig, M., Sakurai, T., and Grumet, M. (1999) Nr-CAM promotes neurite outgrowth from peripheral ganglia by a mechanism involving axonin-1 as a neuronal receptor, *Dev Biol 209*, 340-351.

43. Kamiguchi, H., Long, K. E., Pendergast, M., Schaefer, A. W., Rapoport, I., Kirchhausen, T., and Lemmon, V. (1998) The neural cell adhesion molecule L1 interacts with the AP-2 adaptor and is endocytosed via the clathrin-mediated pathway, *J Neurosci 18*, 5311-5321.
44. Kamiguchi, H., Hlavin, M. L., Yamasaki, M., and Lemmon, V. (1998) Adhesion molecules and inherited diseases of the human nervous system, *Annu Rev Neurosci 21*, 97-125.
45. Kamiguchi, H., and Lemmon, V. (1998) A neuronal form of the cell adhesion molecule L1 contains a tyrosine-based signal required for sorting to the axonal growth cone, *J Neurosci 18*, 3749-3756.
46. Steinberg, M. S. (1963) Reconstruction of tissues by dissociated cells. Some morphogenetic tissue movements and the sorting out of embryonic cells may have a common explanation, *Science 141*, 401-408.
47. Hynes, R. O. (1987) Integrins: a family of cell surface receptors, *Cell 48*, 549-554.
48. Hynes, R. O., Marcantonio, E. E., Stepp, M. A., Urry, L. A., and Yee, G. H. (1989) Integrin heterodimer and receptor complexity in avian and mammalian cells, *J Cell Biol 109*, 409-420.
49. Hynes, R. O. (2002) A reevaluation of integrins as regulators of angiogenesis, *Nat Med 8*, 918-921.
50. Hynes, R. O. (2002) Integrins: bidirectional, allosteric signaling machines, *Cell 110*, 673-687.
51. Hynes, R. O., Lively, J. C., McCarty, J. H., Taverna, D., Francis, S. E., Hodivala-Dilke, K., and Xiao, Q. (2002) The diverse roles of integrins and their ligands in angiogenesis, *Cold Spring Harb Symp Quant Biol 67*, 143-153.
52. Hynes, R. O. (1992) Integrins: versatility, modulation, and signaling in cell adhesion, *Cell 69*, 11-25.
53. Whittaker, C. A., and Hynes, R. O. (2002) Distribution and evolution of von Willebrand/integrin A domains: widely dispersed domains with roles in cell adhesion and elsewhere, *Mol Biol Cell 13*, 3369-3387.
54. Burke, R. D. (1999) Invertebrate integrins: structure, function, and evolution, *Int Rev Cytol 191*, 257-284.
55. Hughes, A. L. (2001) Evolution of the integrin alpha and beta protein families, *J Mol Evol 52*, 63-72.
56. Hynes, R. O., and Zhao, Q. (2000) The evolution of cell adhesion, *J Cell Biol 150*, F89-96.
57. Humphries, M. J. (2000) Integrin cell adhesion receptors and the concept of agonism, *Trends Pharmacol Sci 21*, 29-32.
58. Humphries, J. D., Askari, J. A., Zhang, X. P., Takada, Y., Humphries, M. J., and Mould, A. P. (2000) Molecular basis of ligand recognition by integrin alpha5beta 1. II. Specificity of arg-gly-Asp binding is

determined by Trp157 OF THE alpha subunit, *J Biol Chem 275*, 20337-20345.
59. Humphries, M. J. (2000) Integrin structure, *Biochem Soc Trans 28*, 311-339.
60. Humphries, M. J. (2002) Insights into integrin-ligand binding and activation from the first crystal structure, *Arthritis Res 4 Suppl 3*, S69-78.
61. Bouvard, D., Brakebusch, C., Gustafsson, E., Aszodi, A., Bengtsson, T., Berna, A., and Fassler, R. (2001) Functional consequences of integrin gene mutations in mice, *Circ Res 89*, 211-223.
62. De Arcangelis, A., and Georges-Labouesse, E. (2000) Integrin and ECM functions: roles in vertebrate development, *Trends Genet 16*, 389-395.
63. Hynes, R. O. (1996) Targeted mutations in cell adhesion genes: what have we learned from them?, *Dev Biol 180*, 402-412.
64. Sheppard, D. (2000) In vivo functions of integrins: lessons from null mutations in mice, *Matrix Biol 19*, 203-209.
65. Hogg, N., and Bates, P. A. (2000) Genetic analysis of integrin function in man: LAD-1 and other syndromes, *Matrix Biol 19*, 211-222.
66. Pulkkinen, L., and Uitto, J. (1999) Mutation analysis and molecular genetics of epidermolysis bullosa, *Matrix Biol 18*, 29-42.
67. Kato, A. (1997) The biologic and clinical spectrum of Glanzmann's thrombasthenia: implications of integrin alpha IIb beta 3 for its pathogenesis, *Crit Rev Oncol Hematol 26*, 1-23.
68. Etzioni, A., Doerschuk, C. M., and Harlan, J. M. (1999) Of man and mouse: leukocyte and endothelial adhesion molecule deficiencies, *Blood 94*, 3281-3288.
69. Shimaoka, M., Takagi, J., and Springer, T. A. (2002) Conformational regulation of integrin structure and function, *Annu Rev Biophys Biomol Struct 31*, 485-516.
70. Vinogradova, O., Velyvis, A., Velyviene, A., Hu, B., Haas, T., Plow, E., and Qin, J. (2002) A structural mechanism of integrin alpha(IIb)beta(3) "inside-out" activation as regulated by its cytoplasmic face, *Cell 110*, 587-597.
71. Garcia-Alvarez, B., Bobkov, A., Sonnenberg, A., and de Pereda, J. M. (2003) Structural and functional analysis of the actin binding domain of plectin suggests alternative mechanisms for binding to F-actin and integrin beta4, *Structure 11*, 615-625.
72. Garcia-Alvarez, B., de Pereda, J. M., Calderwood, D. A., Ulmer, T. S., Critchley, D., Campbell, I. D., Ginsberg, M. H., and Liddington, R. C. (2003) Structural determinants of integrin recognition by talin, *Mol Cell 11*, 49-58.
73. Tadokoro, S., Shattil, S. J., Eto, K., Tai, V., Liddington, R. C., de Pereda, J. M., Ginsberg, M. H., and Calderwood, D. A. (2003) Talin

binding to integrin beta tails: a final common step in integrin activation, *Science 302*, 103-106.
74. Takagi, J., Petre, B. M., Walz, T., and Springer, T. A. (2002) Global conformational rearrangements in integrin extracellular domains in outside-in and inside-out signaling, *Cell 110*, 599-511.
75. Takagi, J., and Springer, T. A. (2002) Integrin activation and structural rearrangement, *Immunol Rev 186*, 141-163.
76. Xiong, J. P., Stehle, T., Goodman, S. L., and Arnaout, M. A. (2003) New insights into the structural basis of integrin activation, *Blood 102*, 1155-1159.
77. Xiong, J. P., Stehle, T., Goodman, S. L., and Arnaout, M. A. (2003) Integrins, cations and ligands: making the connection, *J Thromb Haemost 1*, 1642-1654.
78. Adair, B. D., Xiong, J. P., Maddock, C., Goodman, S. L., Arnaout, M. A., and Yeager, M. (2005) Three-dimensional EM structure of the ectodomain of integrin {alpha}V{beta}3 in a complex with fibronectin, *J Cell Biol 168*, 1109-1118.
79. O'Toole, T. E., Katagiri, Y., Faull, R. J., Peter, K., Tamura, R., Quaranta, V., Loftus, J. C., Shattil, S. J., and Ginsberg, M. H. (1994) Integrin cytoplasmic domains mediate inside-out signal transduction, *J Cell Biol 124*, 1047-1059.
80. O'Toole, T. E., Mandelman, D., Forsyth, J., Shattil, S. J., Plow, E. F., and Ginsberg, M. H. (1991) Modulation of the affinity of integrin alpha IIb beta 3 (GPIIb-IIIa) by the cytoplasmic domain of alpha IIb, *Science 254*, 845-847.
81. Du, X. P., Plow, E. F., Frelinger, A. L., 3rd, O'Toole, T. E., Loftus, J. C., and Ginsberg, M. H. (1991) Ligands "activate" integrin alpha IIb beta 3 (platelet GPIIb-IIIa), *Cell 65*, 409-416.
82. Chen, Y. P., O'Toole, T. E., Shipley, T., Forsyth, J., LaFlamme, S. E., Yamada, K. M., Shattil, S. J., and Ginsberg, M. H. (1994) "Inside-out" signal transduction inhibited by isolated integrin cytoplasmic domains, *J Biol Chem 269*, 18307-18310.
83. Martz, E. (1987) LFA-1 and other accessory molecules functioning in adhesions of T and B lymphocytes, *Hum Immunol 18*, 3-37.
84. Vararattanavech, A., Lin, X., Torres, J., and Tan, S. M. (2009) Disruption of the integrin alphaLbeta2 transmembrane domain interface by beta2 Thr-686 mutation activates alphaLbeta2 and promotes micro-clustering of the alphaL subunits, *J Biol Chem 284*, 3239-3249.
85. Larson, R. S., Corbi, A. L., Berman, L., and Springer, T. (1989) Primary structure of the leukocyte function-associated molecule-1 alpha subunit: an integrin with an embedded domain defining a protein superfamily, *J Cell Biol 108*, 703-712.

86. Kishimoto, T. K., Larson, R. S., Corbi, A. L., Dustin, M. L., Staunton, D. E., and Springer, T. A. (1989) The leukocyte integrins, *Adv Immunol 46*, 149-182.
87. Arnaout, M. A. (1990) Structure and function of the leukocyte adhesion molecules CD11/CD18, *Blood 75*, 1037-1050.
88. Staunton, D. E., Dustin, M. L., and Springer, T. A. (1989) Functional cloning of ICAM-2, a cell adhesion ligand for LFA-1 homologous to ICAM-1, *Nature 339*, 61-64.
89. Dustin, M. L., Garcia-Aguilar, J., Hibbs, M. L., Larson, R. S., Stacker, S. A., Staunton, D. E., Wardlaw, A. J., and Springer, T. A. (1989) Structure and regulation of the leukocyte adhesion receptor LFA-1 and its counterreceptors, ICAM-1 and ICAM-2, *Cold Spring Harb Symp Quant Biol 54 Pt 2*, 753-765.
90. Staunton, D. E., Merluzzi, V. J., Rothlein, R., Barton, R., Marlin, S. D., and Springer, T. A. (1989) A cell adhesion molecule, ICAM-1, is the major surface receptor for rhinoviruses, *Cell 56*, 849-853.
91. Dustin, M. L., and Springer, T. A. (1989) T-cell receptor cross-linking transiently stimulates adhesiveness through LFA-1, *Nature 341*, 619-624.
92. Springer, T. A. (1990) Adhesion receptors of the immune system, *Nature 346*, 425-434.
93. Springer, T. A. (1990) Leucocyte adhesion to cells, *Scand J Immunol 32*, 211-216.
94. Diamond, M. S., Staunton, D. E., de Fougerolles, A. R., Stacker, S. A., Garcia-Aguilar, J., Hibbs, M. L., and Springer, T. A. (1990) ICAM-1 (CD54): a counter-receptor for Mac-1 (CD11b/CD18), *J Cell Biol 111*, 3129-3139.
95. Marlin, S. D., and Springer, T. A. (1987) Purified intercellular adhesion molecule-1 (ICAM-1) is a ligand for lymphocyte function-associated antigen 1 (LFA-1), *Cell 51*, 813-819.
96. McDowall, A., Inwald, D., Leitinger, B., Jones, A., Liesner, R., Klein, N., and Hogg, N. (2003) A novel form of integrin dysfunction involving beta1, beta2, and beta3 integrins, *J Clin Invest 111*, 51-60.
97. Arnaout, M. A. (1990) Leukocyte adhesion molecules deficiency: its structural basis, pathophysiology and implications for modulating the inflammatory response, *Immunol Rev 114*, 145-180.
98. Kishimoto, T. K., Hollander, N., Roberts, T. M., Anderson, D. C., and Springer, T. A. (1987) Heterogeneous mutations in the beta subunit common to the LFA-1, Mac-1, and p150,95 glycoproteins cause leukocyte adhesion deficiency, *Cell 50*, 193-202.
99. Anderson, D. C., and Springer, T. A. (1987) Leukocyte adhesion deficiency: an inherited defect in the Mac-1, LFA-1, and p150,95 glycoproteins, *Annu Rev Med 38*, 175-194.

100. Etzioni, A., Frydman, M., Pollack, S., Avidor, I., Phillips, M. L., Paulson, J. C., and Gershoni-Baruch, R. (1992) Brief report: recurrent severe infections caused by a novel leukocyte adhesion deficiency, *N Engl J Med 327*, 1789-1792.
101. Kinashi, T., Aker, M., Sokolovsky-Eisenberg, M., Grabovsky, V., Tanaka, C., Shamri, R., Feigelson, S., Etzioni, A., and Alon, R. (2004) LAD-III, a leukocyte adhesion deficiency syndrome associated with defective Rap1 activation and impaired stabilization of integrin bonds, *Blood 103*, 1033-1036.
102. Etzioni, A., and Alon, R. (2004) Leukocyte adhesion deficiency III: a group of integrin activation defects in hematopoietic lineage cells, *Curr Opin Allergy Clin Immunol 4*, 485-490.
103. Pribila, J. T., Quale, A. C., Mueller, K. L., and Shimizu, Y. (2004) Integrins and T cell-mediated immunity, *Annu Rev Immunol 22*, 157-180.
104. Zhou, X., Li, J., and Kucik, D. F. (2001) The microtubule cytoskeleton participates in control of beta2 integrin avidity, *J Biol Chem 276*, 44762-44769.
105. Xiong, J. P., Stehle, T., Diefenbach, B., Zhang, R., Dunker, R., Scott, D. L., Joachimiak, A., Goodman, S. L., and Arnaout, M. A. (2001) Crystal structure of the extracellular segment of integrin alpha Vbeta3, *Science 294*, 339-345.
106. Xiong, J. P., Stehle, T., Zhang, R., Joachimiak, A., Frech, M., Goodman, S. L., and Arnaout, M. A. (2002) Crystal structure of the extracellular segment of integrin alpha Vbeta3 in complex with an Arg-Gly-Asp ligand, *Science 296*, 151-155.
107. Shimaoka, M., and Springer, T. A. (2003) Therapeutic antagonists and conformational regulation of integrin function, *Nat Rev Drug Discov 2*, 703-716.
108. Shimaoka, M., Xiao, T., Liu, J. H., Yang, Y., Dong, Y., Jun, C. D., McCormack, A., Zhang, R., Joachimiak, A., Takagi, J., Wang, J. H., and Springer, T. A. (2003) Structures of the alpha L I domain and its complex with ICAM-1 reveal a shape-shifting pathway for integrin regulation, *Cell 112*, 99-111.
109. Hogg, N., Clive Landis, R., Bates, P. A., Stanley, P., and Randi, A. M. (1994) The sticking point: How integrins bind to their ligands, *Trends Cell Biol 4*, 379-382.
110. Stewart, M. P., Cabanas, C., and Hogg, N. (1996) T cell adhesion to intercellular adhesion molecule-1 (ICAM-1) is controlled by cell spreading and the activation of integrin LFA-1, *J Immunol 156*, 1810-1817.
111. Woska, J. R., Jr., Shih, D., Taqueti, V. R., Hogg, N., Kelly, T. A., and Kishimoto, T. K. (2001) A small-molecule antagonist of LFA-1 blocks

a conformational change important for LFA-1 function, *J Leukoc Biol 70*, 329-334.
112. Ganpule, G., Knorr, R., Miller, J. M., Carron, C. P., and Dustin, M. L. (1997) Low affinity of cell surface lymphocyte function-associated antigen-1 (LFA-1) generates selectivity for cell-cell interactions, *J Immunol 159*, 2685-2692.
113. Ma, Q., Shimaoka, M., Lu, C., Jing, H., Carman, C. V., and Springer, T. A. (2002) Activation-induced conformational changes in the I domain region of lymphocyte function-associated antigen 1, *J Biol Chem 277*, 10638-10641.
114. Drbal, K., Angelisova, P., Hilgert, I., Cerny, J., Novak, P., and Horejsi, V. (2001) A proteolytically truncated form of free CD18, the common chain of leukocyte integrins, as a novel marker of activated myeloid cells, *Blood 98*, 1561-1566.
115. Hogg, N., Bennett, R., Cabanas, C., and Dransfield, I. (1992) Leukocyte integrin activation, *Kidney Int 41*, 613-616.
116. Dransfield, I., Cabanas, C., Barrett, J., and Hogg, N. (1992) Interaction of leukocyte integrins with ligand is necessary but not sufficient for function, *J Cell Biol 116*, 1527-1535.
117. Hogg, N., Harvey, J., Cabanas, C., and Landis, R. C. (1993) Control of leukocyte integrin activation, *Am Rev Respir Dis 148*, S55-59.
118. Cabanas, C., and Hogg, N. (1993) Ligand intercellular adhesion molecule 1 has a necessary role in activation of integrin lymphocyte function-associated molecule 1, *Proc Natl Acad Sci U S A 90*, 5838-5842.
119. Beals, C. R., Edwards, A. C., Gottschalk, R. J., Kuijpers, T. W., and Staunton, D. E. (2001) CD18 activation epitopes induced by leukocyte activation, *J Immunol 167*, 6113-6122.
120. Lollo, B. A., Chan, K. W., Hanson, E. M., Moy, V. T., and Brian, A. A. (1993) Direct evidence for two affinity states for lymphocyte function-associated antigen 1 on activated T cells, *J Biol Chem 268*, 21693-21700.
121. Rothlein, R., and Springer, T. A. (1986) The requirement for lymphocyte function-associated antigen 1 in homotypic leukocyte adhesion stimulated by phorbol ester, *J Exp Med 163*, 1132-1149.
122. Patarroyo, M., Beatty, P. G., Fabre, J. W., and Gahmberg, C. G. (1985) Identification of a cell surface protein complex mediating phorbol ester-induced adhesion (binding) among human mononuclear leukocytes, *Scand J Immunol 22*, 171-182.
123. Patarroyo, M., and Jondal, M. (1985) Phorbol ester-induced adhesion (binding) among human mononuclear leukocytes requires extracellular Mg++ and is sensitive to protein kinase C, lipoxygenase, and ATPase inhibitors, *Immunobiology 170*, 305-319.

124. Patarroyo, M., Beatty, P. G., Serhan, C. N., and Gahmberg, C. G. (1985) Identification of a cell-surface glycoprotein mediating adhesion in human granulocytes, *Scand J Immunol 22*, 619-631.
125. Dransfield, I., and Hogg, N. (1989) Regulated expression of Mg2+ binding epitope on leukocyte integrin alpha subunits, *EMBO J 8*, 3759-3765.
126. Dransfield, I., Cabanas, C., Craig, A., and Hogg, N. (1992) Divalent cation regulation of the function of the leukocyte integrin LFA-1, *J Cell Biol 116*, 219-226.
127. Buyon, J. P., Slade, S. G., Reibman, J., Abramson, S. B., Philips, M. R., Weissmann, G., and Winchester, R. (1990) Constitutive and induced phosphorylation of the alpha- and beta-chains of the CD11/CD18 leukocyte integrin family. Relationship to adhesion-dependent functions, *J Immunol 144*, 191-197.
128. Merrill, J. T., Slade, S. G., Weissmann, G., Winchester, R., and Buyon, J. P. (1990) Two pathways of CD11b/CD18-mediated neutrophil aggregation with different involvement of protein kinase C-dependent phosphorylation, *J Immunol 145*, 2608-2615.
129. Pardi, R., Inverardi, L., Rugarli, C., and Bender, J. R. (1992) Antigen-receptor complex stimulation triggers protein kinase C-dependent CD11a/CD18-cytoskeleton association in T lymphocytes, *J Cell Biol 116*, 1211-1220.
130. Cairo, C. W., Mirchev, R., and Golan, D. E. (2006) Cytoskeletal regulation couples LFA-1 conformational changes to receptor lateral mobility and clustering, *Immunity 25*, 297-308.
131. Kucik, D. F., Dustin, M. L., Miller, J. M., and Brown, E. J. (1996) Adhesion-activating phorbol ester increases the mobility of leukocyte integrin LFA-1 in cultured lymphocytes, *J Clin Invest 97*, 2139-2144.
132. Litvinov, R. I., Vilaire, G., Li, W., DeGrado, W. F., Weisel, J. W., and Bennett, J. S. (2006) Activation of individual alphaIIbbeta3 integrin molecules by disruption of transmembrane domain interactions in the absence of clustering, *Biochemistry 45*, 4957-4964.
133. Yin, H., Litvinov, R. I., Vilaire, G., Zhu, H., Li, W., Caputo, G. A., Moore, D. T., Lear, J. D., Weisel, J. W., Degrado, W. F., and Bennett, J. S. (2006) Activation of platelet alphaIIbbeta3 by an exogenous peptide corresponding to the transmembrane domain of alphaIIb, *J Biol Chem 281*, 36732-36741.
134. Weber, K. S., Klickstein, L. B., and Weber, C. (1999) Specific activation of leukocyte beta2 integrins lymphocyte function-associated antigen-1 and Mac-1 by chemokines mediated by distinct pathways via the alpha subunit cytoplasmic domains, *Mol Biol Cell 10*, 861-873.
135. Jin, T., and Li, J. (2002) Dynamitin controls Beta 2 integrin avidity by modulating cytoskeletal constraint on integrin molecules, *J Biol Chem 277*, 32963-32969.

136. Crucian, B., Nelman-Gonzalez, M., and Sams, C. (2006) Rapid flow cytometry method for quantitation of LFA-1-adhesive T cells, *Clin Vaccine Immunol 13*, 403-408.
137. Litvinov, R. I., Nagaswami, C., Vilaire, G., Shuman, H., Bennett, J. S., and Weisel, J. W. (2004) Functional and structural correlations of individual alphaIIbbeta3 molecules, *Blood 104*, 3979-3985.
138. Li, R., Mitra, N., Gratkowski, H., Vilaire, G., Litvinov, R., Nagasami, C., Weisel, J. W., Lear, J. D., DeGrado, W. F., and Bennett, J. S. (2003) Activation of integrin alphaIIbbeta3 by modulation of transmembrane helix associations, *Science 300*, 795-798.
139. Kim, M., Carman, C. V., and Springer, T. A. (2003) Bidirectional transmembrane signaling by cytoplasmic domain separation in integrins, *Science 301*, 1720-1725.
140. Fox, J. E., Shattil, S. J., Kinlough-Rathbone, R. L., Richardson, M., Packham, M. A., and Sanan, D. A. (1996) The platelet cytoskeleton stabilizes the interaction between alphaIIbbeta3 and its ligand and induces selective movements of ligand-occupied integrin, *J Biol Chem 271*, 7004-7011.
141. Li, R., Gorelik, R., Nanda, V., Law, P. B., Lear, J. D., DeGrado, W. F., and Bennett, J. S. (2004) Dimerization of the transmembrane domain of Integrin alphaIIb subunit in cell membranes, *J Biol Chem 279*, 26666-26673.
142. Li, W., Metcalf, D. G., Gorelik, R., Li, R., Mitra, N., Nanda, V., Law, P. B., Lear, J. D., Degrado, W. F., and Bennett, J. S. (2005) A push-pull mechanism for regulating integrin function, *Proc Natl Acad Sci U S A 102*, 1424-1429.
143. Auerbach, D., Thaminy, S., Hottiger, M. O., and Stagljar, I. (2002) The post-genomic era of interactive proteomics: facts and perspectives, *Proteomics 2*, 611-623.
144. Yin, H. (2008) Exogenous agents that target transmembrane domains of proteins, *Angew Chem Int Ed Engl 47*, 2744-2752.
145. Almen, M. S., Nordstrom, K. J., Fredriksson, R., and Schioth, H. B. (2009) Mapping the human membrane proteome: a majority of the human membrane proteins can be classified according to function and evolutionary origin, *BMC Biol 7*, 50.
146. Mingarro, I., von Heijne, G., and Whitley, P. (1997) Membrane-protein engineering, *Trends Biotechnol 15*, 432-437.
147. Mingarro, I., Elofsson, A., and von Heijne, G. (1997) Helix-helix packing in a membrane-like environment, *J Mol Biol 272*, 633-641.
148. Lau, T. L., Partridge, A. W., Ginsberg, M. H., and Ulmer, T. S. (2008) Structure of the integrin beta3 transmembrane segment in phospholipid bicelles and detergent micelles, *Biochemistry 47*, 4008-4016.
149. Li, R., Babu, C. R., Valentine, K., Lear, J. D., Wand, A. J., Bennett, J. S., and DeGrado, W. F. (2002) Characterization of the monomeric

form of the transmembrane and cytoplasmic domains of the integrin beta 3 subunit by NMR spectroscopy, *Biochemistry 41*, 15618-15624.
150. Arora, A., Abildgaard, F., Bushweller, J. H., and Tamm, L. K. (2001) Structure of outer membrane protein A transmembrane domain by NMR spectroscopy, *Nat Struct Biol 8*, 334-338.
151. Zhu, H., Metcalf, D. G., Streu, C. N., Billings, P. C., Degrado, W. F., and Bennett, J. S. (2010) Specificity for homooligomer versus heterooligomer formation in integrin transmembrane helices, *J Mol Biol 401*, 882-891.
152. Li, R., Babu, C. R., Lear, J. D., Wand, A. J., Bennett, J. S., and DeGrado, W. F. (2001) Oligomerization of the integrin alphaIIbbeta3: roles of the transmembrane and cytoplasmic domains, *Proc Natl Acad Sci U S A 98*, 12462-12467.
153. Schneider, D., and Engelman, D. M. (2004) Involvement of transmembrane domain interactions in signal transduction by alpha/beta integrins, *J Biol Chem 279*, 9840-9846.
154. DeGrado, W. F., Gratkowski, H., and Lear, J. D. (2003) How do helix-helix interactions help determine the folds of membrane proteins? Perspectives from the study of homo-oligomeric helical bundles, *Protein Sci 12*, 647-665.
155. Tarasova, N. I., Rice, W. G., and Michejda, C. J. (1999) Inhibition of G-protein-coupled receptor function by disruption of transmembrane domain interactions, *J Biol Chem 274*, 34911-34915.
156. Tarasova, N. I., Seth, R., Tarasov, S. G., Kosakowska-Cholody, T., Hrycyna, C. A., Gottesman, M. M., and Michejda, C. J. (2005) Transmembrane inhibitors of P-glycoprotein, an ABC transporter, *J Med Chem 48*, 3768-3775.
157. Russ, W. P., and Engelman, D. M. (2000) The GxxxG motif: a framework for transmembrane helix-helix association, *J Mol Biol 296*, 911-919.
158. Schneider, D., and Engelman, D. M. (2003) GALLEX, a measurement of heterologous association of transmembrane helices in a biological membrane, *J Biol Chem 278*, 3105-3111.
159. Russ, W. P., and Engelman, D. M. (1999) TOXCAT: a measure of transmembrane helix association in a biological membrane, *Proc Natl Acad Sci U S A 96*, 863-868.
160. Kolmar, H., Hennecke, F., Gotze, K., Janzer, B., Vogt, B., Mayer, F., and Fritz, H. J. (1995) Membrane insertion of the bacterial signal transduction protein ToxR and requirements of transcription activation studied by modular replacement of different protein substructures, *EMBO J 14*, 3895-3904.
161. Langosch, D., Brosig, B., Kolmar, H., and Fritz, H. J. (1996) Dimerisation of the glycophorin A transmembrane segment in

membranes probed with the ToxR transcription activator, *J Mol Biol 263*, 525-530.
162. Hurwitz, E., Klapper, L. N., Wilchek, M., Yarden, Y., and Sela, M. (2000) Inhibition of tumor growth by poly(ethylene glycol) derivatives of anti-ErbB2 antibodies, *Cancer Immunol Immunother 49*, 226-234.
163. Gerber, D., Sal-Man, N., and Shai, Y. (2004) Two motifs within a transmembrane domain, one for homodimerization and the other for heterodimerization, *J Biol Chem 279*, 21177-21182.
164. Gerber, D., and Shai, Y. (2001) In vivo detection of hetero-association of glycophorin-A and its mutants within the membrane, *J Biol Chem 276*, 31229-31232.
165. Gerber, D., and Shai, Y. (2002) Chirality-independent protein-protein recognition between transmembrane domains in vivo, *J Mol Biol 322*, 491-495.
166. Kim, S., Jeon, T. J., Oberai, A., Yang, D., Schmidt, J. J., and Bowie, J. U. (2005) Transmembrane glycine zippers: physiological and pathological roles in membrane proteins, *Proc Natl Acad Sci U S A 102*, 14278-14283.
167. Porte, D., Oertel-Buchheit, P., Granger-Schnarr, M., and Schnarr, M. (1995) Fos leucine zipper variants with increased association capacity, *J Biol Chem 270*, 22721-22730.
168. Schnarr, M., Oertel-Buchheit, P., Kazmaier, M., and Granger-Schnarr, M. (1991) DNA binding properties of the LexA repressor, *Biochimie 73*, 423-431.
169. Dmitrova, M., Younes-Cauet, G., Oertel-Buchheit, P., Porte, D., Schnarr, M., and Granger-Schnarr, M. (1998) A new LexA-based genetic system for monitoring and analyzing protein heterodimerization in Escherichia coli, *Mol Gen Genet 257*, 205-212.
170. Zhao, T. X., Martinko, A. J., Le, V. H., Zhao, J., and Yin, H. (2010) Development of agents that modulate protein-protein interactions in membranes, *Curr Pharm Des 16*, 1055-1062.
171. Slivka, P. F., Wong, J., Caputo, G. A., and Yin, H. (2008) Peptide probes for protein transmembrane domains, *ACS Chem Biol 3*, 402-411.
172. Kortemme, T., and Baker, D. (2004) Computational design of protein-protein interactions, *Curr Opin Chem Biol 8*, 91-97.
173. Kang, S. G., and Saven, J. G. (2007) Computational protein design: structure, function and combinatorial diversity, *Curr Opin Chem Biol 11*, 329-334.
174. Shifman, J. M., and Mayo, S. L. (2003) Exploring the origins of binding specificity through the computational redesign of calmodulin, *Proc Natl Acad Sci U S A 100*, 13274-13279.
175. Reina, J., Lacroix, E., Hobson, S. D., Fernandez-Ballester, G., Rybin, V., Schwab, M. S., Serrano, L., and Gonzalez, C. (2002) Computer-

aided design of a PDZ domain to recognize new target sequences, *Nat Struct Biol 9*, 621-627.
176. Ogihara, N. L., Ghirlanda, G., Bryson, J. W., Gingery, M., DeGrado, W. F., and Eisenberg, D. (2001) Design of three-dimensional domain-swapped dimers and fibrous oligomers, *Proc Natl Acad Sci U S A 98*, 1404-1409.
177. Partridge, A. W., Liu, S., Kim, S., Bowie, J. U., and Ginsberg, M. H. (2005) Transmembrane domain helix packing stabilizes integrin alphaIIbbeta3 in the low affinity state, *J Biol Chem 280*, 7294-7300.
178. Luo, B. H., Springer, T. A., and Takagi, J. (2004) A specific interface between integrin transmembrane helices and affinity for ligand, *PLoS Biol 2*, e153.
179. Gottschalk, K. E. (2005) A coiled-coil structure of the alphaIIbbeta3 integrin transmembrane and cytoplasmic domains in its resting state, *Structure 13*, 703-712.
180. Yin, H., Slusky, J. S., Berger, B. W., Walters, R. S., Vilaire, G., Litvinov, R. I., Lear, J. D., Caputo, G. A., Bennett, J. S., and DeGrado, W. F. (2007) Computational design of peptides that target transmembrane helices, *Science 315*, 1817-1822.
181. Caputo, G. A., Litvinov, R. I., Li, W., Bennett, J. S., Degrado, W. F., and Yin, H. (2008) Computationally designed peptide inhibitors of protein-protein interactions in membranes, *Biochemistry 47*, 8600-8606.
182. Hebert, T. E., Moffett, S., Morello, J. P., Loisel, T. P., Bichet, D. G., Barret, C., and Bouvier, M. (1996) A peptide derived from a beta2-adrenergic receptor transmembrane domain inhibits both receptor dimerization and activation, *J Biol Chem 271*, 16384-16392.
183. Baldwin, J. M. (1993) The probable arrangement of the helices in G protein-coupled receptors, *EMBO J 12*, 1693-1703.
184. Anand-Srivastava, M. B., Sehl, P. D., and Lowe, D. G. (1996) Cytoplasmic domain of natriuretic peptide receptor-C inhibits adenylyl cyclase. Involvement of a pertussis toxin-sensitive G protein, *J Biol Chem 271*, 19324-19329.
185. Merkouris, M., Dragatsis, I., Megaritis, G., Konidakis, G., Zioudrou, C., Milligan, G., and Georgoussi, Z. (1996) Identification of the critical domains of the delta-opioid receptor involved in G protein coupling using site-specific synthetic peptides, *Mol Pharmacol 50*, 985-993.
186. Lee, C. H. (2004) Reversing agents for ATP-binding cassette (ABC) transporters: application in modulating multidrug resistance (MDR), *Curr Med Chem Anticancer Agents 4*, 43-52.
187. Stein, W. D., Bates, S. E., and Fojo, T. (2004) Intractable cancers: the many faces of multidrug resistance and the many targets it presents for therapeutic attack, *Curr Drug Targets 5*, 333-346.

188. Leonard, G. D., Fojo, T., and Bates, S. E. (2003) The role of ABC transporters in clinical practice, *Oncologist 8*, 411-424.
189. Locher, K. P., Lee, A. T., and Rees, D. C. (2002) The E. coli BtuCD structure: a framework for ABC transporter architecture and mechanism, *Science 296*, 1091-1098.
190. Chang, G., and Roth, C. B. (2001) Structure of MsbA from E. coli: a homolog of the multidrug resistance ATP binding cassette (ABC) transporters, *Science 293*, 1793-1800.
191. Popot, J. L., and Engelman, D. M. (1990) Membrane protein folding and oligomerization: the two-stage model, *Biochemistry 29*, 4031-4037.
192. Popot, J. L., and Engelman, D. M. (2000) Helical membrane protein folding, stability, and evolution, *Annu Rev Biochem 69*, 881-922.
193. Schneider, D., and Engelman, D. M. (2004) Motifs of two small residues can assist but are not sufficient to mediate transmembrane helix interactions, *J Mol Biol 343*, 799-804.
194. Ladokhin, A. S., and White, S. H. (2004) Interfacial folding and membrane insertion of a designed helical peptide, *Biochemistry 43*, 5782-5791.
195. Mehrabi, D., DiCarlo, J. B., Soon, S. L., and McCall, C. O. (2002) Advances in the management of psoriasis: monoclonal antibody therapies, *Int J Dermatol 41*, 827-835.
196 Cairo, C.W. and Golan, D.E. (2008) T cell adhesion mechanisms revealed by receptor lateral mobility. *Biopolymers 5*, 409-19.

CHAPTER TWO

SYNTHESIS AND CHARACTERIZATION OF EGFP-B2 TM CONSTRUCTS[1, 2, 3]

[1] We acknowledge Dr. Sandra Marcus, Biological Services, Department of Chemistry, University of Alberta for training on molecular biology techniques, provision of pBAD-His vector, *E. coli* strain LMG148, and helpful discussions.

[2] We acknowledge Dr. Robert E. Campbell, Department of Chemistry, University of Alberta, for provision of the EGFP gene in the pBAD-His vector.

[3] We acknowledge Flow cytometry instrument access from Dr. James Stafford, Department of Biological Sciences, University of Alberta.

2.1. INTRODUCTION

About one third of eukaryotic and prokaryotic proteins are membrane associated or transmembrane proteins(1). Generally, transmembrane proteins consist of an extracellular portion, known as the ectodomain, and a hydrophobic membrane buried region, known as the transmembrane (TM) domain, which links the ectodomain to a cytoplasmic domain. TM proteins can be single-pass, with just a single membrane-spanning portion or multiple-pass with numerous portions spanning the membrane. Single pass TM proteins can be Type I, II or III while multiple-pass TM proteins are classified as Type IV. Type I proteins are anchored via a stop-transfer anchor sequence to the membrane orientating the protein during translocation with their *N*-terminus facing the endoplasmic recticulum (ER) lumen. Type II TM proteins are anchored using a signal-anchor with their *N*-terminus facing the cytosolic compartment. Type III TM proteins are anchored with a signal-anchor but their *N*-terminus is oriented to face the extracellular compartment. Type IV TM can either be IVa with their *N*-terminus targeted to the cytosol or IVb when they have their *N*-terminus in the extracellular lumen (2). Studies of TM proteins are challenging due to issues with solubility and aggregation. TM proteins are known to be the targets for over 60% of available pharmaceuticals (3). Thus, understanding TM proteins becomes critical as the design and exploitation of exogenous agents that specifically target TM domains of proteins could provide new therapeutic strategies. (3-5). This arena already

forms the basis for the development of new therapeutics proven beneficial in animal models (6-8).

As discussed in Chapter 1, conventional methods that have been used in studying TM proteins include mutational, structural studies, and the use of synthetic peptides to disrupt receptor function (3, 9). Synthetic peptides that mimic the TM domains of the G-protein–coupled receptors (GPCRs) have been shown to specifically inhibit signaling and the *in vitro* replication of HIV-1 (9-10). Michejda *et al*. used synthetic peptides derived from the TM domains of GPCR (TM2) to disrupt the function of receptors (10). This resulted from the synthetic peptide binding and inserting into the membrane, thereby competing with the actual TM domain. Another approach has been the use of computed helical anti-membrane protein (CHAMP) (5, 9, 11). Previous studies on the TM domains of the ErbB receptor or epidermal growth factor receptor (EGFR) family indicated that the TM contains two GXXXG-like motifs implicated in the formation of homo and heterodimers in the ErbB1 and ErbB2 receptor (4-5, 9, 12). Mutation of a Thr residue in the GXXXG motif found in the TM domain of β_2 integrin has been shown to be crucial for dimerization of the integrin TM (12). CHAMP generated peptides have been used to target the α-subunit of the platelet integrin $\alpha_{IIb}\beta_3$ (13-14). TM domains of peptides tend to form homodimers in lipid micelles and in *E. coli* membranes (15).

LFA-1 is a receptor expressed exclusively on leukocytes and is involved in leukocyte recruitment and trafficking. LFA-1 is formed by the heterodimeric

association of the α_L and β_2 integrin TM domains on the surface of T cells. Like many other integrins, this heterodimerization is important in maintaining the receptor in its inactive state on cell surface. Disruption of the association has been observed during integrin-mediated activation in the platelet $\alpha_{IIb}\beta_3$ and a similar phenomenon has been observed in $\alpha_L\beta_2$ integrin using structural and mutational analysis.

LFA-1 is constitutively expressed on the surface of T lymphocytes. LFA-1 is a receptor involved in a number of immunological processes in the body involving cell-cell adhesion, cell-ECM interaction and has equally been associated with diseases including human leukocyte adhesion deficiency, bovine leukocyte adhesion deficiency and chronic inflammatory diseases such as arthritis, psoriasis, and asthma. Binding of LFA-1 to its counter-receptor, the intercellular adhesion molecule (ICAM) 1-3 is crucial in mediating immune response. During leukocyte trafficking, T cells adhere to blood endothelia using LFA-1 receptors. This leads to an arrest of T lymphocytes at the site of signal initiation with subsequent extravasation and finally the propagation of the immune response.

2.2. HYPOTHESIS

We proposed that fluorescent proteins containing the TM domain of the β_2 integrin would bind or insert and interfere with the function of LFA-1 on the cell surface of lymphocytes. The inclusion of EGFP in these molecules will allow fluorescence microscopy or flow cytometry (FC) to be used for detection of

binding. We hypothesized that if the β_2-TM proteins disrupt LFA-1 function, they should bind to the cells with high affinity.

In this chapter we discuss the engineering of the EGFP-β_2 TM constructs, their purification and characterization, and their binding to an LFA-1 (+) cell line, Jurkat lymphocytes. These proteins are recombinantly expressed with an *N*-terminal EGFP, thus providing a convenient label for detection and EGFP would enhance the solubility of the chimeric proteins cognizance of the hydrophocity of the fused TM proteins. We wanted to study the effect of a short segment of the cytoplasmic domain of β_2 integrin on binding to the cells. Furthermore, since the TM domain of interest is considerably longer compared to synthetic peptides that have been used in similar studies, we designed some proteins with truncations. We generated four proteins with lengths of 23, 28, 33, and 45 amino acid (a.a.) residues (excluding the EGFP tag). The peptide designated EGFPβ_2TM+CD (45 a.a.) was expressed from the gene encoding 10 a.a. of the β_2 tail domain, the whole TM domain and 12 a.a. of the cytoplasmic domain. The EGFPβ_2TM-CD protein contains a truncation of the 12 a.a. cytoplasmic domain. The EGFPβ_2TM-5B is derived from truncation of 15 base pairs (bp) from the 3' end of the gene for the TM domain. The last variant made was a truncation of 30 bp from the 3' end of the gene for the TM domain of β_2 integrin.

We describe the use of these proteins to label Jurkat cells. We decided to use molecular biology approach in engineering these proteins due to the limitations associated with using solid phase peptide synthesis in generating

hydrophobic proteins of greater than 26 a.a. residues. To the best of our knowledge, this is the first work that has been done on TM protein using recombinant proteins expressed in bacterial systems. We have used recombinant fluorescent protein tags carrying the β_2-TM domain, and truncated variants, to label Jurkat cells (clone E6.1) which expresses the lymphocyte function association-antigen-1 (LFA-1) receptors on their surfaces.

2.3. RESULTS

2.3.1. Design and synthesis of the β_2-TM genes

The genes for the fluorescent protein tags were constructed by PCR amplification of the gene for the TM domain of the β_2 integrin downstream from the gene for enhanced green fluorescent protein (EGFP). The resulting gene would express an *N*-terminal EGFP protein with a *C*-terminal β_2 integrin TM.

The sequence for the β_2 integrin target region and the gene is outlined for all the recombinant proteins shown below in Figure 2.1 (16). Figure A1 (appendix section) shows the full sequence of the proteins and the different a.a. truncated. We introduced a mutation (C695S) of the integrin β_2 tail domain to prevent the formation of disulfide bonds. In effect, we were attaching a 45 a.a. peptide on to the *C*-terminus of the EGFP protein with the whole TM region of the β_2 integrin (23 a.a.) sandwiched between 10 a.a. of the tail domain, and 12 a.a. of the cytoplasmic domain. We fused the peptide at its *N*-terminus so that the EGFP end of the recombinant protein would be expressed in the extracellular lumen as LFA-

1 is a Type I TM protein. This design will allow us to study the effect of the cytoplasmic tail on the binding of the protein to the cell membrane and also investigate the effect of the different lengths of the proteins on binding. This peptide is considerably longer when compared to synthetic peptides that have been employed in similar studies ranging from 18 – 26 a.a. (4, 10, 13-14).

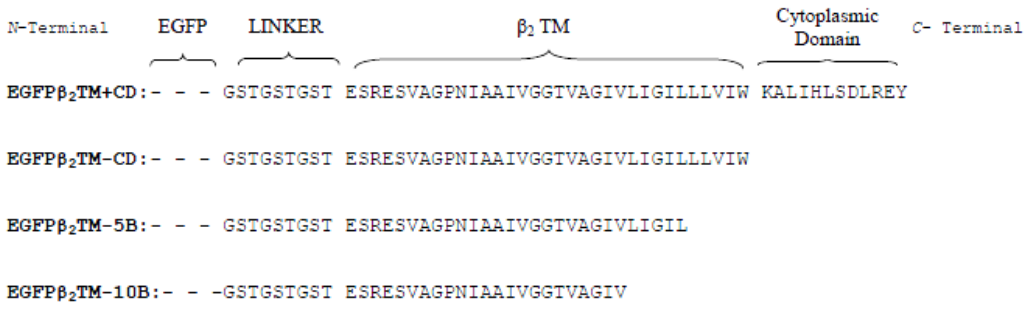

Figure 2.1: EGFPβ$_2$-TM recombinant proteins

All of the β$_2$-TM proteins have an *N*-terminal EGFP linked via a 9-mer linker (GSTGSTGST) at the β$_2$-TM. The linker is designed to enhance the solubility of the peptides.

2.3.1.1. The pBAD/His A, B and C vector

The pBAD vector is a pBR332-derived expression vector that has been engineered for the expression and purification of recombinant proteins in *E. coli* (*64*). The vector utilizes the araBAD promoter (pBAD) which optimizes the yield of soluble protein expressed. It also includes an AraC cassette which regulates the P_{BAD} promoter. The P_{BAD} expression is induced in the presence of L-arabinose, whose concentration is critical in optimizing the yield of soluble protein. The protein includes an *N*-terminal poly-histidine tag which forms the basis for the

purification of proteins using immobilized metal affinity chromatography with Ni-NTA resins. In addition, there is an ampicillin resistant gene (β-lactamase) which provides for easy selection of plasmid in *E. coli*.

2.3.1.2. Synthesis of recombinant genes

The gene coding for the EGFP protein (*egfp* (gene A)) was provided within the Xho I and EcoR I restriction enzyme (RE) sites of the multiple cloning (MC) site of the pBAD-His vector. This is in frame with the poly-histidine sequence for easy purification of the expressed protein.

The gene for the recombinant EGFP β_2 TM with a short cytoplasmic tail gene (*egfp$\beta_2$tm+cd*) (gene B) was synthesized from the *egfp* and the *ksiβ_2* gene (synthetic fusion of the β_2 TM with the bacterial Ketosteroid isomerase protein) templates by polymerase chain reaction (PCR). PCR amplification of the gene was achieved using four primers; two outer primers A and D and two inner primers B and C. The EGFP protein was linked to the β_2 integrin via a 9-mer consisting of the amino acids GSTGSTGST. The resulting construct, *egfp-linker-β_2-TM* would be used for the expression of the EGFPβ_2TM+CD protein. The gene for recombinant EGFP β_2 transmembrane without the short cytoplasmic tail gene (*egfp$\beta_2$tm-cd*) (gene C) was constructed in a like manner from the *egfp* and *ksiβ_2* genes using four primers A, B, C and EGFPTM-CD (acting as D). *egfp$\beta_2$tm-cd* was made to exclude the short cytoplasmic tail of the β_2 integrin. Using the same template the gene for the recombinant EGFP β_2 with truncation of five amino acid residues (15 bp) from the *C*-terminus of the TM domain (*egfp$\beta_2$tm-5b*) (gene D),

was PCR amplified using primers A, B, C and EGFPTM-5B. The gene for the recombinant EGFP β_2 with truncation of ten a.a. residues (30 bp) from the *C*-terminus of the TM domain (*egfp$\beta_2$tm-10b*) (gene E) was the PCR amplification product of genes 1 and 5. Gene 5 was made by PCR amplification of *ksiβ_2* gene template with primers C and EGFPTM-10B.

2.4. EXPRESSION OF GENES AND PURIFICATION OF PROTEINS.

2.4.1. Expression of genes

The resulting plasmids pBADHis–gene (A–E) were amplified in chemically competent (cc) *E. coli* bacteria strain DH5α cells, and purified using the Plasmid miniprep GeneJet purification kit (Fermentas Canada Inc, Burlington, ON) and expressed in a bacterial system. Expression was confirmed by growing transformed bacteria on ampicillin-containing lysogeny broth (LB) agar plates. Since pBAD vector has an ampicillin resistant gene, only cells that contain the plasmid will be able to grow on ampicillin-containing plates.

2.4.2. Purification of proteins

Following a mini-scale protein extraction using bacterial protein extraction reagent (B-PER); (PIERCE, Rockford, IL), a large scale protein purification using immobilized metal affinity chromatography (IMAC) with nickel-nitrilotriacetic acid (Ni-NTA) resins was performed. The expected amino acid sequence and molecular weight of the recombinant proteins expressed downstream from the poly-His tag gene of pBADHis vector were obtained (Table 2.3).

2.5. CHARACTERISATION OF PROTEINS

2.5.1. Characterization of purified proteins by SDS-PAGE

Purified proteins were characterized by sodium dodecyl sulfate polyacrylamide gel electrophoreses (SDS-PAGE) to confirm their molecular weights relative to known protein standards. A 12% denaturing-resolving SDS-PAGE was used to characterize the proteins. Coomasie blue and fluor orange stains of the gels were imaged using a 302 nm UV transilluminator, (ImageQuant RT ECL; GE Healthcare Bioscience, Piscataway, NJ) (Figure 2.2). The gel images confirmed the purity of the proteins.

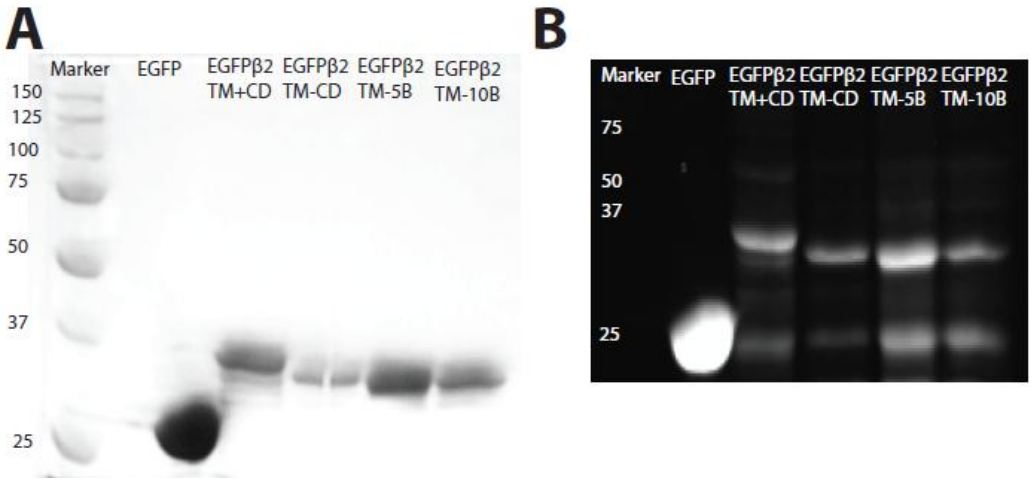

Figure 2.2. Purification of the β_2-TM proteins

Purified proteins were loaded onto a 12% SDS-PAGE gel under reducing condition. The gel was stained with **A**: Coomassie blue and visualized under white light or **B**: stained with coomassie orange fluor and imaged at 302 nm and viewed using a 572 nm filter. Lane 1 is MW (kDa), lane 2 EGFP (28.5 kDa), lane 3 EGFPβ_2TM+CD (34.5 kDa), lane 4 EGFPβ_2TM-CD (33.0 kDa), lane 5 EGFPβ_2TM-5B (32.4 kDa) and lane 6 EGFPβ_2TM-10B (31.9 kDa).

2.5.2. CD Spectroscopy

Circular dichroism (CD) is an analytical technique that reveals the secondary structures of proteins (17-19). A CD spectrum is affected by the presence of the three basic secondary structures of a protein: α-helix, β-sheet and random coil. CD spectra depend on several factors including concentration of the protein, buffer used and temperature (20-23). Generally observed values of molar ellipticity reported for α-helix, β-sheet and random coil are given in Table 2.1 (22, 24-25).

Secondary protein structure	Transition	Observed wavelengths (nm)	Molar ellipticity ($deg \cdot cm^2 \cdot dmol^{-1}$)
α-helix	π - π*	190 - 195	80,000 – 80,000
	n - π*	208	-40,000 ± 3,000
	n - π*	222	-40,000 ± 3,000
β-sheet	π - π*	195 - 200	30,000 – 50,000
	n - π*	215 - 220	-10,000 – -20,000
Random coil	π - π*	200	-20,000
	n - π*	220	n/a

Table 2.1. Typical molar ellipticity values for protein secondary structure.

Adapted from references 17, 26-28.

We obtained CD spectra of the purified β_2-TM proteins. EGFP is a predominantly β sheet protein with a characteristic minimum at 217 nm, and a corresponding molar ellipticity value of -13710 $deg \cdot cm^2 \cdot dmol^{-1}$ similar to literature values (24-25). This peak results from an electronic transition from n – π* for β-sheet structures. There is also a conspicuous maximum around 196 nm

with a molar ellipticity value of 38570 deg·cm^2·dmol^{-1} as a result of a $\pi - \pi^*$ electronic transition. The CD spectrum of 5 μM of EGFP is shown on Figure 2.3.

The CD Spectrum for EGFPβ_2TM+CD shows a maximum at 195 nm with a molar ellipticity of 71290 deg·cm^2·dmol^{-1} corresponding to the $\pi - \pi^*$ electronic transition of the β-sheet. There are the characteristic α-helix minima at 210 nm (-58490 deg·cm^2·dmol^{-1}) and 218 nm (-56280 deg·cm^2·dmol^{-1}). Figure 2.3 shows the spectrum for 4.5 μM EGFPβ_2TM+CD protein (17, 26-28). EGFPβ_2TM-CD protein with the short cytoplasmic tail completely removed shows a conspicuous α-helical peak with very intense minima at 217 nm (-74460 deg·cm^2·dmol^{-1}) and 211 nm (-70180 deg·cm^2·dmol^{-1}) corresponding to electronic transitions between $n - \pi^*$. There is also a maximum at 195 nm (126370 deg·cm^2·dmol^{-1}) for the β-sheet. Figure 2.3 shows the CD spectrum of EGFPβ_2TM-CD obtained using 4.75 μM of the protein solution. As the β_2 TM begins to be truncated, we observed a decrease in the helical property of the corresponding proteins. EGFPβ_2TM-5B though still very α-helical, shows a decrease in the maxima for the β-sheet at 195 nm to 92030 deg·cm^2·dmol^{-1} compared to that of EGFPβ_2TM-CD and both minima at 211 nm (- 61560 deg·cm^2·dmol^{-1}) and 217 nm (-60040 deg·cm^2·dmol^{-1}). Figure 2.3 shows the obtained spectrum with 5.26 μM of the EGFPβ_2TM-5B protein.

This same trend is observed too with the truncation of ten amino acid residues from the *C*-terminus of the TM domain. The protein EGFPβ_2TM-10B shows a maximum corresponding to a β-sheet at 195 nm with a molar ellipticity

of 60180 deg·cm^2·dmol^{-1}. The corresponding α-helix minima equally appears at 211 nm (-37030 deg·cm^2·dmol^{-1}) and 217 nm (-38850 deg·cm^2·dmol^{-1}). Figure 2.3 shows the spectrum for the EGFPβ_2TM-10B protein with a concentration of 4.8 µM. These CD data are consistent with the presence of α-helical structure due to fusion of the β_2 TM protein to the primarily β-sheet EGFP protein.

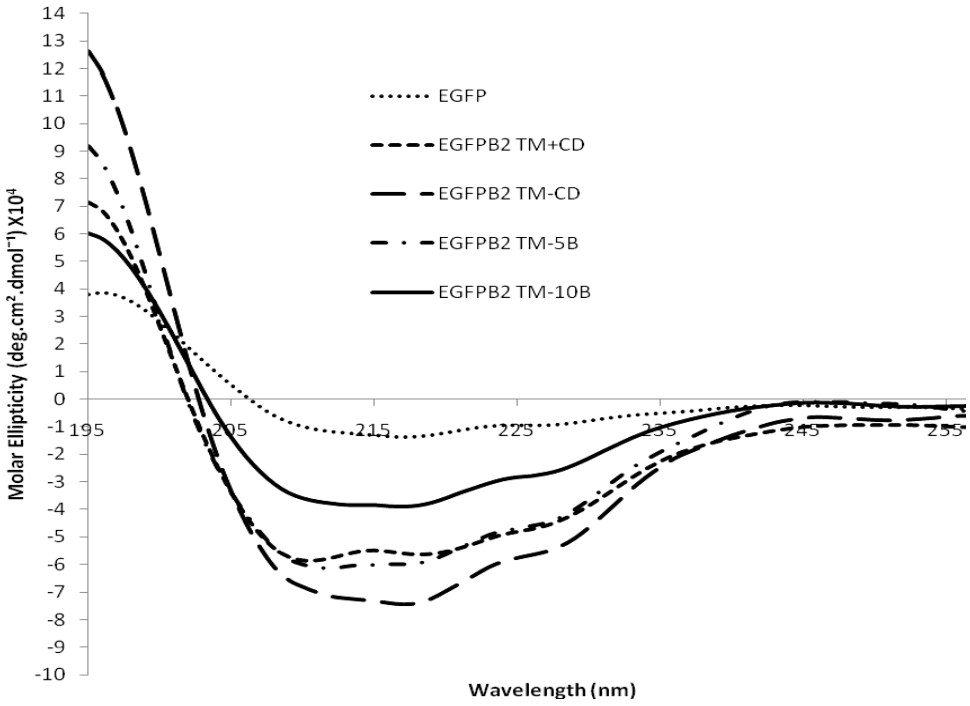

Figure 2.3: CD spectra of EGFP and fusion proteins.

CD spectra of purified EGFP and the β_2-TM proteins were obtained. EGFP (5 µM) is predominantly β-sheet containing protein. EGFPβ_2TM-CD (4.75 µM) has the most helical structure followed by its truncated variant; EGFPβ_2TM-5B (5.26 µM). EGFPβ_2TM+CD (4.5 µM) is next followed lastly by EGFPβ_2TM-10B (4.8 µM). The reduced helicity of EGFPβ_2TM+CD may be due to the presence of the short cytoplasmic tail attached. EGFP shows a minimum between 215 – 220 nm. The attached β_2 integrin TM introduce α-helix character as observed in the minima at about 211 and 217 nm. All proteins were in a solution of 100 mM NaCl, 50 mM NaH_2PO_4 and 0.05% elugent at 25 ^oC.

2.5.3. Fluorescence and absorbance measurements of β_2-TM proteins

The absorbance of proteins at 280 nm can be used to determine the relative abundance of the three amino acids tryptophan, tyrosine and cysteine that mainly absorb at this wavelength. The peptide backbone of the protein also has an absorbance at 205 nm. The absorbance spectra obtained for the five proteins using the SpectraMax M2e spectrophotometer (Molecular Devices, Sunnyvale, CA) with an absorption scan from 200 – 600 nm were as follows: EGFP, three peaks at 280, 390 and 475 nm; while all the β_2-TM proteins had two peaks at 280 and 390 nm.

Since the proteins all have EGFP as an *N*-terminal protein, the chromophore in EGFP can be excited at 480 nm (29-30). Thus, using a fixed emission wavelength of 510 nm, an excitation scan from 300 – 500 nm was performed. This scan showed three excitation maxima for all proteins at 471 nm, 485 nm and 495 nm. When an emission scan was performed at a fixed excitation of 475 nm we observed a single emission maximum at 508 nm. The fluorescence measurements were done on the QuantaMaster Model QM-4/2005 Spectrofluorometer (Photon Technology International, Birmingham, NJ). EGFP emits light at about 509 nm (30-31). The quantum yeild of the four chimeric proteins was slightly reduced compared to that of EGFP. Table 2.2 and Figure A2 (appendix) shows the fluorescence spectra of all the proteins.

protein	λ_{max} *(Abs) (nm)*	λ_{max} *(Exc) at* λ_{510} *(Emm) (nm)*	λ_{max} *(Emm) at* λ_{475} *(Exc) (nm)*
EGFP	280, 390, 475	471, 485, 495	508
EGFPβ_2TM+CD	280, 390	471, 485, 495	508
EGFPβ_2TM-CD	280, 390	471, 485, 495	508
EGFPβ_2TM-5B	280, 390	471, 485, 495	508
EGFPβ_2TM-10B	280, 390	471, 485, 495	508

Table 2.2: Summary of the absorption, excitation and emission maxima of EGFP and the β_2-TM proteins

An absorption scan from 200 – 600 nm was performed on proteins while an excitation scan from 300 – 500 nm was done with a fixed emission of 510 nm. For the emission spectra, we used a fixed excitation of 475 nm. All proteins were at a concentration of 2.0 μM. See figure A2 in appendix.

2.5.4. Mass Spectrometry

Mass spectrometry has been widely applied in the determination of the molecular weight, structure, and modification patterns of carbohydrates on proteins. Matrix-assisted laser desorption/ionization-time of flight mass spectrometry (MALDI-TOF MS) was used to confirm the molecular weights of the purified proteins while liquid chromatography mass spectroscopy tandem (LC MS/MS) technique was used to confirm the a.a. sequence after trypsin digest of proteins. The results are summarized on Table 2.3. The sequences of all five proteins were confirmed with sequence coverage of between 44-66%.

protein designation	*expected Molecular weight (dalton)*	*MALDI weight (Da)*	*expected sequence of amino acid*	*LC MS/MS (Coverage area of expected a.a. in bold and underlined)*
EGFP (276 a.a.)	31100.8	31195	MGGSHHHHHH GMASMTGGQQ MGRDLYDDDD KDRWGSEMVS KGEELFTGVV PILVELDGDV NGHKFSVSGE GEGDATYGKL TLKFICTTGK LPVPWPTLVT TLTYGVQCFS RYPDHMKQHD FFKSAMPEGY VQERTIFFKD DGNYKTRAEV KFEGDTLVNR IELKGIDFKE DGNILGHKLE YNYNSHNVYI MADKQKNGIK VNFKIRHNIE DGSVQLADHY QQNTPIGDGP VLLPDNHYLS TQSALSKDPN EKRDHMVLLE FVTAAGITLG MDELYK	MGGSHHHHHH GMASMTGGQQ MGRDLYDDDD KDRWGSEMVS K**GEELFTGVV PILVELDGDV NGHKFSVSGE GEGDATYGKL TLKFICTTGK** LPVPWPTLVT TLTYGVQCFS RYPDHMKQHD FFK**SAMPEGY VQERTIFFKD DGNYK**TR**AEV KFEGDTLVNR** IELK**GIDFKE DGNILGHKLE YNYNSHNVYI MADK**QKNGIK VNFKIR**HNIE DGSVQLADHY QQNTPIGDGP VLLPDNHYLS TQSALSKDPN EKRDHMVLLE FVTAAGITLG MDELYK** (Sequence Coverage of **66%** with P<0.05)
EGFP β_2 TM+CD (330 a.a.)	36560.2	36651	MGGSHHHHHH GMASMTGGQQ MGRDLYDDDD KDRWGSEMVS KGEELFTGVV PILVELDGDV NGHKFSVSGE GEGDATYGKL TLKFICTTGK LPVPWPTLVT TLTYGVQCFS RYPDHMKQHD FFKSAMPEGY VQERTIFFKD DGNYKTRAEV KFEGDTLVNR IELKGIDFKE DGNILGHKLE YNYNSHNVYI MADKQKNGIK VNFKIRHNIE DGSVQLADHY QQNTPIGDGP VLLPDNHYLS TQSALSKDPN EKRDHMVLLE FVTAAGITLG MDELYKGSTG STGSTESRES VAGPNIAAIV GGTVAGIVLI GILLLVIWKA LIHLSDLREY	MGGSHHHHHH GMASMTGGQQ MGRDLYDDDD KDRWGSEMVS K**GEELFTGVV PILVELDGDV NGHKFSVSGE GEGDATYGK**L TLK**FICTTGK** LPVPWPTLVT TLTYGVQCFS RYPDHMKQHD FFK**SAMPEGY VQERTIFFK**D DGNYKTRAEV K**FEGDTLVNR** IELK**GIDFKE DGNILGHKLE YNYNSHNVYI MADK**QKNGIK VNFKIRHNIE DGSVQLADHY QQNTPIGDGP VLLPDNHYLS TQSALSKDPN EK**RDHMVLLE FVTAAGITLG MDELYKGSTG STGSTESR**ES VAGPNIAAIV GGTVAGIVLI GILLLVIWK**A LIHLSDLR**EY (Sequence Coverage of **44%** with P<0.05)

EGFP β_2 TM-CD (318 a.a.)	35120.5	35212	MGGSHHHHHH GMASMTGGQQ MGRDLYDDDD KDRWGSEMVS KGEELFTGVV PILVELDGDV NGHKFSVSGE GEGDATYGKL TLKFICTTGK LPVPWPTLVT TLTYGVQCFS RYPDHMKQHD FFKSAMPEGY VQERTIFFKD DGNYKTRAEV KFEGDTLVNR IELKGIDFKE DGNILGHKLE YNYNSHNVYI MADKQKNGIK VNFKIRHNIE DGSVQLADHY QQNTPIGDGP VLLPDNHYLS TQSALSKDPN EKRDHMVLLE FVTAAGITLG MDELYKGSTG STGSTESRES VAGPNIAAIV GGTVAGIVLI GILLLVIW	MGGSHHHHHH GMASMTGGQQ MGRDLYDDDD KDRWGSEMVS K**GEELFTGVV** **PILVELDGDV** **NGHKFSVSGE** **GEGDATYGK**L TLKFICTTGK LPVPWPTLVT TLTYGVQCFS RYPDHMKQHD FFK**SAMPEGY** **VQERTIFFKD** **DGNYK**TRAEV K**FEGDTLVNR** IELK**GIDFKE** **DGNILGHKLE** **YNYNSHNVYI** **MADK**QKNGIK VNFKIR**HNIE** **DGSVQLADHY** **QQNTPIGDGP** **VLLPDNHYLS** **TQSALSKDPN** **EKRDHMVLLE** **FVTAAGITLG** **MDELYKGSTG** **STGSTESR**ES VAGPNIAAIV GGTVAGIVLI GILLLVIW (Sequence coverage of **58%** with P<0.05)
EGFP β_2 TM-5B (313 a.a.)	34495.7	34588	MGGSHHHHHH GMASMTGGQQ MGRDLYDDDD KDRWGSEMVS KGEELFTGVV PILVELDGDV NGHKFSVSGE GEGDATYGKL TLKFICTTGK LPVPWPTLVT TLTYGVQCFS RYPDHMKQHD FFKSAMPEGY VQERTIFFKD DGNYKTRAEV KFEGDTLVNR IELKGIDFKE DGNILGHKLE YNYNSHNVYI MADKQKNGIK VNFKIRHNIE DGSVQLADHY QQNTPIGDGP VLLPDNHYLS TQSALSKDPN EKRDHMVLLE FVTAAGITLG MDELYKGSTG STGSTESRES VAGPNIAAIV GGTVAGIVLI GIL	MGGSHHHHHH GMASMTGGQQ MGRDLYDDDD KDRWGSEMVS K**GEELFTGVV** **PILVELDGDV** **NGHKFSVSGE** **GEGDATYGK**L TLKFICTTGK LPVPWPTLVT TLTYGVQCFS RYPDHMKQHD FFK**SAMPEGY** **VQERTIFFK**D DGNYKTRAEV K**FEGDTLVNR** IELK**GIDFKE** **DGNILGHKLE** **YNYNSHNVYI** **MADKQKNGIK** **VNFK**IRHNIE DGSVQLADHY QQNTPIGDGP VLLPDNHYLS TQSALSKDPN EK**RDHMVLLE** **FVTAAGITLG** **MDELYKGSTG** **STGSTESR**ES VAGPNIAAIV GGTVAGIVLI GIL (Sequence coverage of **44%** with P<0.05)

EGFP β_2 TM-10B (308 a.a.)	33986.0	34190	MGGSHHHHHH GMASMTGGQQ MGRDLYDDDD KDRWGSEMVS KGEELFTGVV PILVELDGDV NGHKFSVSGE GEGDATYGKL TLKFICTTGK LPVPWPTLVT TLTYGVQCFS RYPDHMKQHD FFKSAMPEGY VQERTIFFKD DGNYKTRAEV KFEGDTLVNR IELKGIDFKE DGNILGHKLE YNYNSHNVYI MADKQKNGIK VNFKIRHNIE DGSVQLADHY QQNTPIGDGP VLLPDNHYLS TQSALSKDPN EKRDHMVLLE FVTAAGITLG MDELYKGSTG STGSTESRES VAGPNIAAIV GGTVAGIV	MGGSHHHHHH GMASMTGGQQ MGRDLYDDDD KDRWGSEMVS K**GEELFTGVV** **PILVELDGDV** **NGHKFSVSGE** **GEGDATYGK**L TLK**FICTTGK** LPVPWPTLVT TLTYGVQCFS RYPDHMKQHD FFK**SAMPEGY** **VQERTIFFKD** **DGNYK**TRAEV K**FEGDTLVNR** IELK**GIDFKE** **DGNILGHKLE** **YNYNSHNVYI** **MADK**QKNGIK VNFKIR**HNIE** **DGSVQLADHY** **QQNTPIGDGP** **VLLPDNHYLS** **TQSALSKDPN** **EKRDHMVLLE** **FVTAAGITLG** **MDELYKGSTG** **STGSTESR**ES VAGPNIAAIV GGTVAGIV (Sequence Coverage of **60%** with P<0.05)

Table 2.3: Summary of the molecular weights and expected amino acid sequences of purified recombinant proteins.

From the gene sequence of the recombinant proteins, the following amino acid sequence and respective molecular weights of the proteins is predicted (ExPASy Proteomics Server). Using the Mascot server, the sequence identity coverage was determined following trypsin on-gel digestion. All proteins had individual ion scores > 7 indicating an identity of extensive homology (P<0.05). These results are present on the Mascot server under Job ID 2864 to 2869. The percentage coverage ranges from 43% for EGFPβ_2TM+CD to 66% for EGFP proteins. MALDI values with ± 100 mass units are indicative of the molecular weights of the proteins.

2.6. BINDING ASSAYS

Michejda and co-workers showed that small synthetic peptides which mimic sections of transmembrane proteins could inhibit the function of GPCR and the ABC transporters *in vivo* on cell membranes by disrupting their proper assembly (10, 32). Thus, the recombinant proteins were tested for their binding ability to Jurkat cells. These cells express the LFA-1 molecule on their surface (10). If proteins bind with the membrane, we will be able to detect labeled cells by the technique of flow cytometry (FC) using a flow cytometer that uses laser excitation of the the EGFP chromophore. We set out to determine the affinity of the TM proteinsfor cells relative to EGFP.

2.6.1. Binding of EGFP protein to Jurkat ells (clone E6.1)

As a control experiment, we tested the binding of the EGFP protein to Jurkat cells and detected cells with green fluorescence. Cells were harvested at mid-log phase and incubated with different amounts of the EGFP protein. The cells were then analysed for fluorescence by gating them using a flow cytometer (FC) whose parameters had been adjusted to show the number of fluorescent cells from a total cell population of 5,000 events. A histogram is obtained from the fluorescence channel showing the population of labelled cell. To quantify binding, we fit the data to two different equations in order to obtain the binding constant (K_d) and the 50% saturation concentration (EC_{50}). Fitting the data into a ligand binding one-site competition plot of log of protein concentration against percentage of labelled cells shown on Figure 2.4 A1 we obtained a very high EC_{50}

value of > 100 µM while fitting the concentration (transformed) against the response (percentage labelled) into the ligand – binding, one-site saturation gave us a B_{max} of 73 ± 32% with a K_d > 100 µM (Figure 2.4 A2). EC_{50} in this case is defined as the concentration of the protein (agonist) that is required to give 50 % response. The upper plateau for EGFP could not be established as it was well above 250 µg/mL. The high K_d value indicates that EGFP binds only weakly to cells, and it does not reach saturation even at high protein concentration. B_{max} is the maximum percentage of cells labelled at saturation concentration of protein. K_d is the equilibrium dissociation constant of the protein. The histogram obtained from treating the cells with 40 µg/mL of EGFP protein overlaid on the control cells is shown on Figure 2.5 B. Table A1 (appendix) shows the raw data obtained from EGFP labelling.

2.6.2. Binding of EGFPβ_2TM+CD protein to Jurkat cells

Jurkat cells were treated with concentrations of the EGFPβ_2TM+CD protein over the same range used for EGFP alone. Table A2 (appendix) shows the raw data obtained from the FC experiments with three runs per sample; while Figure 2.5 C shows the overlaid histogram at 40 µg/mL protein treatment; and Figures 2.4 B1 and B2 shows the binding curves obtained as semi-log and linear plots, respectively. The EC_{50} from the one-site ligand competitive curve is 750 ± 30 nM while the one-site ligand saturation binding plot gave a B_{max} of 100 ± 6% with a K_d of 480 ± 90 nM. The K_d value for EGFPβ_2TM+CD suggest that the protein is binding to the membrane and causing labelling of the cells.

2.6.3. Binding of EGFPβ_2TM-CD protein to Jurkat cells

The FC data obtained is shown on Table A3 (appendix) while the overlaid histogram obtained from labeling with 40 µg/mL of protein is shown on Figure 2.5 D. The binding curve (Figure 2.4 C1 and C2) gave an EC_{50} of 1,460 ± 40 nM and fitting the data to the one-site specific binding equation we obtained a B_{max} of 44 ± 4% with a K_d of 420 ± 120 nM. This K_d value also indicates the protein binds with high affinity to the cells compared to EGFP.

2.6.4. Binding of EGFPβ_2TM-5B protein to Jurkat cells

The FC experiment resulted in the data shown on Table A4 (appendix). The corresponding overlaid histogram obtained from treating the cells with 40 µg/mL of protein is shown on Figure 2.5 E. The binding curves on Figure 2.4 D1 and D2 show an EC_{50} value of 790 ± 50 nM fitting the data to the one-site specific binding equation we obtained a B_{max} of 44 ± 4% with a K_d value of 280 ± 80 nM was obtained. This protein as indicated by its K_d binds to cells with a much higher affinity compared to the other β_2-TM proteins.

2.6.5. Binding of EGFPβ_2TM-10B protein to Jurkat cells

The same concentrations of EGFPβ_2TM-10B protein was incubated with Jurkat cells and sorted for labelled cells. The data obtained are presented on Table A5 (appendix) while the overlaid histogram obtained from treatment of the cells with 40 µg/mL protein is shown on Figure 2.5 F. The plot of log of protein concentration against percent of labeled cells shown on Figure 2.4 E1 gave an

EC_{50} of 490 ± 40 nM while Figure 2.4 E2 on the one-site saturation equation resulted in a B_{max} value of 80 ± 5 % with a corresponding K_d of 440 ± 80 nM .

The data obtained suggests that the fusion of the β_2-TM protein to the EGFP has a substantial influence on the binding of the protein to the cells. This is evident with the greater than 200-fold increase in binding achieved with the recombinant proteins. Table 2.6 summarizes the values obtained.

protein	*EC_{50} values (nM)*	*B_{max} (%)*	*K_d (nM)*
EGFP	> 100 µM	73 ± 32	> 100 µM
EGFPβ_2TM+CD	750 ± 350	100 ± 6.19	480 ± 90
EGFPβ_2TM-CD	1,460 ± 40	44.05 ± 4.0	420 ± 120
EGFPβ_2TM-5B	790 ± 50	44.45 ± 3.8	280 ± 80
EGFPβ_2TM-10B	490 ± 40	80.4 ± 4.5	440 ± 80

Table 2.4: Fit values for EGFPβ_2TM protein binding to cells.

The EC_{50} values were obtained by substituting % labelled cells, as determined by FC, data into the one-site ligand binding competition equation, Y=Bottom + (Top-Bottom)/(1+10^((LogEC_{50}-X))), while B_{max} and K_d values were both obtained from the one-site ligand binding saturation equation, $Y = B_{max}*X/(K_d + X)$.

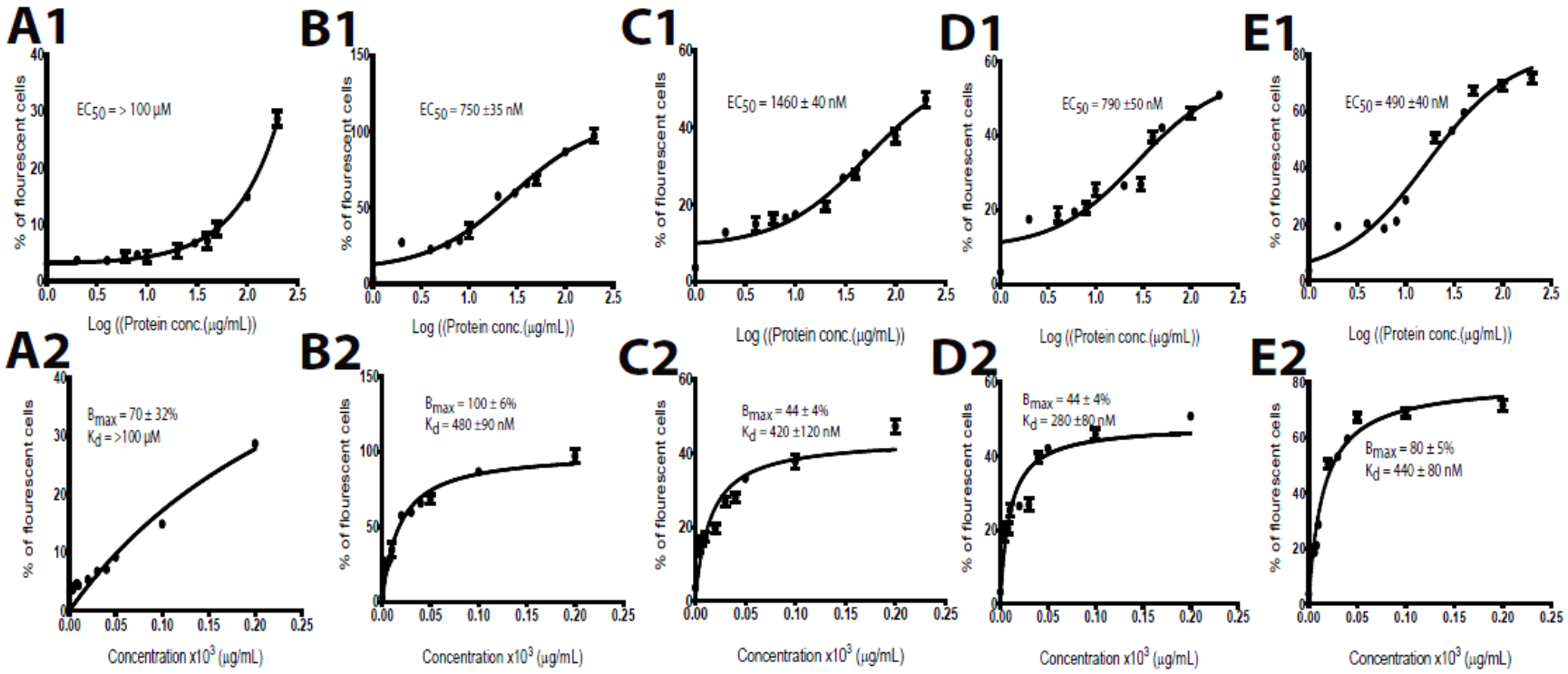

Figure 2.4: One-site competitive ligand binding and saturation curves for the β_2-TM recombinant proteins.

Binding of β_2-TM proteins to Jurkat cells was determined by FC. **A1**: The competitive ligand-binding curve for EGFP with R^2 value of 0.99. **A2**: EGFP Saturation curve with R^2 of 0.89 **B1**: Competitive binding curves for EGFPβ_2TM+CD protein with R^2 value is 0.96. **B2**: The saturation curve for EGFPβ_2TM+CD with R^2 of 0.95. **C1**: The competitive ligand-binding curve for EGFPβ_2TM-CD with R^2 value of 0.95. **C2**: The saturation curve for EGFPβ_2TM-CD with a calculated R^2 of 0.87. **D1**: The competitive ligand-binding curve for EGFPβ_2TM-5B protein with R^2 value of 0.92. **D2**: Saturation curve for EGFPβ_2TM-5B protein with R^2 value of 0.87. **E1**: The competitive ligand-binding curve for EGFPβ_2TM-10B protein with R^2 value of 0.96. **E2**: Saturation curve for EGFPβ_2TM-10B with R^2 is 0.96. The number of replicates is four (n=4) and errors are represented by SD and some error bars may be obscured by the symbols.

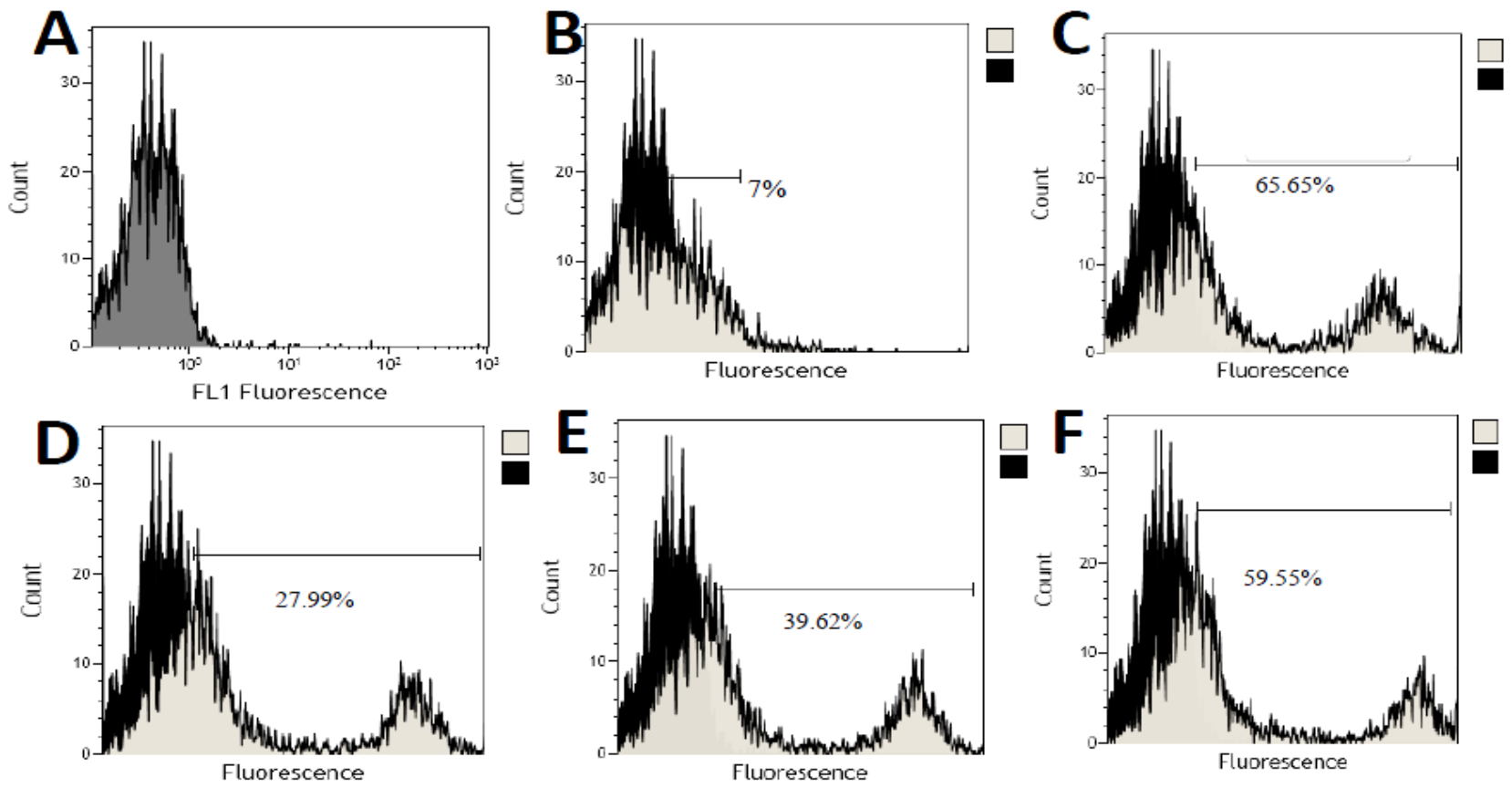

Figure 2.5: Overlaid histograms showing binding of recombinant proteins to Jurkat cells following treatment.

A: Fluorescence of control cells (untreated) as seen in the FL1 channel. **B**: Cells treated with 40 µg/mL of EGFP protein observed in the FL1 channel. **C**: 40 µg/mL of EGFPβ_2TM+CD protein treated cells under the FL1 channel. **D**: Cells labelled by binding to 40 µg/mL of EGFPβ_2TM-CD protein and seen under the FL1 channel. **E**: 40 µg/mL EGFPβ_2TM-5B protein treated cells and seen under the FL1 channel. **F**: Binding of cells to 40 µg/mL of EGFPβ_2TM-10B protein seen under the FL1 channel. Excitation wavelength is 488 nm while emission in the FL1 channel is at a BP525 filter. Black is untreated cells while white is treated cells

2.7. FLUORESCENCE MICROSCOPY

Labelled cells were fixed and mounted on microscope slides for fluorescence imaging. The images (Figure 2.6) were taken using a 60X oil immersion objective either with DIC or epi-fluorescence imaging. Epi-fluorescence was done at an excitation of 488 nm using an argon laser source and viewed through a 525 nm filter. Images doesn't clearly indicate if proteins are being inserting into the membrane, binding, or just forming aggregates on the membrane. Also some of the protein may be incorporated into endosomes and internalized.

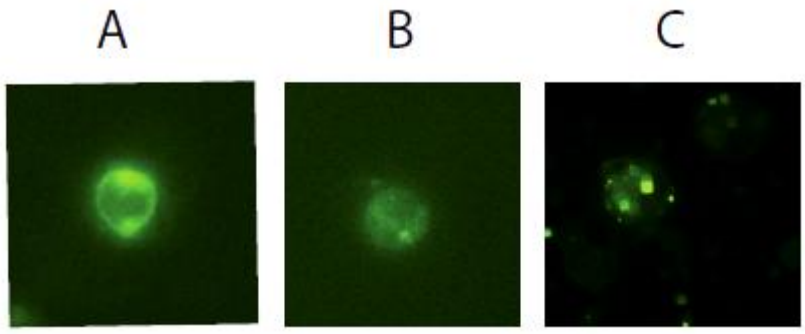

Figure 2.6: Microscopy images of cells treated with EGFP and EGFPβ_2TM+CD proteins.

A is an epi-fluorescence image of EGFPβ_2TM+CD protein treated cells viewed under the 60X oil immersion objective. **B** is an epi-fluorescent image of EGFP protein treated cells viewed with the 60X oil immersion objective. **F** is another epi-fluorescence image obtained from EGFPβ_2TM+CD protein treated cells viewed under the 60X oil immersion objective. **A** shows some association of the protein with the membrane while **C** is probably internalization of the proteins resulting to possible endosomes formation in the cell.

2.8. DISCUSSION

We have shown that recombinantly expressed proteins label Jurkat cells *in vitro* by binding to the cells in a similar way synthetic peptides mimicking TM protein exhibit their function in disrupting membrane receptors. We made four variants of a fluorescent protein having an *N*-terminal EGFP linked via a 9-mer to a β_2 integrin TM domain. The lengths of the proteins were shortened by truncation of the *C*- terminal end of the β_2 integrin. These proteins were shown to have remarkable affinity for Jurkat cells as low as 300 nM. Structural characterization of the peptides using CD spectroscopy confirmed the presence of an α-helical β_2-TM protein fused to the β-sheeted EGFP protein. We used FC to analyze the percentage of cells that were labelled with these peptides. Fluorescence microscopy supports that the proteins may associate to the cell membrane. Our data do not exclude the possibility that the protein bind to cells as aggregates. We computed the K_d values for each protein and found that EGFPβ_2TM-5B had the highest binding affinity for the cells with a K_d value of 280 ± 80 nM. The protein that bound with least affinity was EGFPβ_2TM+CD (K_d of 480 ± 90 nM). EGFPβ_2TM-CD had a K_d of 420 ± 120 nM while EGFPβ_2TM-10B had a K_d of 440 ± 80 nM. Compared to EGFP (K_d value > 100 μM) we can conclude that the recombinant proteins have a nanomolar affinity for Jurkat cells, with as much as 370-fold enhancement from EGFP alone.

Four variants of a fluorescent protein that targets β_2 integrin (CD18) TM domain were made by recombinantly expressing the genes in LMG194 and

DH10B *E. coli* bacteria strains. Table 2.5 shows the resulting proteins and their corresponding K_d values. The characteristic GXXXG-like motif which forms the framework for folding of the helical TM domain is present as GTVAG (33-34).

TM domains have a high tendency of forming homodimers through these GXXXG and SXXXS motifs (34-40). By their small size, glycine residues have the tendency to come closer allowing two TM helices to come together. The three variable a.a. residues (XXX) improve specificity by the formation of binding ridges or clefts. The lengths of the peptides (excluding the EGFP) and the type of a.a. residues are a key factor to their insertion into the lipid membrane. These are also attributed to their secondary structures shown by their corresponding CD spectrum. A short peptide of 24 a.a. residues corresponding to TM 2 of CXCR4 has been shown to have a high effect on signal transduction by disruption of the receptor (10). A peptide antagonist with a length of 15 a.a. residues has equally been show to have an inhibitory effect by disruption of the ABC TM assembly of P-gp (32). Thus the lengths of the interfering peptides would have a tremendous effect on their binding and insertion ability into the membrane.

Protein	*Sequence*	*K_d values (nM)*	*Fold over EGFP*
EGFP	EGFP	> 100 μM	1
EGFPβ_2TM+CD	*EGFP*-GSTGSTGSTESRESVAGPN IAAIVG**GTVAG**IVLIGILL LVIWKALIHLSDLREY	480 ± 90	220
EGFPβ_2TM-CD	*EGFP*-GSTGSTGSTESRESVAGPN IAAIVG**GTVAG**IVLIGILL LVIW	420 ± 120	250
EGFPβ_2TM-5B	*EGFP*-GSTGSTGSTESRESVAGPN IAAIVG**GTVAG**IVLIGIL	280 ± 80	370
EGFPβ_2TM-10B	*EGFP*-GSTGSTGSTESRESVAGPN IAAIVG**GTVAG**IVL	440 ± 80	240

Table 2.5: Summary of the recombinant proteins and their corresponding K_d values for Jurkat

Proteins varied in length from 23 a.a. to 45 a.a. which are attached to the *C*–terminus of EGFP via a 9-mer. The characteristic GXXXG like motifs are indicated in bold. EGFP denoted the protein.

The proposed mechanism of binding and insertion of membrane peptides involves three steps which takes into account the two stage model of membrane folding and oligomerization (41-43). Firstly, the protein binds to the cell in a fully soluble membrane conformation. The protein then moves on the fluid mosiac membrane, orienting itself into a conformation that favors membrane insertion. It

then insert into the membrane and adopts the desired conformation for associating with either the lipid bilayer or other TM proteins in the membrane bilayer (36-38). Polar and ionisable a.a. residues including D-amino acids are important in enhancing membrane solubility of peptides (44-47). TM helices expose their non-polar residues to the surrounding medium (48-49). Our peptides have a significant number of such residues including Ser, Arg, Glu, and Thr which could affect binding.

Insertion of the protein in the membrane involves a spontaneous orientation of the TM segment (made up primarily of hydrophobic and non-polar a.a.) favoring the formation of helix-helix association. The hydrophobicity of the TM segment is required for the TM conformation (50). Apart from EGFPβ_2TM+CD which have a Lys residue, the peptides are completely free of Asp and Pro which have been shown to hinder peptide insertion, though can be tolerated when present near the center of the domain (51-52). A measure of the propensity of residues to form helical structures are in the order Ile > Leu > Val > Met > Phe > Ala > Gln > Try > Thr > Ser > Asn > Gly > Pro (53). Val, Ile and Gly are considered as α–helix destabilizing residues in soluble proteins where Leu, Ala are major contributors to helicity (49-50, 54-59).

Binding of EGFP to Jurkat cells resulted in a non-saturated curve when fitted to the one-site specific binding equation with a K_d >100 μM. The corresponding EC_{50} value obtained from a fit to the one-site competition binding equation gives > 100 μM. Comparing these values with those obtained from the

treatment of the cells with the recombinant peptides, we observe more than 200-fold decreases in the K_d and EC_{50} values. The K_d of the EGFPβ_2TM-5B protein is the lowest at 280 ± 80 nM. EGFPβ_2TM+CD has the highest K_d (480 ± 90 nM) while EGFPβ_2TM-CD and EGFPβ_2TM-10B have respective K_d values of 420 ± 120 nM and 440 ± 80 nM. These data suggest that the length of a TM helix segment is important in binding to the membrane bilayer. The presence of the GXXXG motif is essential for helix formation and the GXXXG motif should be flanked by some residues as seen by the drastic increase in K_d value for EGFPβ_2TM-10B which has just three a.a. residues after the GXXXG. The short cytoplasmic domain attached to the EGFPβ_2TM+CD protein containing polar amino acid residues as well as the length of the protein may be accounted for the high K_d relative to the other recombinant peptides.

2.9. CONCLUSION

Recombinant proteins bearing a *C*-terminal hydrophobic peptide can bind to cells in a similar manner as synthetic hydrophobic TM peptides interfere with receptor function by disrupting TM-TM association. The length of the recombinant protein (attached hydrophobic domain) may have a role in facilitating insertion into the membrane. Furthermore, anionic residues are important for the binding and insertion process. In this chapter, we have shown that our recombinant proteins can bind with nanomolar affinity to Jurkat cells and cause labelling of the cells. In Chapter 3, we will report on the influence of these

peptides on the function of our target LFA-1 receptor. We will show the effect of these peptides on the binding of LFA-1 to specific mAb epitopes.

2.10. MATERIALS AND METHODS

2.10.1. Materials

The following restriction enzymes were obtained from their respective vendors: EcoRI (Invitrogen), XhoI (Invitrogen), BamHI (Fermentas), NdeI (Fermentas), dNTP-deoxynucleotide triophosphates (Invitrogen) Taq DNA Polymerase (Invitrogen), T4 DNA ligase (Invitrogen), Pfu Ultra II fusion HS DNA polymerase (Stratagene).The cell lines used were Sub-cloning efficiency DH5α competent cells (Invitrogen), *E. coli* SURE cells (Stratagene), *E. coli* BL21 DE3 (Novagen), *E. coli* pLysS DE3 (Novagen), *E. coli* LMG194 (Sigma) *E. coli* JM109 (Stratagene), *E. coli* XL1Blue (Stratagene). Vectors used, pET28a vector (Novagen) and pBAD vector (Invitrogen). Protein purification B-PER, bacterial Protein Extraction Reagent (PIERCE), kanamycin (Sigma), Ampicillin (Sigma), Chloramphenicol (Sigma), Tetracycline (Sigma), IPTG- isopropyl-β-D-thiogalactopyranoside (Fisher Scientific), L-Arabinose (Sigma) GuHCl-Guanidinium HCl (Calbiochem), SDS-sodium dodecylsulphate (BioRad), Urea (Caledan), TX100 (VWR International), β-OG, n-octyl-β-D-glucopyranoside (Calbiochem), CHAPS (Sigma-Aldrich), Ultra pure agarose (Invitrogen), Normal 2% agarose (Invitrogen), SYBR Safe DNA gel stain in DMSO (Invitrogen), Gene Ruler 1 kb DNA ladder (Fermentas), Gene ruler 100 bp DNA ladder (Fermentas), Nuclease free water (Gibco), Complete EDTA free protease inhibitor tablets

(Roche Diagnostics), DNaseI (Boehringer Mannhem), lysozyme from chicken egg white (Sigma), β-mercarptoethanol (Bioshops Biotechnology), DTT,Dithiothreitol (Fisher Biotech), Imidazole (Sigma-Aldrich), Fermentas Genejet Plasmid miniprep kit, Qiagen QIAquick PCR purification kit. Other reagents used were purchased from Invitrogen, Sigma or Fisher Scientific.

2.10.2. Experimental Methods

2.10.2.1. PCR amplification and introduction of genes into plasmid

2.10.2.1.1. Amplification of the Ksiβ$_2$ gene

The gene *Ksiβ$_2$* (543 bp) was codon optimized for *E. coli*, synthesized and ligated between the NdeI and BamHI RE sites of the PUC 57 plasmid (2710 bp) (BioBasic, Canada), Figure 2.6 below. The bacterial protein ketosteroid isomerase (Ksi) was linked to the β_2 integrin via a 7-mer (GGGGSDP) with the introduction of an Aspartate – Proline (DP) site for acid cleavage to release the β_2 integrin (60-61). The outline for the gene sequence is shown on Figure 2.6 below. This was provided as a 4 µg lyophilized gene. A stock solution of 500 ng/µL was made by adding 8 µL sterile water. 2 µg (4 µL) of the product was then digested to give approximately 0.4 µg of the *Ksiβ$_2$* (20%). Digestion was performed using Fermentas double digest with NdeI and BamHI REs and incubating overnight at 37 °C.As a control pET28a (110 ng/µL) was digested with similar enzymes and incubated overnight at 37°C. This was subsequently used for expressing the KSIβ_2 protein.

Following overnight digestion, a 1% agarose gel was run to separate gene of interest from the plasmid. Gene purification was done using QIAquick Gel Extraction kit protocol using a microcentrifuge (Qiagen) as per manufacturer`s instruction. The concentration of purified *ksiβ*$_2$ was 7.7 ng/µL.

2.10.2.1.2. Recombinant PCR

All genes were amplified using the technique of recombinant PCR. The strategy uses two outer primers, A and D; and two inner primers B and C. Primers A and B are used to amplified a gene template (*egfp*) to make gene product 1, while primers C and D amplify a gene template (*ksiβ*$_2$), to make gene product 2. The general principle for the PCR is depicted below in Figure 2.7. Table 2.6 shows the primer names and sequence of all primers used in making all the fusion genes while Table 2.7 shows the targeted regions of the proteins.

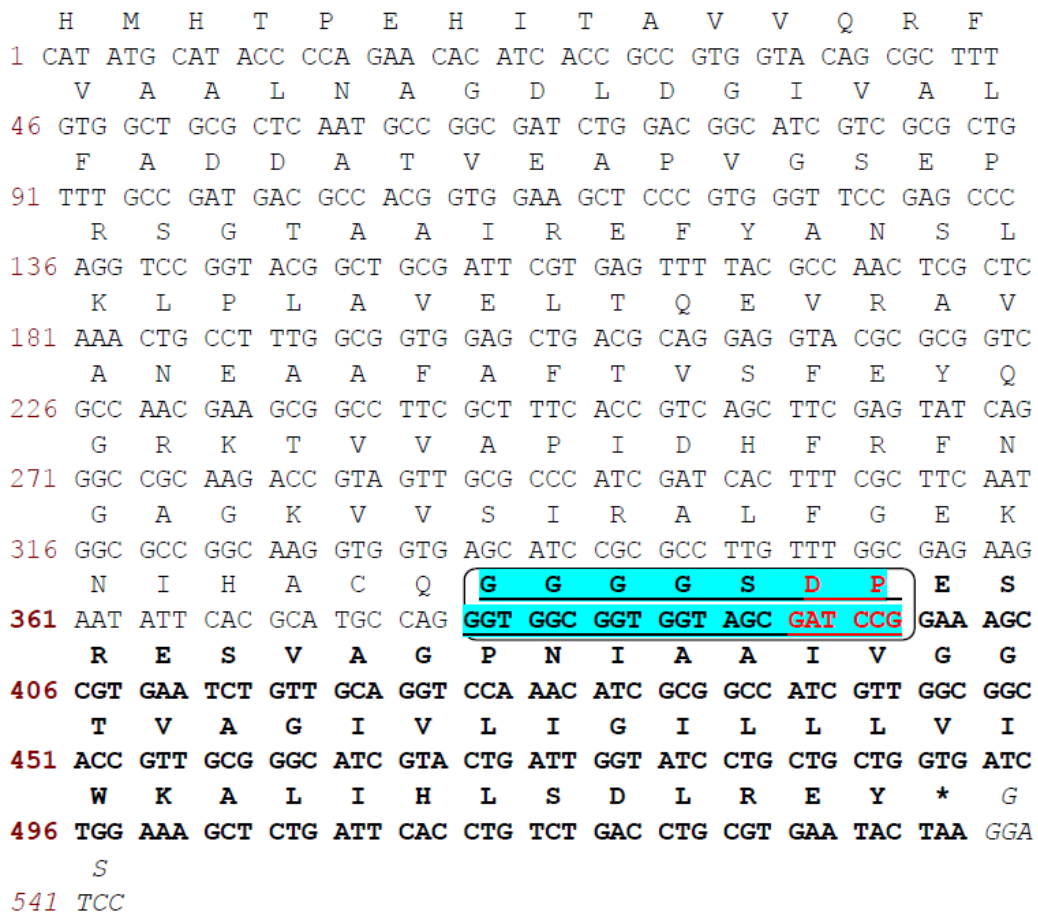

Figure 2.6: Codon optimized sequence and expected amino acid sequence of the *ksiβ_2* gene

The gene for the bacteria ketosteriod isomerise protein was synthesized upstream the gene for the TM domain of β_2 integrin containing a short cytoplasmic tail. Ksi is linked to β_2 integrin TM via a DP sequence to serve as a site for mild acid cleavage. In bold is the sequence for the desired protein while within the oval rectangle is the sequence for the DP containing linker. * denotes a stop codon.

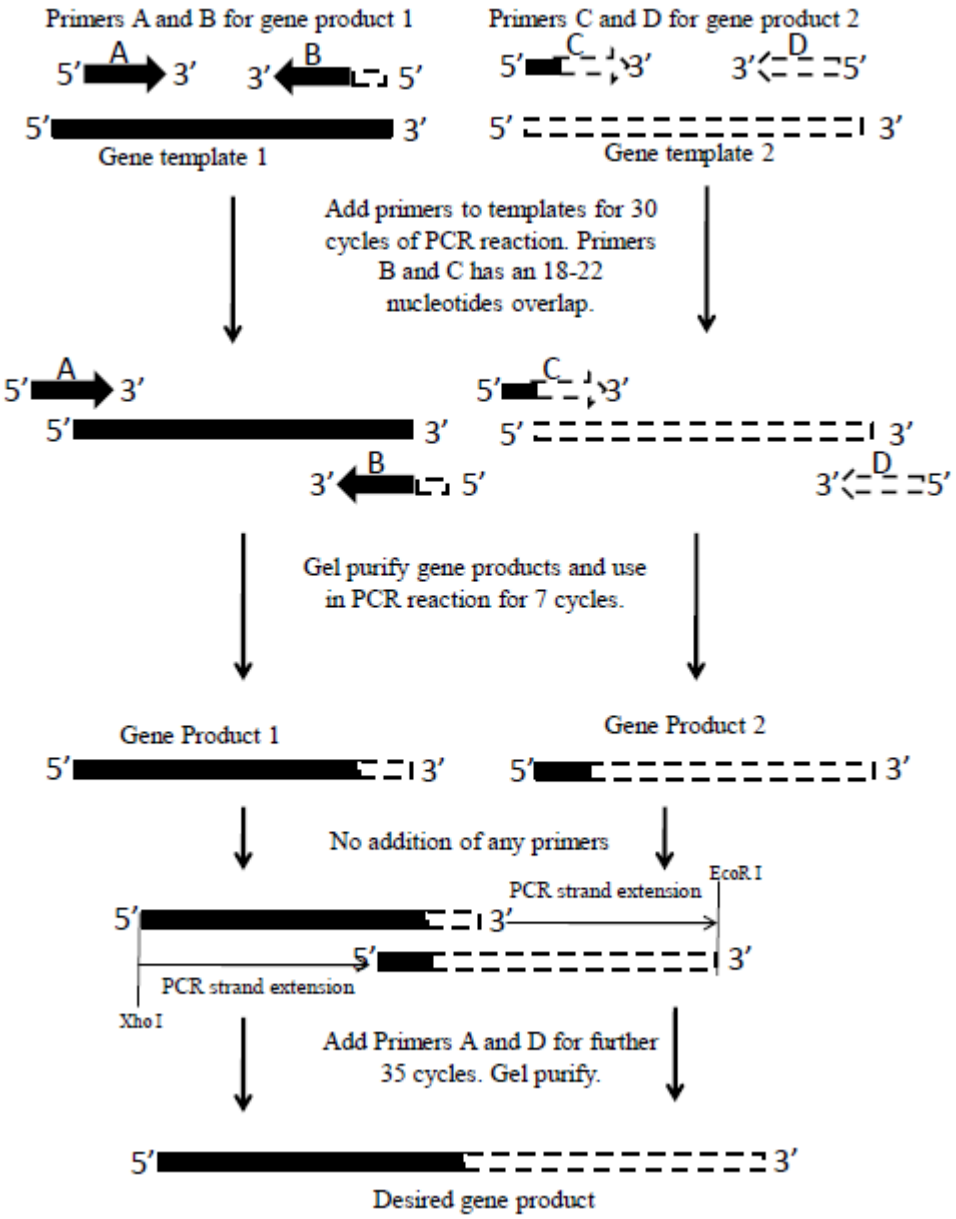

Figure 2.7: Steps involve in polymerase chain reaction for the amplification of gene fragments

PCR can be use to amplify a small amount of DNA. Here the technique of PCR is utilized in amplifying two gene templates using primers which bind to the gene sequences. The amplified templates are then ligated together using primers which overlap in their sequence. Adapted and modified from Dr. SA Marcus written protocol for PCR.

Primers	*Sequence*	*Description*
A	5'-GTT TAT CTC GAG CAT GGT GAG CAA GGG CGA GGA G-3'	Sense strand for *N*-terminal end of EGFP protein containing a restriction enzyme site for Xho I (underlined)
B	5′-GCA ACA GAT TCA CGG CTT TCA GTC GAA CCA GTC GAA CCA GTC GAA CCC TTG TAC AGC TCG TCC ATG C-3′	Reverse compliment of primer C for amplifying the end of EGFP-linker ESRES of the β_2 integrin.
C	5′-GCA TGG ACG AGC TGT ACA AGG GTT CGA CTG GTT CGA CTG GTT CGA CTG AAA GCC GTG AAT CTG TTG C-3′	Amplifying the EGFP-linker-ESRES of β_2 integrin
D	5'-ATT AAT GAA TTC TTA GTA TTC ACG CAG GTC AG-3'	Reverse primer D for the sense strand end of β_2 integrin with an EcoRI restriction enzyme site (underlined).
EGFPTM-CD	5′-ATT AAT GAA TTC TTT CCA GAT CAC CAG CAG-3′	For the sense strand of the β_2 integrin without the cytoplasmic end. It has an EcoRI restriction enzyme site underlined.
EGFPTM-5B	5′-ATT AAT GAA TTC TAC GAT GCC CGC AAC-3′	For the sense strand of the β_2 integrin with truncation of 5 a.a. residues from the *C*-terminal end of the TM domain with an EcoRI restriction enzyme site (underlined)
EGFPTM-10B	5`-ATT AAT GAA TTC GGC CGC GAT GTT TGG-3`	For the sense strand of the β_2 integrin with truncation of 10 a.a. residues from the *C*-terminal end of the TM domain with an EcoRI restriction enzyme site (underlined

Table 2.6. A description of primers used for PCR reactions. All primers were synthesized by Integrated DNA Technology.

Primers were synthesized by the IDT and provided in microgram concentrations.

Primer	*Target section of recombinant protein.*	*DNA and amino acid sequences of targeted section of protein.*
Primer A	Sense strand for *N*-terminal of the EGFP protein.	S S S M V S K G E E AGC TCG AGC ATG GTG AGC AAG GGC GAG GAG
Primers B and C	End of EGFP – linker – ESRES of β_2 integrin	M D E L Y K G S T G S T G GCATG GAC GAG CTG TAC AAG GGT TCG ACT GGT TCG ACT GGT S T E S R E S V TCG ACT GAA AGC CGT GAA TCT GTT GC
Primer D	Sense strand end of β_2 integrin end for the EGFPβ_2TM+CD protein.	W K A L I H L S D L R E Y TGG AAA GCT CTG ATT CAC CTG TCT GAC CTG CGT GAA TAC
Primer EGFPTM-CD	For the sense strand end of the β_2 integrin end for the EGFPβ_2TM-CD protein	L L V I W K CTG CTG GTG ATC TGG AAA
Primer EGFPTM-5B	For the sense strand end of the β_2 integrin end for the EGFPβ_2TM-5B protein	V A G I V GTT GCG GGC ATC GTA
Primer EGFPTM-10B	For the sense strand end of the β_2 integrin end for the EGFPβ_2TM-10B protein	P N I A A CCA AAC ATC GCG GCC

Table 2.7. Target regions of primers used in PCR amplifications.

Primers were used with either EGFP or KSIβ_2 genes as template for the PCR amplification of the recombinant genes.

To make a recombinant PCR fusion of *egfpβ$_2$tm+cd* we used four different primers designated EGFPβ$_2$ A to D synthesized by Integrated DNA technologies (Toronto, ON). *egfpβ$_2$tm-cd* was made using primer EGFPTM-CD (acts as primer D). Gene product 4 for synthesizing *egfpβ$_2$tm-5B* was amplified using primers C and EGFPTM-5B (as primer D). Finally, gene product 5 for synthesis of *egfpβ$_2$tm-10b* was made using primers C in addition to primer EGFPTM-10B. All PCR reactions were done using standard PCR protocol. All concentrations were measured using NanoDrop Spectrophotometer ND 1000 (NanoDrop Technologies, Inc. Wilmington, DE USA). Store all DNA at – 20 ºC for future use. The resulting gene products have XhoI and EcoRI restriction sites at the 5' and 3' ends respectively.

2.10.2.1.3. pBAD-His plasmid transformation with PCR products

Following manufacturer's protocol (Invitrogen) a double digestion mix was set up for a total of 8 h for both the plasmid and the PCR products. React 2 is suitable with Xho I but EcoR I is compatible with React 3 instead. Thus we added the required amount of 1 M NaCl for a final 100 mM before proceeding with EcoR I digestion for 4 h. Following digestion, a 1% analytical agarose gel was run and using QIAquick gel extraction kit, we excised and purify the correct gene bands. Also, the pBAD-His vector was extracted from the gel using the same QIAquick extraction kit. To check for the correctness of the DNA sequence of the purified plasmid, DNA sequencing was done using different primers that can target the different sections of the plasmid DNA for use in sequencing.

We used RecAI (5'-ATGCCATAGCATTTTTATCC-3') and RecBI (5'-GATTTAATCTGTATCAGG-3') primers for both the forward and reverse strands respectively for sequencing pBAD. Since the reversed strand was not well sequenced, we also used a primer DBZ28 (5`-ATGGTCCTGCTGGAGTTCCTG-3`) in addition to the EGFPβ_2D primer for the sequencing.

Sequencing was performed using BigDye Premix with all reactions being set up on ice using standard procedure. Use the program BDSEQ on the Techne PCR machine. Precipitation of the sequencing product was done using for BigDye premix following standard protocol. Air dry or dry briefly (2-5 m) in a vacuum centrifuge and submit samples for sequencing. Sequencing was done using the Genetic Analyzer 3730 (Applied Biosystems) with BigDye Terminator V 3.1 at the Molecular Biology Service Unit (MBSU) at the department of Biological Sciences, University of Alberta. Sequencing results confirmed the presence of PCR gene product in the plasmid following ligation using T4 DNA ligase (Invitrogen) as per manufacturer's protocol with an insert (I) to vector (V) ratio of 3:1. The DNA was amplified by transforming DH5α cc cells and then growing a single colony in 5 mL LB ampicillin broth overnight and purifying the plasmid using Fermentas miniprep purification kit for double stranded DNA. Transformation of *E. coli* cells with amplified plasmid DNA was by electroporation (BioRad's GenePulser). The *pBADHis- EGFPβ_2TM+CD* plasmid was introduced into *E. coli* LMG194 cells while all other plasmids were introduced into *E. coli* DH10B cells for expression of the proteins.

2.10.2.2. Protein expression

The conditions used for large-scale expression of the different proteins varied with the different *E. coli* cell strain used. For the EGFPβ_2TM+CD protein using the LMG194 cells, we used a low salt LB broth. LMG194 cells containing *pBADHis-egfp$\beta_2$tm+cd* construct were grown overnight while shaking at 225 rpm in a 2 mL LB amp broth. A litre of low salt LB ampicillin (containing 50 μg/mL amp, 10 g tryptone, 5 g yeast extract, and 5 g NaCl) broth for the culture of the cells was made in a 4 L baffle flask. The 2 mL of overnight culture (OD_{600} ~ 2.0) was transferred to the 4 L baffle flask containing the medium. Then flask was incubated at 37 °C while shaking at 225 rpm until OD_{600} ~ 0.60. 1 mL of 20% of L-arabinose was then added to a final concentration of 0.02%. Growth of cell culture was continued at 37 °C while shaking at 225 rpm for 4 h. Cells were harvested by spinning in JA10 rotor at 8000 rpm for 30 m. Pellet was weighed and stored at – 20 °C.

For protein expression in DH10B cells, we used a normal salt containing LB ampicillin broth (containing 50 μg/mL amp, 10 g tryptone, 5 g yeast extract, and 10 g NaCl). Grow a single colony in 2 mL of LB medium overnight at 37 ºC while shaking at 225 rpm. The OD_{600} should be between 1 and 2. Then the overnight culture was transferred to a 4 L baffle flask containing 1 L of LB ampicillin medium. This culture was grown at 37 ºC while shaking until OD_{600} ~ 0.6. 1 mL of 20% L-arabinose (final concentration of 0.02%) was added and the incubator's temperature lowered to 20 ºC. Growth of culture was continued for 6

– 8 h. Cells were harvested by centrifuging in a JA10 rotor at 8000 rpm for 30 m at 4 ºC. Supernatant was discarded and pellet weighed out and stored at – 20 ºC if protein extraction was not done immediately.

2.10.2.3. Protein purification

Purification was done under native conditions with the following buffers; lysis buffer (50 mM NaH_2PO_4, 300 mM NaCl, 10 mM imidazole , 0.2% TX-100 (can be substituted with 0.2% elugent) pH 8.0) wash buffer (50 mM NaH_2PO_4, 300 mM NaCl, 20 mM imidazole, pH 8.0) elution buffer (50 mM NaH_2PO_4, 300 mM NaCl, 250 mM imidazole, pH 8.0). Cell pellet was re-suspended in 50 mL of lysis buffer. A tablet of complete EDTA-free protease inhibitor and 50 µL of 5 mg/mL DNaseI were added and mixed well until cells were completely re-suspended. Lyses of cells was performed using Constant Cell disrupter (Low March, Daventry, Northants) at 24 kPsi in just one cycle. The cell lysate was spinned at 18,000 rpm in JA20 tubes for 30 min at 4 °C. Supernatant was decanted and stored at 4 °C. Both pellet and supernatant were fluoresced under UV at 510 nm.

Purification was performed using an immobilized metal affinity chromatography with nickel nitrilotriacetic acid (Ni-NTA) as a bead (QIAGEN). The recombinant proteins all have an *N*-terminal poly-histidine tag which readily chelate with the two free sites of the Ni ions in the Ni-NTA agarose column. Thus using a BioRad 10 mL column, 2.5 mL of the Ni-NTA agarose bead was loaded and allowed to settle at room temperature. The column was washed for 30 m with

the wash buffer at a flow rate of 1 mL/m followed by the passage of the clarified lysate at a rate of 0.5 mL/m to maximize binding of the protein to the column. After the flow through was collected, the wash buffer was still passed over the column at the same rate of 0.5 mL/m. Then the protein was eluted with the elution buffer and fractions collected in 1.5 mL tubes. To completely elute protein from the column, 0.1% elugent was added to the elution buffer and the concentration of imidazole was raised up to 500 mM. Tubes containing large amount of the protein were seen to fluoresce without the use of UV but much protein could be seen stocked on the column (as the column appeared green). The use of elugent was subsequently adopted as the proteins were to be used on human Jurkat cells.

The overall yield per litre of bacterial cultures was about 3.2 mg/mL for all recombinant protein whereas the yield for EGFP protein was about 6 mg/mL. Purified proteins were stored for long-term usage in 20 - 50% glycerol at -20 ºC. Before use, proteins are dialyzed in a buffer (containing 0.05% elugent, 100 mM NaCl, 50 mM NaH_2PO_4) for 4 h at 4 ºC in a 10,000 MWCO Slide-A-lyzer dialysis cassette.

2.10.2.4. Protein characterization

2.10.2.4.1. SDS PAGE

Denaturing SDS PAGE was used to characterize the purified proteins for confirmation of molecular weight. The stacking gel was 4% while the resolving gel was either 15% or 12%. Following protein purification, 2X SDS PAGE sample buffer was added to a small amount of the protein. Protein samples were

boiled on a heat block for 5 min at 95 ºC and placed on ice. Gels were loaded with 10 µL of the boiled protein sample and let run at a voltage of 150 V (BioRad minigel electrophoresis chamber, Hercules, CA). Gel was stopped after blue front of sample buffer was at the base of the gel, removed and washed with DI water and stained with either coomasie blue or coomasie fluor orange. Destaining was done using a destain solution and gel was imaged using the ImageQuant RT ECL (GE Healthcare Bioscience, Baie d'Urfe, QC) with either white light chemiluminescence (coomasie blue) or UV at an excitation of 302 nm and observing with the 557 nm emission filter.

2.10.2.4.2. CD spectroscopy

Protein solutions were dialyzed in a 100 mM NaCl, 50 mM NaH_2PO_4 and 0.05% elugent solution for 4 h at 4 ºC until protein started losing its solubility by forming insoluble protein. The solution was spinned down to completely separate the insoluble fraction from the soluble suspension. The soluble fraction is filtered using a 0.22 µm filter (Millipore) and using a 2 mm path length quartz cuvette, 150 µL of the protein solution was added and run using the ConvCD Olis Spectrometer (Quantum Northwest, Inc., Liberty Lake, WA). The scans (repeated scans of five) were collected with a monochromator excitation scan of 195 – 260 nm (far IR) with a fixed emission of 400 nm. The bandwidth was set at 2 nm and the samples were run at 25 ºC. Analysis was performed using the OlisGlobalworks software.

2.10.2.4.3. Mass spectrometry

We used MALDI-TOF for protein samples. All protein samples were dialyzed in a buffer containing reduced amounts of salt (50 mM NaCl, 25 mM NaH_2PO_4) using a 10 kDa MWCO dialysis cassette for 5-8 h at 4 ºC. Lyophilize all protein samples before proceeding with MALDI-TOF analysis. Make a 1 µg/µL protein concentration using different ratios of organic and inorganic solvents depending on the solubility of the protein. We used 50% acetonitril/methanol in 0.1% formic acid. The matrix used is sinapinic acid (SA) which is made of two different layers. In layer 1; we used a final 10 mg/mL SA in a solution of 4:1 acetone/methanol. Layer 2 is made from 10 mg/mL SA in a 1:1 acetonitrile/0.1% trifluoroacetic acid (TFA). Note that the second layer should have lesser organic solvent to prevent dissolution of the first layer. Wash the MALDI plate with organic solvent and clean starting and finishing with acetone. The SA layer solutions can be stored for up to a month at –20 ºC. Put a drop of layer on the plate and let dry. Then add layer 2 and let dry. Put your sample on the layer and allow to air dry too. Run the samples on the AB Sciex Voyager Elite MALDI instrument (AB Sciex, Foster city, CA, USA).

Liquid chromatography mass spectroscopy (ES LC MS/MS) was performed on the protein following an in-gel digestion as follows. Cast SDS gels and run immediately. Then excise gel bands and proceed with in-gel digestion otherwise store gel bands at – 80 ºC if digestion is not to be done immediately. For digestion, thaw gel bands at ambient temperature and wash with distilled

water for 10 min. Cover bands with acetonitrile (ACN), vortex for 20 s and let shrink (or till it turn white). Vacuum dry the band in a speed-vacuum for 10 – 30 min until dry. Then cover bands with 4.5 mM dithiothreitol (DTT) in 0.1 M NH_4HCO_3 and leave at 50 ºC for 30 min. then add iodoacetamide to a final concentration of 9 mM, vortex and let stand for 30 min in dark. Replace solution from gel with ACN and dehydrate as above (shrink and dry). Then cover gel bands with 5-10 ng/µL modified trypsin in 0.1 M NH_4HCO_3 and digest overnight at 30 ºC. Extract peptides from gel by three changes of 50% ACN in 0.2% TFA with 20 min of vortexing between each turn. Run samples on the Waters (micromass) Q-TOF Premier instrument (Waters, Milford, MA, USA).

2.10.2.5. Cell culture

Jurkat cells (clone E6.1) was obtained from ATCC (ATCC Number: TIB-15) as a frozen suspension. These cells are from Homo sapiens (humans) T lymphocytes from patient with acute T cell leukemia. T lymphocytes express T cell antigen receptors including LFA-1molecules, ICAM 1 and CD3 among other receptors and antigens. Jurkat clone E6.1 is a derivative of the Jurkat cell line that expresses high amounts of interleukin 2 (IL-2). Culturing of the Jurkat cells is done under sterile conditions using ATCC RPMI 1640 medium supplemented with 10% fetal bovine serum (FBS). 1% penicillin/streptomycin antibiotics is also added to prevent the growth of bacteria. The cells are cultured in a T-75 culture flask inside a 95% air, 5% CO_2 and 37 ºC incubator. Sub culturing is performed following manufacturer's protocol. Cells are grown to a density of $1x10^6$ to $3x10^6$

cells/mL which corresponds to cells in the late log phase. The culture is maintained by added fresh medium to small volume of the cells (depending on the density) Adding 9 mL of fresh medium to 1 mL of cells in their late log phase was found to keep the cells viable. Medium was change every 2-3 days depending on the number of cells seeded. Cultures can also be maintained by centrifuging at 1200 rpm for 2 m, followed by washing and re-suspension in fresh medium. The number of cells re-suspended depends on the density at the beginning preceding the wash steps.

2.10.2.5.1. Cell preparation for binding assays

Harvest cells (mid-late log phase) by spinning down in a 15 mL sterile tube for 2 m at 1200 rpm. Spinning at lower speeds for a few more minutes equally maintains the morphology of the cells. Wash cells two times using PBSSB buffer (1X PBS containing 1% BSA and 0.1% NaN_3 pH 7.2 - 7.4) Re-suspend cells in same buffer and put in 37 ºC incubator if cells are not used immediately. Count the number of cells and aliquot in sterile 1.5 mL eppendorf tubes in the BioSafety cabinet. Add proteins to cells to the desired final concentration as needed.

2.10.2.5.2. Binding assay

The binding of the recombinant proteins to human Jurkat cells clone E6.1 was done by incubating the various proteins with the cells followed by analysis with a flow cytometer. Washed cells were re-suspended in PBSSB buffer (1.5-2.0 x 10^6 cells/mL) and incubated with various concentrations of the recombinant

proteins. Protein stock solutions were dialyzed into a solution containing 100 mM NaCl, 50 mM Na_2HPO_4 and 0.05% elugent for 4 h at 4 ºC. This solution had both the soluble and insoluble protein in it except for the EGFP that is still completely soluble in the solution. The protein solutions were then centrifuged to pellet the insoluble form of the protein while the protein solution (containing soluble protein) was then used for the binding assays.

Total concentrations of the protein added to cells were as follows: 0, 2, 4, 6, 8, 10, 20, 30, 40, 50, 100, and 200 µg/mL. The same protein concentrations were used for all five proteins samples. Following addition of the protein, slightly vortex the tubes for protein to mix and place tubes horizontally on a flat surface. Total volume (of cells plus proteins) used in these experiments was 250 µL in a 1.5 mL tube. Incubate cells for 1 h at 37 ºC in a 95% air, 5% CO_2 incubator. After 1 hr of incubation, spin down tubes at 1200 rpm for 4 m and discard supernatant by carefully aspirating making sure the cell pellet stay intact. Then wash the cells with two volumes (500 µL) of PBSSB and re-suspend cells in same PBSSB. Fix the cells with one volume of 0.25% paraformaldehyde (PFA) on ice for 30 m. Wash cells again with two volumes of PBSSB buffer and re-suspend in same buffer (100 µL). Then add 20 µL of the fixed cells unto a 96 well plate containing 200 µL PBSSB/well and re-suspend by pipetting up and down. The samples are now ready for flow cytometry (FC) using the Beckman Coulter Cell Lab Quanta Flow cytometer (Brea, CA, USA).

2.10.2.5.3. Flow cytometry

Place a 96 welled plate containing samples on the plate holder. Select the program 'NGE- Cairo Lab', select the wells containing the samples and run. This program has been set to analyse cells that show high fluorescence and low fluorescence (62-63). The FL1 window is set to show the fluorescence (GFP) against electronic volume (EV) of the cells. With the following settings; Gain of 1.69, side scattering (SS) of 3.90, flow rate of 39.0 µL/m, the photon multiplier tube (PMT) voltage of the FL1 set at 6.13, we are able to distinguished clearly the labeled from unlabelled cells. The number of fluorescent cells is analyzed from a total of 5000 cells that the machine is set to count. Cells were gated (Region 1) from the region of the cell population with a mean cell diameter of about 10 µm. From this population of cells, green fluorescence cells are sorted into region 2 which appears on the FL1 channel. The cytometer uses an argon laser source at 488 nm to excite the EGFP chromophore and emission is observed at 525 nm.

2.10.2.5.4. Analysis of FC data

The percentage of fluorescence is proportional to the mean fluorescence intensity of the sorted cells. Three runs were performed for each cell treatment (n=3) and the mean percentage of fluorescent cells calculated. Since the cell population followed a binomial distribution with mean cell diameter of 10 µm (seen on the EV vs SS plot) we computer the error for each sample runs using standard deviation of the mean (SD). The data obtained from all protein were analysed to determine the EC_{50}, B_{max} and K_d of each peptide. By fitting the data to

a standard EC_{50} curve (eq. 1) we could obtain the respective EC_{50} values (Plot of log of protein concentration against % of labeled cells).

$F = BOTTOM+TOP-BOTTOM/(1 + 10^{(X-LogEC_{50})})$ **Equation 2.1**

Similarly, fitting the data to a standard single-site binding model (eq.2) we obtained the B_{max} and K_d values of all proteins by plotting protein concentration against % of labeled cells.

$Y = B_{max}*X/(K_d + X)$ **Equation 2.2**

All analysis was performed using the GraphPad software, Prism (GraphPad Software Inc, La Jolla, CA). The overlaid histogram analyses were done using the Beckman Coulter flow cytometry analysis software, Kaluza V 1.1.

2.10.2.6. Fluorescence microscopy

Prepare cells as above for flow cytometry and incubate with the required final protein concentration for 1 h at 37 ºC. Wash cells following protein treatment two times with two volumes of PBSSB buffer at pH 7.2. Re-suspend cells in same buffer and place 10 µL on a 1.5 mm microscope slide. Cover slides with a 1.5 inch slide cover and let dry. Mount on microscope and observe under a 60X oil immersion objective at room temperature. Use the diascopic and epi-fluorescence light source for image collection. Using the EPI light, we used the GFP BP filter to observe for fluorescent cells. All images was done using the Nikon Eclipse Ti fluorescent microscope (Nikon Instruments, Melville, NY, USA)

2.11. REFERENCES

1. Auerbach, D., Thaminy, S., Hottiger, M. O., and Stagljar, I. (2002) The post-genomic era of interactive proteomics: facts and perspectives, *Proteomics 2*, 611-623.
2. Molecular Cell Biology by Harvey Lodish et al.`, 6th Edition.
3. Yin, H. (2008) Exogenous agents that target transmembrane domains of proteins, *Angew Chem Int Ed Engl 47*, 2744-2752.
4. Gerber, D., Sal-Man, N., and Shai, Y. (2004) Two motifs within a transmembrane domain, one for homodimerization and the other for heterodimerization, *J Biol Chem 279*, 21177-21182.
5. Slivka, P. F., Wong, J., Caputo, G. A., and Yin, H. (2008) Peptide probes for protein transmembrane domains, *ACS Chem Biol 3*, 402-411.
6. Gerber, D., Quintana, F. J., Bloch, I., Cohen, I. R., and Shai, Y. (2005) D-enantiomer peptide of the TCRalpha transmembrane domain inhibits T-cell activation in vitro and in vivo, *FASEB J 19*, 1190-1192.
7. Manolios, N., Collier, S., Taylor, J., Pollard, J., Harrison, L. C., and Bender, V. (1997) T-cell antigen receptor transmembrane peptides modulate T-cell function and T cell-mediated disease, *Nat Med 3*, 84-88.
8. Gollner, G. P., Muller, G., Alt, R., Knop, J., and Enk, A. H. (2000) Therapeutic application of T cell receptor mimic peptides or cDNA in the treatment of T cell-mediated skin diseases, *Gene Ther 7*, 1000-1004.
9. Zhao, T. X., Martinko, A. J., Le, V. H., Zhao, J., and Yin, H. (2010) Development of agents that modulate protein-protein interactions in membranes, *Curr Pharm Des 16*, 1055-1062.
10. Tarasova, N. I., Rice, W. G., and Michejda, C. J. (1999) Inhibition of G-protein-coupled receptor function by disruption of transmembrane domain interactions, *J Biol Chem 274*, 34911-34915.
11. Yin, H., Slusky, J. S., Berger, B. W., Walters, R. S., Vilaire, G., Litvinov, R. I., Lear, J. D., Caputo, G. A., Bennett, J. S., and DeGrado, W. F. (2007) Computational design of peptides that target transmembrane helices, *Science 315*, 1817-1822.
12. Vararattanavech, A., Lin, X., Torres, J., and Tan, S. M. (2009) Disruption of the integrin alphaLbeta2 transmembrane domain interface by beta2 Thr-686 mutation activates alphaLbeta2 and promotes micro-clustering of the alphaL subunits, *J Biol Chem 284*, 3239-3249.
13. Caputo, G. A., Litvinov, R. I., Li, W., Bennett, J. S., Degrado, W. F., and Yin, H. (2008) Computationally designed peptide inhibitors of protein-protein interactions in membranes, *Biochemistry 47*, 8600-8606.
14. Yin, H., Litvinov, R. I., Vilaire, G., Zhu, H., Li, W., Caputo, G. A., Moore, D. T., Lear, J. D., Weisel, J. W., Degrado, W. F., and Bennett, J. S. (2006) Activation of platelet alphaIIbbeta3 by an exogenous peptide corresponding to the transmembrane domain of alphaIIb, *J Biol Chem 281*, 36732-36741.

15. Li, R., Babu, C. R., Lear, J. D., Wand, A. J., Bennett, J. S., and DeGrado, W. F. (2001) Oligomerization of the integrin alphaIIbbeta3: roles of the transmembrane and cytoplasmic domains, *Proc Natl Acad Sci U S A 98*, 12462-12467.
16. http://www.ncbi.nlm.nih.gov/protein/124056465
17. Bovey, F. A., and Hood, F. P. (1967) The circular dichroism spectrum of poly-L-acetoxyproline, *Biopolymers 5*, 915-919.
18. Beychok, S. (1966) Circular dichroism of biological macromolecules, *Science 154*, 1288-1299.
19. Beychok, S., Armstrong, J. M., Lindblow, C., and Edsall, J. T. (1966) Optil rotatory dispersion and circular dichroism of human carbonic anhydrases B and C, *J Biol Chem 241*, 5150-5160.
20. Miles, D. W., Robins, R. K., and Eyring, H. (1967) Optical rotatory dispersion, circular dichroism, and absorption studies on some naturally occurring ribonucleosides and related derivatives, *Proc Natl Acad Sci U S A 57*, 1138-1145.
21. Miles, D. W., Robins, R. K., and Eyring, H. (1967) Substituent effects on the optical activity of some purine nucleosides, *J Phys Chem 71*, 3931-3941.
22. Greenfield, N. J. (1996) Methods to estimate the conformation of proteins and polypeptides from circular dichroism data, *Anal Biochem 235*, 1-10.
23. Tiffany, M. L., and Krimm, S. (1972) Effect of temperature on the circular dichroism spectra of polypeptides in the extended state, *Biopolymers 11*, 2309-2316.
24. Quadrifoglio, F., and Urry, D. W. (1968) Ultraviolet rotatory properties of polypeptides in solution. I. Helical poly-L-alanine, *J Am Chem Soc 90*, 2755-2760.
25. Greenfield, N., and Fasman, G. D. (1969) Computed circular dichroism spectra for the evaluation of protein conformation, *Biochemistry 8*, 4108-4116.
26. Chen, Y. H., Yang, J. T., and Chau, K. H. (1974) Determination of the helix and beta form of proteins in aqueous solution by circular dichroism, *Biochemistry 13*, 3350-3359.
27. Saxena, V. P., and Wetlaufer, D. B. (1971) A new basis for interpreting the circular dichroic spectra of proteins, *Proc Natl Acad Sci U S A 68*, 969-972.
28. Rucker, A. L., and Creamer, T. P. (2002) Polyproline II helical structure in protein unfolded states: lysine peptides revisited, *Protein Sci 11*, 980-985.
29. Tsien, R. Y. (1998) The green fluorescent protein, *Annu Rev Biochem 67*, 509-544.
30. Shimomura, O., Johnson, F. H., and Saiga, Y. (1962) Extraction, purification and properties of aequorin, a bioluminescent protein from the luminous hydromedusan, Aequorea, *J Cell Comp Physiol 59*, 223-239.

31. Morise, H., Shimomura, O., Johnson, F. H., and Winant, J. (1974) Intermolecular energy transfer in the bioluminescent system of Aequorea, *Biochemistry 13*, 2656-2662.
32. Tarasova, N. I., Seth, R., Tarasov, S. G., Kosakowska-Cholody, T., Hrycyna, C. A., Gottesman, M. M., and Michejda, C. J. (2005) Transmembrane inhibitors of P-glycoprotein, an ABC transporter, *J Med Chem 48*, 3768-3775.
33. Russ, W. P., and Engelman, D. M. (2000) The GxxxG motif: a framework for transmembrane helix-helix association, *J Mol Biol 296*, 911-919.
34. Senes, A., Engel, D. E., and DeGrado, W. F. (2004) Folding of helical membrane proteins: the role of polar, GxxxG-like and proline motifs, *Curr Opin Struct Biol 14*, 465-479.
35. Javadpour, M. M., Eilers, M., Groesbeek, M., and Smith, S. O. (1999) Helix packing in polytopic membrane proteins: role of glycine in transmembrane helix association, *Biophys J 77*, 1609-1618.
36. Kim, S., Jeon, T. J., Oberai, A., Yang, D., Schmidt, J. J., and Bowie, J. U. (2005) Transmembrane glycine zippers: physiological and pathological roles in membrane proteins, *Proc Natl Acad Sci U S A 102*, 14278-14283.
37. Walters, R. F., and DeGrado, W. F. (2006) Helix-packing motifs in membrane proteins, *Proc Natl Acad Sci U S A 103*, 13658-13663.
38. Schneider, D., and Engelman, D. M. (2004) Motifs of two small residues can assist but are not sufficient to mediate transmembrane helix interactions, *J Mol Biol 343*, 799-804.
39. Dawson, J. P., Weinger, J. S., and Engelman, D. M. (2002) Motifs of serine and threonine can drive association of transmembrane helices, *J Mol Biol 316*, 799-805.
40. Dawson, J. P., Melnyk, R. A., Deber, C. M., and Engelman, D. M. (2003) Sequence context strongly modulates association of polar residues in transmembrane helices, *J Mol Biol 331*, 255-262.
41. Popot, J. L., and Engelman, D. M. (1990) Membrane protein folding and oligomerization: the two-stage model, *Biochemistry 29*, 4031-4037.
42. Popot, J. L., and Engelman, D. M. (2000) Helical membrane protein folding, stability, and evolution, *Annu Rev Biochem 69*, 881-922.
43. Ladokhin, A. S., and White, S. H. (2004) Interfacial folding and membrane insertion of a designed helical peptide, *Biochemistry 43*, 5782-5791.
44. Lew, S., Caputo, G. A., and London, E. (2003) The effect of interactions involving ionizable residues flanking membrane-inserted hydrophobic helices upon helix-helix interaction, *Biochemistry 42*, 10833-10842.
45. Wimley, W. C., and White, S. H. (2000) Designing transmembrane alpha-helices that insert spontaneously, *Biochemistry 39*, 4432-4442.
46. Melnyk, R. A., Partridge, A. W., Yip, J., Wu, Y., Goto, N. K., and Deber, C. M. (2003) Polar residue tagging of transmembrane peptides, *Biopolymers 71*, 675-685.

47. Maeda, M., Melnyk, R. A., Partridge, A. W., Liu, L. P., and Deber, C. M. (2003) Transmembrane segment peptides with double D-amino acid replacements: helicity, hydrophobicity, and antimicrobial activity, *Biopolymers 71*, 77-84.
48. Rees, D. C., DeAntonio, L., and Eisenberg, D. (1989) Hydrophobic organization of membrane proteins, *Science 245*, 510-513.
49. Gratkowski, H., Lear, J. D., and DeGrado, W. F. (2001) Polar side chains drive the association of model transmembrane peptides, *Proc Natl Acad Sci U S A 98*, 880-885.
50. Krishnakumar, S. S., and London, E. (2007) The control of transmembrane helix transverse position in membranes by hydrophilic residues, *J Mol Biol 374*, 1251-1269.
51. Hessa, T., Kim, H., Bihlmaier, K., Lundin, C., Boekel, J., Andersson, H., Nilsson, I., White, S. H., and von Heijne, G. (2005) Recognition of transmembrane helices by the endoplasmic reticulum translocon, *Nature 433*, 377-381.
52. Zhou, F. X., Cocco, M. J., Russ, W. P., Brunger, A. T., and Engelman, D. M. (2000) Interhelical hydrogen bonding drives strong interactions in membrane proteins, *Nat Struct Biol 7*, 154-160.
53. Li, S. C., and Deber, C. M. (1994) A measure of helical propensity for amino acids in membrane environments, *Nat Struct Biol 1*, 558.
54. Li, S. C., and Deber, C. M. (1993) Peptide environment specifies conformation. Helicity of hydrophobic segments compared in aqueous, organic, and membrane environments, *J Biol Chem 268*, 22975-22978.
55. Krishnakumar, S. S., and London, E. (2007) Effect of sequence hydrophobicity and bilayer width upon the minimum length required for the formation of transmembrane helices in membranes, *J Mol Biol 374*, 671-687.
56. White, S. H., and Wimley, W. C. (1999) Membrane protein folding and stability: physical principles, *Annu Rev Biophys Biomol Struct 28*, 319-365.
57. MacKenzie, K. R., and Engelman, D. M. (1998) Structure-based prediction of the stability of transmembrane helix-helix interactions: the sequence dependence of glycophorin A dimerization, *Proc Natl Acad Sci U S A 95*, 3583-3590.
58. Zhou, F. X., Merianos, H. J., Brunger, A. T., and Engelman, D. M. (2001) Polar residues drive association of polyleucine transmembrane helices, *Proc Natl Acad Sci U S A 98*, 2250-2255.
59. Russ, W. P., and Engelman, D. M. (1999) TOXCAT: a measure of transmembrane helix association in a biological membrane, *Proc Natl Acad Sci U S A 96*, 863-868.
60. Jaroniec, C. P., Kaufman, J. D., Stahl, S. J., Viard, M., Blumenthal, R., Wingfield, P. T., and Bax, A. (2005) Structure and dynamics of micelle-

associated human immunodeficiency virus gp41 fusion domain, *Biochemistry 44*, 16167-16180.
61. Piszkiewicz, D., Landon, M., and Smith, E. L. (1970) Anomalous cleavage of aspartyl-proline peptide bonds during amino acid sequence determinations, *Biochem Biophys Res Commun 40*, 1173-1178.
62. Dundr, M., McNally, J. G., Cohen, J., and Misteli, T. (2002) Quantitation of GFP-fusion proteins in single living cells, *J Struct Biol 140*, 92-99.
63. Dundr, M., Hoffmann-Rohrer, U., Hu, Q., Grummt, I., Rothblum, L. I., Phair, R. D., and Misteli, T. (2002) A kinetic framework for a mammalian RNA polymerase in vivo, *Science 298*, 1623-1626.
64. http://tools.invitrogen.com/content/sfs/manuals/pbad_man.pdf.

CHAPTER THREE

EFFECTS OF B_2 TM CONSTRUCTS AND GLYCOSIDASES ON LFA-1 EPITOPES[4,5,6,7,8]

[4] TS2/4 monoclonal antibody was provided by Christopher M. Sadek, Department of Chemistry, University of Alberta.
[5] MBP- Neu3 enzyme was provided by Amgad Albohy, Department of Chemistry, University of Alberta.
[6] GST-Neu4 was provided by Ruixiang Zheng (Blake), Department of Chemistry,University of Alberta.
[7] OKT3 monoclonal antibody was provided by Chun Xia (Cecilia), Department of Chemistry, University of Alberta.
[8] We acknowledge flow cytometer access by Dr. James Stafford, Department of Biological Sciences, University of Alberta.

3.1. INTRODUCTION

The function of receptors can be influenced by molecules that either activate or inhibit specific pathways through which these receptors function. The function of LFA-1 receptors on T lymphocytes is well known to be modulated by small molecules, kinases, metal ions and others (1, 2). As such, some compounds or molecules can either inhibit or activate the receptor resulting to either a decrease or an increase in their binding ability to monoclonal antibody (mAb) that target specific epitopes on this receptor. In this chapter we explore the effects of recombinant β_2 TM proteins on the binding properties of LFA-1 via mAbs that bind specific epitopes on the receptor.

Our initial approach in testing the biological significance of our recombinant proteins had been to do an adhesion assay with Jurkat cells or other LFA-1 expressing cell lines. We were unable to obtain reproducible results with a functional adhesion assay using ICAM-1 and LFA-1 to evaluate the change in adhesion of the Jurkat cells to fluosphere beads conjugated with these proteins. Thus we resulted in utilising mAbs directed against epitopes on either the α_L or β_2 integrins. We utilized the T cell activation epitopes: MEM48, MEM148 against the β_2 integrin and the TS1/22 inhibitory epitope against the α_L integrin. The OKT3 mAb is a murine Ab that belongs to the IgG2a Ig isotype and specifically targets the ε- chain of the CD3 receptor on mature T cells (3). OKT3 has been used for treatment of renal graft rejections, and for the treatment of acute rejection in liver and heart transplant recipients (4-6). The CD18 activating Ab MEM48 is a

monoclonal Ab that specifically recognises an epitope consisting of residues 534-546 cystein rich repeats on CD18 antigen (7).

Another CD18 antibody we utilized in the study is MEM148 which is also an activation-dependent antibody that binds an inaccessible epitope on intact β_2 integrin on resting leukocytes (8-10). This epitope is exposed on the activated leukocyte having the high-affinity state of LFA-1 molecule or on un-associated β_2 integrin (8). To study the effect of our recombinant peptides on LFA-1, we utilized other antibodies specific for the CD11a integrin. TS1/22 is an inhibitory mAb that specifically binds to an epitope on the I-domain of CD11a causing inhibition of T cell chemotaxis in response to interleukin-2 and lymphocyte chemotactic factor (LCF) and suppresses T cell migration via human umbilical vein endothelia cell (HUVEC) monolayer (11). TS1/22 is a competitive inhibitor of ICAM-1 that binds to the same epitope. We used the anti- CD11a antibody, TS2/4 as a positive control antibody which binds to the β-propeller of CD11a integrin (12-14).

The change in binding of these mAb was monitored through FC for cells that were bound to 1 μm red or yellow-green fluosphere beads labelled with the mAb. Fluospheres are fluorescent probes which serve as sensitive tools for obtaining functional and structural information on a number of cellular and functional processes. Due to their high sensitivity, they can be use for receptor tracking on cell surfaces especially as such receptors are usually expressed in very small concentrations. They can thus be used for flow cytometry and fluorescent

microscopy experiments with instruments having the appropriate lasers for detecting the beads.

Very little is known about the role of glycosylation on LFA-1. Previous work by Asada and coworkers on the glycosylation of LFA-1 has predicted that there are 12 sites for N-linked glycosylationon the α_L chain and 6 sites on the β_2 chain (47). Since our group is interested in understanding the role of glycosylation on LFA-1 and we have access to the protein, we decided to study the effect of glycosidases on LFA-1. The function of carbohydrates on LFA-1 receptor was investigated through the use of glycosidases including mammalian neuraminadase (MBP-NEU3 and GST-NEU4), bacterial neuraminidase (NEUX), two endoglycosidases: Endo H_f and PNGase F. Lastly we investigated the effect of the interfering proteins made on the adhesiveness of LFA-1 receptor through their effects on the binding of the different mAbs.

Our hypothesis is that the recombinant proteins can insert into membranes and cause receptor disruption. If this model is correct, we expect to observe a change in the binding of MEM48 or MEM148 labelled beads to their respective epitopes since these epitopes are activating and accessible only on the high affinity form of LFA-1 or isolated form of the β_2 integrin. Cells were first incubated with the β_2 TM proteins followed by washing to remove unbound proteins. The cells were then treated with fluosphere beads labelled with the different mAbs. Following incubation of the cells with the labelled beads, the cells were washed to remove unbound beads, resuspended and sorted for

fluorescently labelled cells. This experiment makes use of red fluosphere beads as the β_2 TM proteins all contain a green fluorescent protein. Therefore we used the red fluorophore of the beads to detect mAb binding separately from EGFP. A change in binding of the cells to mAb labelled beads can be followed by plotting green vs red fluorescence and tracking the shift in cell population.

We used pIgG (from fetal bovine serum) as a control Ab, OKT3 mAb (human) as a TCR mAb. To target β_2 (CD18) integrin, we used MEM48, a mAb against human CD18 which is an activating epitope. MEM148 mAb is also used to target CD18 integrin, another activating epitope. TS1/22 inhibitory mAb against LFA-1 (against CD11a integrin) was used along side with the TS2/4 mAb that targets intact LFA-1 receptor. The use of phorbol 12-myristate 13-acetate (PMA), cytochalasin D (cyto D) and TS2/4 mAb to either inhibit (cyto D, TS2/4) or activate (PMA) the LFA-1 was also investigated.

3.2. EFFECTS OF ACTIVATORS AND INHIBITORS ON LFA-1 BINDING EPITOPES

The use of phorbol esters has been widely applied in stimulating lymphocytes. The exact mechanism of LFA-1 activation via phorbol esters is through protein kinase-c (PKC) activation (15). Phorbol esters such as phorbol-12-myristate-13-acetate (PMA) have been shown to activate LFA-1 by forming clusters through cross linking of receptors (16-18). This clustering does not result in an increase in expression of the LFA-1 molecules on T-cells but probably leads to an increase in the number of high affinity forms of the receptor (16).

To inhibit LFA-1 adhesion, cytochalasin D (cyto D), a cell-permeable fungal mycotoxin which acts by binding to actin filaments, was used (19). Its binding leads to disruption of actin filaments and inhibition of actin polymerization. In effect, it inhibits polymerization and depolymerisation of actin sub-units. We treated cells with a total of 5 µg/mL cyto D for 30 min before labelling cells for an additional one hour with fluosphere beads containing different mAb. Cyto D inhibit LFA-1 binding in a similar way as cyto B has been shown to inhibit LFA-1 (+) T cells (18). Lastly LFA-1 receptors were pre-blocked using soluble TS2/4 mAb that recognises and binds to the intact LFA-1 receptor on cell surfaces.

3.2.1. Effects of PMA on LFA-1 epitopes

The effect of treating Jurkat cells clone E6.1 with 100 ng/mL of PMA was investigated by measuring their ability to bind to fluosphere beads conjugated with different mAbs recognising different epitopes on the LFA-1 receptor. Table A6 shows the data obtained while Tables A7 and A8 shows the respective normalized data to buffer condition and pIgG beads (see appendix). Figure 3.1 shows bar graph plots obtained when all treatment are normalized to the buffer condition (as control). By normalizing the data set to the labelling under the buffer condition, we observed an increase in binding to the MEM48 and MEM148 epitopes associated with PMA treatment. There was a greater than 100% (two-fold) increase in binding of the cells to MEM48 and MEM148-conjugated beads. This suggests an increase in the number of high affinity forms of LFA-1 as these

epitopes are all activation dependent. Beads conjugated with TS1/22 (4%) and TS2/4 (- 6%) did not have a significant binding change since the epitopes for these mAbs are not activation.

3.2.2. Effect of cytochalasin D on LFA-1 epitopes

The buffer normalized data shows a decrease in binding of mAb to the cells when treated with cyto D. We observed a 65% decrease in binding of LFA-1 to OKT3-conjugated beads while a reduction of about 33% and 32% was seen with MEM48 and MEM148 conjugated beads respectively. There was a 41% reduction in the binding ability of LFA-1 to TS1/22-conjugated beads while a very small reduction of 7% for TS2/4 conjugated beads. Cyto D thus has an inhibitory effect on the LFA-1 receptors both on its β_2 and α_L integrins and on a TCR. This is probably due to their direct disruption of actin filaments and inhibition of actin polymerization.

3.2.3. Effects of soluble TS2/4 mAb blocking on LFA-1 epitopes

The buffer normalized data shows a reduction in the binding of OKT3-conjugated beads by 77% when cells are treated with TS2/4 mAb. A decrease in binding of 14% was observed for MEM48-conjugated beads while almost no change (1%) was observed with MEM148-conjugated beads. There was a corresponding 9% reduction in binding to the TS1/22-conjugated beads and a drastic reduction of 80% to TS2/4-conjugated beads, indicating that the mAb was effectively blocking binding. The reduction in binding seen with OKT3 may be attributed to the fact that soluble TS2/4 mAb recognises a similar epitope on TCR

which OKT3 too binds too. The reduction is similar to observed reduction in the case of TS2/4-conjugated beads implying a strong binding of soluble TS2/4. In the case of MEM48-conjugated beads, the slight reduction may be due to an overlap of the TS2/4 binding epitope with that of MEM48 on the β_2 integrin. Since no change was observed with MEM148-conjugated beads, it suggests that the two epitopes are completely separated. TS1/22 epitopes may overlap with TS2/4 or completely separate too from the observed 9% reduction with TS1/22-conjugated beads.

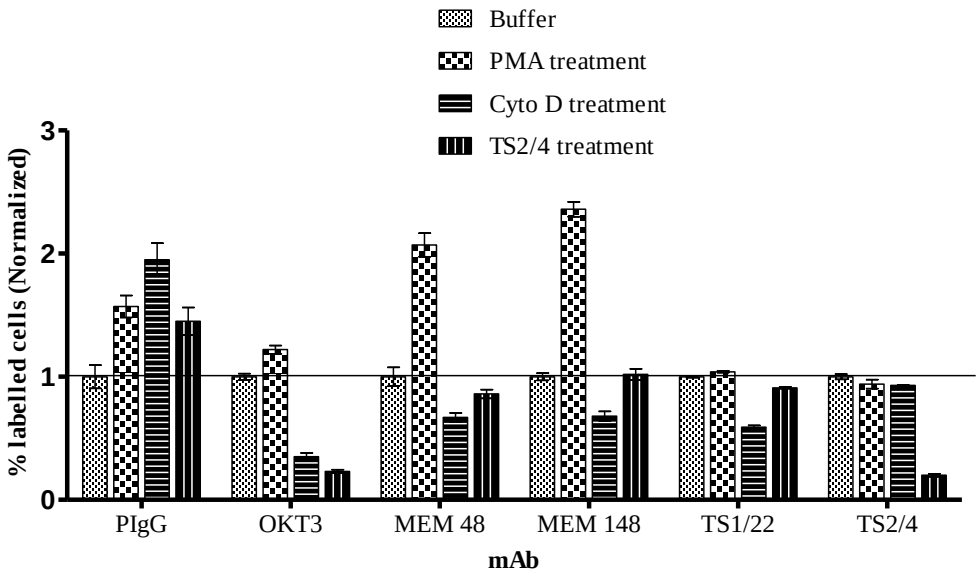

Figure 3.1: mAb epitopes on Jurkat cells under treatments with agonist and antagonists.

FC data for YG beads conjugated to mAbs was normalized to buffer treatment for each antibody. MEM48 and MEM148-conjugated beads binding following treatment with PMA is consistent with literature in which PMA has been shown to induce activation of LFA-1 receptors (17).

3.3. EFFECTS OF GLYCOSIDASES ON LFA-1 BINDING EPITOPES

Glycosidases are hydrolytic enzymes that cleave glycans from glycoproteins and glycolipids (20-22). Glycosidases will cleave carbohydrate residues on protein or lipid thereby modifying their functions. Approximately 50% of mammalian proteins are either co-translationally or post-translationally modified with carbohydrates either through O-link (involving the hydroxyl groups of Ser and Thre or carboxyl groups of Glu and Asp) or N-linked (involving amine groups of Asn, Gln, Lys, Arg and His) (48). We used human fusion neuraminadases (MBP-NEU3 and GST-NEU4) (44), the *Clostridium perfringens* bacterial neuraminidase (NEUX), *Streptomyces plicatus* bacterial endoglycosidases, Endo-β-N-acetylglucosaminidase H (Endo H_f) and the *Flavobacterium meningosepticum* bacterial endoglycosidase, peptide-N^4-(N-acetyl-beta-D-glucosaminyl)-asparagine amidase (PNGase F) which are all enzymes that remove carbohydrate residues from high mannose, hybrid and/or complex oligosaccharides from N-linked glycoproteins (23, 24). The data obtained from treatment with neuraminidases is presented on Table A9 (appendix). The normalized data to the buffer PBSSB pH 5.5 is shown on Table A10 (appendix) while the data normalized to the labelling with pIgG conjugated beads are shown on Figure A11 (See Appendix). Figure 3.2 show the bar charts obtained from the normalized data to the buffer condition.

3.3.1. Effects of NEU3 treatment on LFA-1 epitopes

Treatment of Jurkat cells with NEU3 and subsequent labelling with fluosphere beads conjugated with mAb showed a general increase in binding compared to cells that were not treated. There was an 86% increase in binding with OKT3-conjugated beads, a 15% increase with MEM48-conjugated beads, 22% increase with MEM148 beads, 56% increase in case of TS1/22 and a 13% increase with TS2/4 beads. Treatment of cells with NEU3 therefore results in an increase in binding of the mAb-conjugated beads to their epitopes on LFA-1.

3.3.2. Effects of NEU4 treatment on LFA-1 epitopes

Results showed a general decrease in binding to mAb-conjugated beads compared to cells that were not treated. There is a 14% decrease in binding with OKT3-conjugated beads, a 43% decrease with MEM48-conjugated beads, 33% decrease with MEM148-conjugated beads, 6% decrease in case of TS1/22-beads and a 2% increase with TS2/4-beads. In general, NEU4 causes a reduction in the binding of mAb-conjugated beads to their epitopes on LFA-1 receptor.

3.3.3. Effects of bacterial NEUX treatment on LFA-1 epitopes

Results showed a general increase in binding compared to cells that were not treated. There was a 119% increase in binding with OKT3-conjugated beads, a 55% increase with MEM48-conjugated beads, 70% increase with MEM148-conjugated beads, 26% increase in case of TS1/22 and an 8 % increase with TS2/4 conjugated beads. Thus, bacterial neuraminidase enzyme greatly increased the

binding of mAb-conjuagated beads to their respective epitopes on LFA-1 receptor.

3.3.4. Effect of Endo H_f treatment on LFA-1 epitopes

Results showed a general decrease in binding compared to cells that were not treated. There was a 2% decrease in binding with OKT3-conjugated beads, a 1% decrease with MEM48-conjugated beads, 13% decrease with MEM148-conjugated beads, 36% decrease in case of TS1/22 and a 1 % increase with TS2/4 conjugated beads. In effect Endo H_f have a very negligible effect on the epitopes on LFA-1 except for the MEM148 and TS1/22 where it had a inhibitory effect.

3.3.5. Effects of PNGase F treatment on LFA-1 epitopes

Treatment of Jurkat cells with bacterial PNGase F and subsequent labelling with fluosphere beads conjugated with mAb showed a general increase in binding compared to cells that were not treated. There was a 53% increase in binding with OKT3-conjugated beads, a 15% increase with MEM48-conjugated beads, 25% increase with MEM148-conjugated beads, 16% increase in case of TS1/22 and no increase with TS2/4 conjugated beads. In effect PNGase F has a positive effect on the binding of LFA-1 epitopes to their mAb by increasing binding of these epitopes.

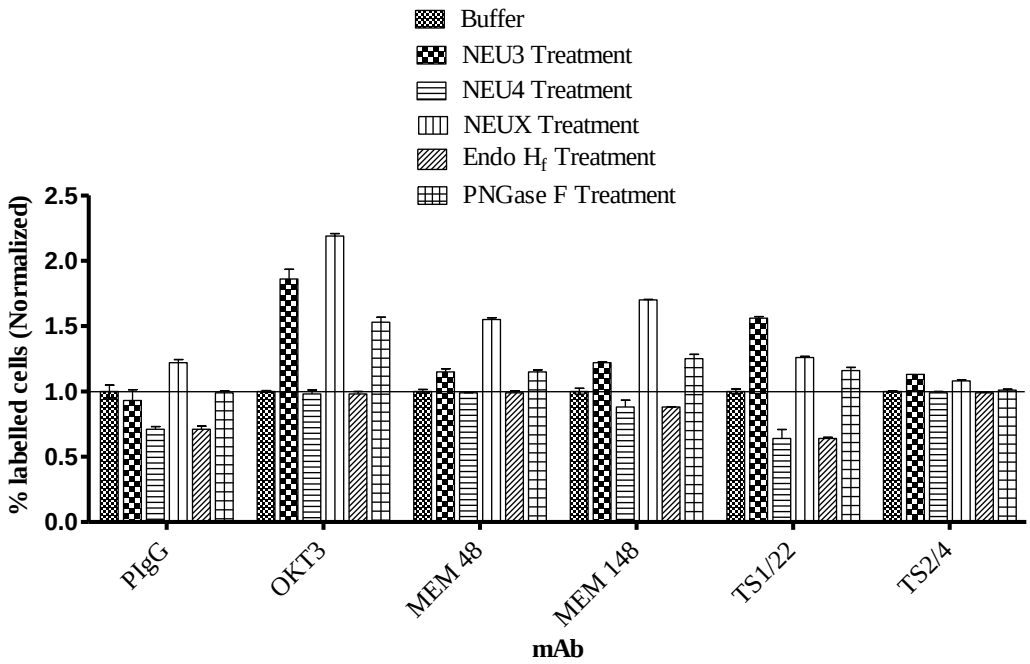

Figure 3.2: Binding of mAb to glycosidase-treated cells normalized to buffer condition

Labelling of Jurkat cells with mAb conjugated fluospheres after glycosidase treatment. Data are plotted as the normalized change in labelled cells relative to buffer treatment. MBP-NEU3 and GST-NEU4 were used at a final concentration of 20 µg/mL while NEUX was used at 20 mU/mL. Endo H_f was used at 10000 U/mL final concentration while PNGase F was at 5000 U/mL.

3.4. EFFECTS OF INTERFERING PROTEINS ON LFA-1 BINDING EPITOPES

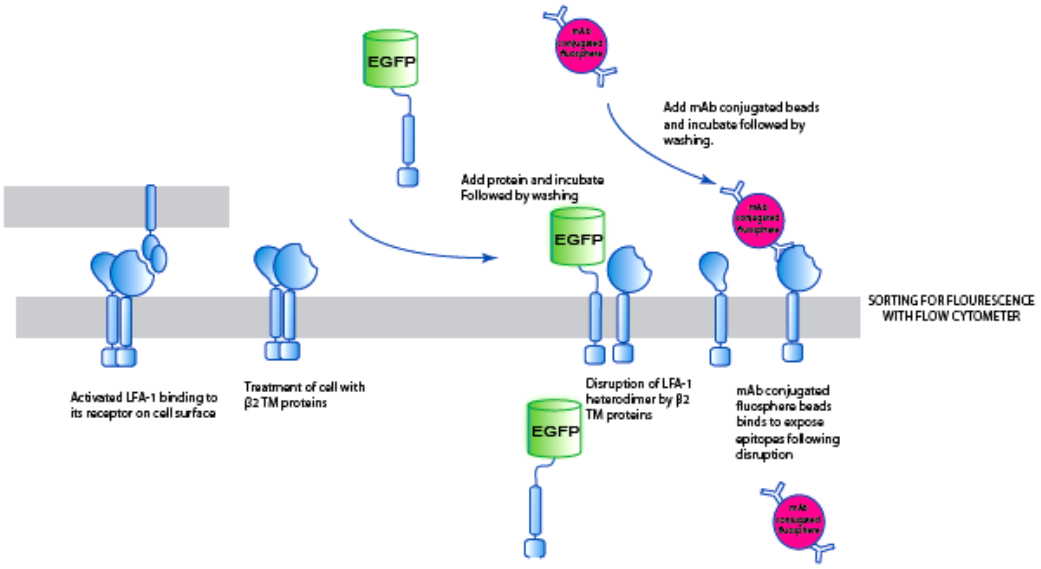

Figure 3.3: Schematic representation of the in vitro protein binding and mAb conjugated fluosphere beads labeling.

Proteins bind to cell membrane and disrupt LFA-1 receptor through the homomeric association of the β_2 TM with WT TM. This leads to exposure of activating epitopes on the β_2 integrin resulting to a change in binding of the mAb-conjugated fluospheres to their respective epitopes.

We have seen from Chapter 2 that the recombinant fluorescently tagged proteins bind and may insert into the membrane of Jurkat cells. To test if these proteins interfere with the structure of the LFA-1 molecule on the surface of Jurkat cells, we pre-treated cells with the proteins followed by incubation with fluosphere beads containing mAbs against specific epitopes on LFA-1. If our hypothesis of the protein binding and inserting into the membrane followed by the

disruption of the LFA-1 receptor with the displacement of β_2 integrin, we will expect a decrease in binding of LFA-1 mAb to the cells or an increase in binding to mAb beads that recognise β_2 integrin when not intact. 1 μm red fluosphere beads were conjugated with the mAbs by adding soluble mAb to the beads and incubating at room temperature.

The raw data from these experiments are shown on Table A12. Table A13 shows the data with the background (No mAb) labelling subtracted (appendix section). Normalizing the data to EGFP treatment, we have the results presented on Table A14; while normalizing the data to pIgG binding data, we obtain the data on Table A15 (appendix). These results are plotted in Figures 3.4 for the EGFP treatment normalized data.

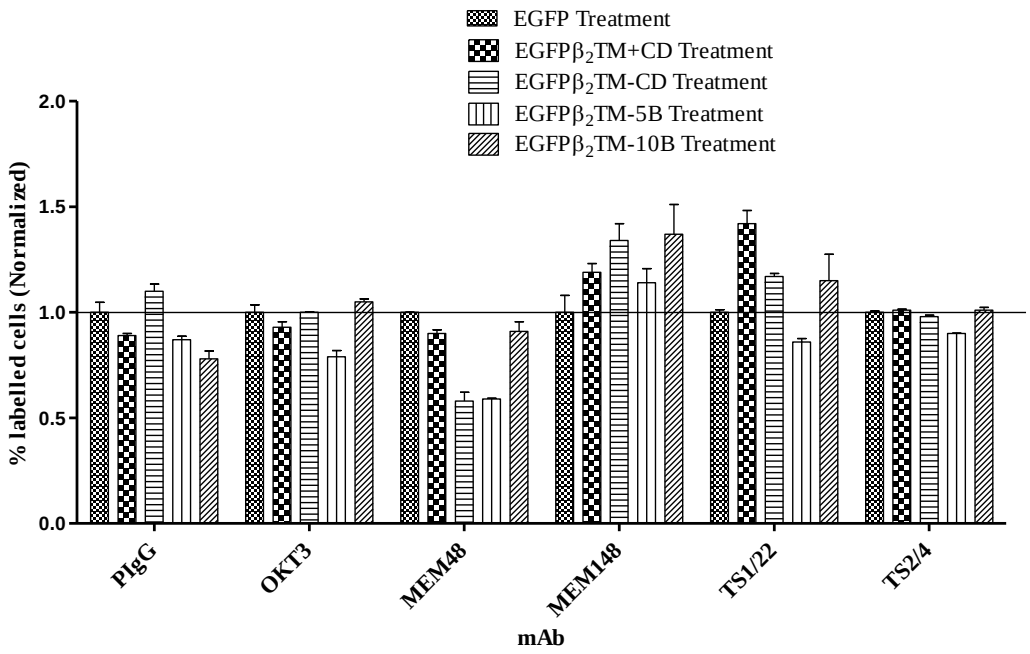

Figure 3.4: Flow cytometry analysis of β_2 TM proteins effects on LFA-1 epitopes normalized to EGFP condition

Labelling of Jurkat cells with mAb-conjugated red fluosphere beads following treatment with β_2 TM proteins. The data is plotted as normalized change in labelled cells relative to EGFP treatment. All proteins were used at 20 µg/mL final concentrations. The concentrations of the mAb used in labelling the beads varied with 10 µg/mL final used for pIgG, OKT3 and TS2/4 Ab while 20 µg/mL was used for the MEM48, MEM148 and TS1/22 mAbs. The observed increase in binding is probably due to disruption of the LFA-1 receptor following insertion of the recombinant protein in the membrane.

3.4.1. Effect of proteins on OKT3 binding epitope

The observed trend in binding of the cells to OKT3 mAb labelled beads was a decrease in binding except for the EGFPβ_2TM-10B protein that showed a 4% increase. There was a 7% decrease in binding from treating the cells with EGFPβ_2TM+CD protein, a 1% decrease in the case of EGFPβ_2TM-CD protein and 21% decrease with EGFPβ_2TM-5B protein. Thus the β_2 TM proteins have a slight effect on OKT3 epitopes by decreasing binding of the epitopes to OKT3-conjugated beads.

3.4.2. Effects of proteins on MEM48 binding epitope

Binding to MEM48 epitope was disrupted with an observed decrease in binding following treatment with the β_2 TM proteins. There was a 10% decrease in binding in the case of EGFPβ_2TM+CD protein, a 42% decrease resulting from EGFPβ_2TM-CD protein treatment, a corresponding 42% decrease in binding from EGFPβ_2TM-5B protein and lastly a 9% decrease resulting from EGFPβ_2TM-10B protein pre-incubation. Therefore, recombinant β_2 TM proteins all had a remarkable effect on MEM48 epitopes by reducing the binding of MEM48-conjugated beads to these epitopes.

3.4.3. Effects of proteins on MEM148 binding epitope

Binding to MEM148 epitope was enhanced with an observed increase in binding to MEM148-conjugated beads following treatment with the β_2TM proteins. There was a 19% increase in binding in the case of EGFPβ_2TM+CD protein, a 34% increase resulting from EGFPβ_2TM-CD protein treatment, a

corresponding 13% increase in binding from EGFPβ_2TM-5B protein and lastly a 36% increase resulting from EGFPβ_2TM-10B protein pre-incubation. In general, β_2 TM proteins increased binding of MEM148-conjugated beads to their epitopes on LFA-1 following treatment with the proteins.

3.4.4. Effects of proteins on TS1/22 binding epitope

The trend observed with the TS1/22 epitope showed a general increase in binding to the TS1/22-conjugated beads following protein treatment with the exception of the EGFPβ_2TM-5B protein treatment that resulted in a 15% decrease in binding of cells to TS1/22 labelled beads. EGFPβ_2TM+CD protein enhanced binding by 41% while EGFPβ_2TM-CD and EGFPβ_2TM-10B proteins enhanced binding by 16% and 15% respectively. Thus treatment of the cells with recombinant proteins followed by incubation with TS1/22-conjugated beads increased binding to their epitopes.

3.4.5. Effect of proteins on TS2/4 binding epitope

Several proteins had little effect on TS2/4 mAb binding; while a slight decrease was observed with some other proteins. EGFPβ_2TM-CD and EGFPβ_2TM-5B proteins reduced the binding of TS2/4 beads by 3% and 10% respectively. On the other hand, EGFPβ_2TM+CD and EGFPβ_2TM-10B proteins did not affect the binding of TS2/4-conjugated beads to the cells. Thus, recombinant proteins had very little or no effect on the binding of TS2/4-conjugated beads to their epitopes on LFA-1 receptor.

The cytometry images showing the population of cells gated, green fluorescent cells and those labelled with red beads are shown in the appendix section. A cell population with cell diameter from 7 µm – 15 µm was gated with population following a binomial distribution with a mean cell diameter of 12 µm. (Plot of EV against EV). The EV vs SS of the population gated is shown in Region 1. Region 2 in the FL1 channel is a representation of the cells that are labelled with the green fluorescent protein. Region 3 denotes cells labelled with red fluosphere beads in the FL2 channel while Region 4 represents cells labelled with the red fluospheres in the FL3 channel. The excitation wavelength of the laser used is 488 nm. Emission in the FL1 channel is at 525BP while FL2 and FL3 are respectively at 575BP and 670BP. All excitation was with the 488 nm laser source of the cytometer. Figure 3.5 shows the 2D plots obtained from FL1 and FL2 plots showing the change in binding to the MEM148 and TS1/22 epitopes following treatment with recombinant proteins.

Target integrin	*mAb targeted epitope*			*Effect of activator (PMA)*		*Effects of inhibitor (Cyto D)*		*Effect of glycosidases*		*Effect of β_2TM proteins*	
	Epitope	*Description*	*Source of mAb and isotype of Ab*	*Expected effect*	*Observed effect*	*Expected effect*	*Observed effect*	*Expected effect*	*Observed effect*	*Expected effect*	*Observed effect*
β_2	MEM48	Activating	Mouse IgG1	Stimulatory	Stimulatory	Inhibitory	Inhibitory	Not applicable	Stimulatory	Stimulatory	Inhibitory
	MEM148	Activating	Mouse IgG1	Stimulatory	Stimulatory	Inhibitory	Inhibitory	Not applicable	Varied	Stimulatory	Stimulatory
α_L	TS1/22	Inbibitory	Mouse IgG1	No effect	Not significant	Inhibitory	Inhibitory	Not applicable	Varied	Stimulatory	Stimulatory
	TS2/4	Immuno-precipitates the CD11a/CD18 complex	Mouse IgG1 k isotype	No effect	Not significant	No effect	Not significant	Not applicable	Not significant	No Effect	No effect

Table 3.1: Summary of the effects of PMA, cytochalasin D, glycosidases and recombinant β_2TM proteins on the α_L and β_2 integrins of LFA-1 receptor.

The table shows the expected and observed changes to the MEM48, MEM148, Ts1/22 and TS2/4 epitopes of LFA-1 following treatment with the different activator and inhibitor. 'Inhibitory' implies a decrease in binding was observed which was significant while 'Stimulatory' indicates an observed increase in binding. 'Not significant' indicates a very negligible change while 'No effect' implies nochange was observed. 'Varied' is either a stimulatory or inhibitory effect base on the glycosidase used.

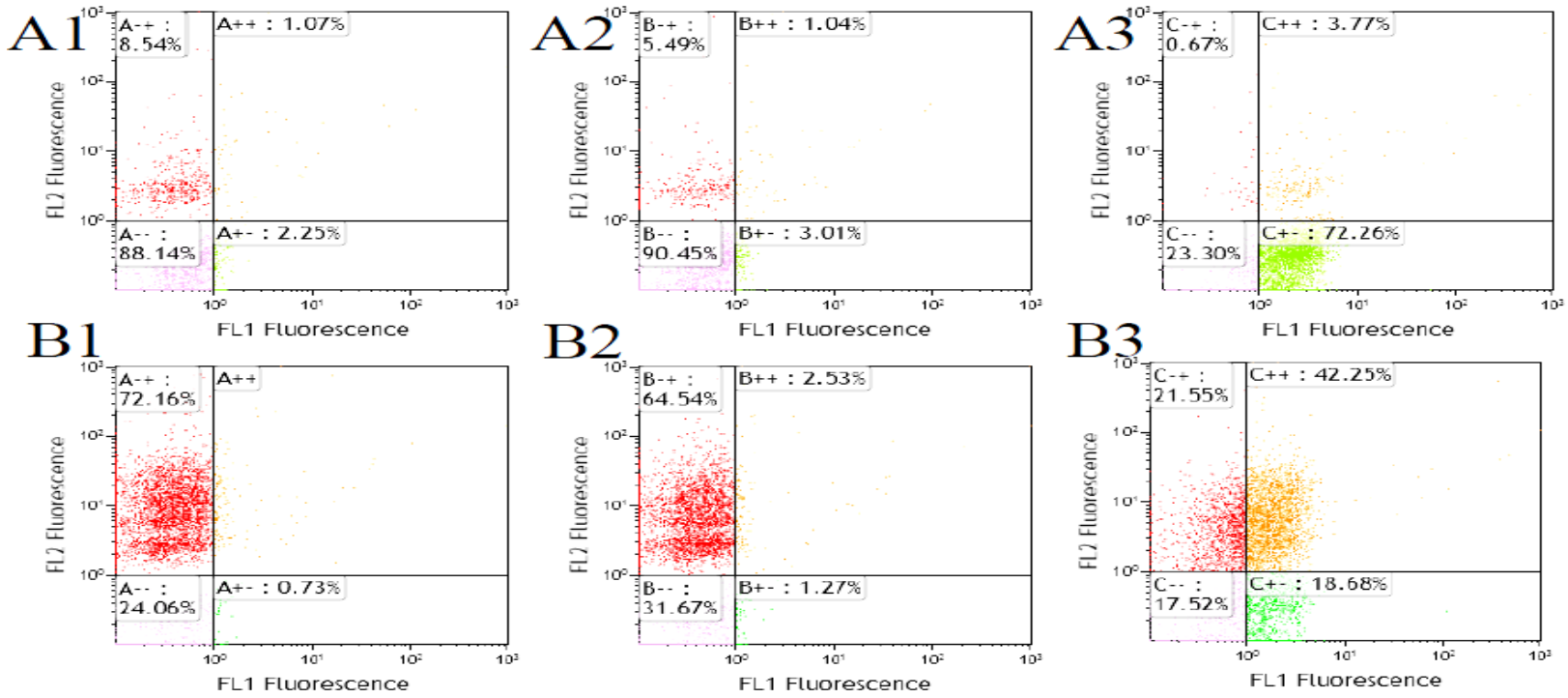

Figure 3.5: Two dimensional plot showing the change in epitopes resulting from treatment of the cells with β_2TM proteins.

A1: Cells labelled with MEM148 conjugated beads (red). **A2**: Same cells treated with EGFP (green) prior to labelling with MEM148 conjugated beads (red). **A3**: Same cells treated with the EGFPβ_2TM+CD protein (green) prior to labelling with MEM148 conjugated beads (red). **B1**: Cells labelled with TS1/22 conjugated beads (red). **B2**: Same cells treated with EGFP (green) prior to labelling with TS1/22 conjugated beads (red). **B3**: Same cells treated with the EGFPβ_2TM+CD protein (green) prior to labeling with TS1/22 conjugated beads (red). (--) represents no labeled cells. (-+) indicates cells labeled with beads (red), (+-) for cells greenly labeled while (++) represents cells that are both green and red fluorescent. The cells were excited at 488nm and observed at 525 (FL1) and 625 (FL2) channels.

3.5. DISCUSSION

The function of the LFA-1 receptor can be regulated by small molecule compounds that may activate or inhibit activity. Phorbol esters, such as PMA, have been shown to increase binding of mononuclear leukocytes following their incubation between minutes and 12 h when activation is complete (17, 25). PMA activates through PKC, leading to LFA-1 cross-linking of receptors and this does not affect the density of LFA-1 on the cell surface (16-18, 26). PMA does this by increasing the avidity of LFA-1 to ICAM-1 molecules (27, 28). Here we have shown the effect on the binding of LFA-1 to mAbs that bind specific epitopes on the receptor. We used two different mAb specific to the CD18 integrin, and showed that after treating cells with 100 ng/mL total concentration of PMA for 30 min and then incubating cells with 1 μm fluospheres beads containing these mAbs, their binding was enhance almost two fold.

Cyto D is an inhibitor of LFA-1 function by its action on actin units and sub-units (29). It inhibits polymerisation of actin filaments by promoting depolymerisation (19, 30-34). Cross-linking of receptors is facilitated by actin filaments in the cell membrane, thus inhibition of their formation would in turn inhibit the binding of LFA-1 molecule to their receptors (16, 28). We observed a 30% decrease in the binding of LFA-1 to the mAb beads that binds to MEM48 and MEM148 epitopes. While the inhibitory mAb, TS1/22 beads showed an almost 40% decrease in its binding to LFA-1.

The role of glycosylation on the β_1 integrin has been described, whereas very little is known about glycosylation on the β_2 integrin (35, 36). Studies on the characterisation of glycoproteins are done using endoglycosidases and exoglycosidases (23). The pattern of glycosylation on integrins is important to their function and is mediated in the β_1 integrin by TGF β_1 which plays a key role in integrin β_1 maturation (36). Alteration of the glycosylation pattern also affects the interaction of oligosaccharides with the integrin (35). Hypersialylation of β_1 integrin involving (beta-galactosamide α-2, 6) ST6Gal-I sialyltransferase I through the PKC/Ras/ERK has been attributed to the progress of different cancers including colon adenocarcinoma, and ovarian adenocarcinoma (37-41). Hyposialylation of β_1- and desialylation of α_5- integrins has been shown to increase their binding to fibronectin (42).

Treatment of cells with the endoglycosidase Endo H_f led to a negligible decrease in binding in the case of OKT3, MEM48 and TS2/4 epitopes whereas there was an observed decreased in the case of MEM148 (18%) and TS1/22 (41%) epitopes. PNGase F treatment on the other hand led to an increase in the binding of the various epitopes ranging from 15–53 % while TS2/4 binding showed no change in binding. Treatment with the mammalian sialidases; NEU3 and NEU4 gave interesting results with NEU3 increasing binding while NEU4 generally reduced binding. The bacterial neuraminadase (NEUX) equally caused an increased in the binding of LFA-1 epitopes to their respective mAb. NEU3 probably cleaves similar to NEUX by hydrolyzing α(2→3), α(2→6), and α(2→8)-

glycosidic linkages of terminal sialic residues (23, 24, 43, 44). Endo H_f equally decreased the binding of LFA-1 epitopes to their mAb. PNGase F which hydrolyzes all classes of Asn linked glycans leaving the free Asn residue also enhanced the binding of LFA-1 epitopes to their corresponding mAb beads.

3.6. CONCLUSION

The studies with LFA-1 agonist, PMA (100 ng/mL) on the MEM48 and MEM148 epitopes showed a greater than two fold increase in binding of the receptor to beads containing mAb against these epitopes. Cyto D at a 5 µg/mL final concentration has an inhibitory effect on LFA-1 epitopes, inhibiting binding of beads containing mAb by almost 25%. TS2/4 was used to block LFA-1 epitope (against TS2/4) but this epitope is located on a different site on the LFA-1 from the other epitopes studied. The effect of glycosidases on LFA-1 epitopes was intriguing, as treatment of cells with human MBP-NEU3, bacterial NEUX and PNGase F all resulted in an increase in binding to the different epitopes tested. Treatment with the human GST-NEU4 showed a decrease in binding when cells were incubated with beads containing mAb against different epitopes. There was little or no decrease in binding due to Endo H_f treatment.

Lastly the use of the β_2TM recombinant proteins to interfere with the epitopes on LFA-1 receptor was investigated. Following treatment of the cells with the proteins and incubating cells with mAb-conjugated beads we observed changes with the binding of the beads to their respective epitopes. Interestingly, we observed a general reduction in binding of the MEM48-conjugated beads to

their epitopes whereas there was an increase in binding to MEM148 epitope upon treatment with recombinant proteins. This suggests that, if the β_2 TM proteins are binding to the cell, they may be causing disruption of the LFA-1 receptor in a way we hypothesized. This disruption would expose the MEM148 epitope present on un-associated LFA-1 leading to the increased binding to the MEM148-conjugated beads. This observation may also be explained by the fact that the β_2 TM proteins bind to the cell and induce a conformational change to the LFA-1 receptor which either exposes (in the case of MEM148) or bury (in the case of MEM48) the epitopes on the β_2 integrin. The decrease in binding seen with the MEM48-conjugated beads following treatment with the β_2 TM proteins may be resulting from disruption of the $\alpha_L$and β_2 heterodimerization as β_2 homodimers begin to form from the β_2 TM proteins and the β_2 integrin. This may block the epitope for MEM48 leading to the reduction in binding observed. This again is in line with our hypothesis. On the other hand, the slight increase in binding of the cells to the TS1/22-conjugated beads may be due to disruption of the LFA-1 receptor exposing the epitope on the α_L integrin favouring binding of the TS1/22-conjugated beads.

3.7. MATERIALS AND METHODS

3.7.1. Materials

The following monoclonal antibodies were purchased; MEM48 (Enzo Life Sciences), MEM148 (Enzo life Sciences) TS1/22 (Thermo Scientific), Polyclonal IgG (fetal bovine serum pIgG), TS2/4 (mouse), OKT3 (mouse) antibodies were made. The following glycosidases were obtained; Neuraminidase from Clostridium perfringens (C. welchi) (Sigma) EndoHf (New England BioLabs), PNGase F (New England BioLabs), Mammalian NEU3 was provided as MBP-NEU3 while NEU4 was available as GST-NEU4. Dulbecco's Phosphate Buffered Saline (Gibco), NaCl (Caledon Laboratories chemicals), HEPES (Sigma) Boric acid (Fluka) EDTA (Sigma), NaN_3 (Sigma) Dextran from *Leuconostoc mesenteroides* (Sigma-Aldrich) Albumin from bovine serum (Sigma), Paraformaldehyde (Sigma Aldrich) Polyethyleneglycol Bishpenol A Epichlorohydrin copolymer 15-20 KDa (Sigma) Phorbol myristate ester, Cytochalasin D , RPMI 1640 (Gibco) Penicillin/Streptomycin (Gibco), Fetal bovine serum (Gibco) Jurkat cells clone E6.1 was obtained from ATCC. One micron red and yellow-green FluorSpheres beads (Molecular Probe, Invitrogen).

3.7.2. Methods

3.7.2.1. Beads labelling with mAb

Beads were labelled at room temperature. A stock solution of 1.25% beads in Borate buffer containing 0.1% NaN_3 was made from the 2.5% beads solution from Molecular Probes. Store beads away from light at 4 ºC. Sonicate the 1.25%

stock for approximately 7 m in a water bath sonifier prior to use. For a final volume of 100 µL, add 10 µL of beads to a sterile 1.5 mL tube and add the calculated amount of borate buffer (100 mM Borate, 1 mM EDTA, 0.1% NaN_3 pH 8.5) and sonicate for 3 m. Then add the required amount of mAb to a final volume of 100 µL. Mix by vortexing immediately for 20 s. We used 10 µg/mL final concentrations of TS2/4, OKT3 and pIgG anti-bodies while TS1/22, MEM48 and MEM148 mAbs were used at 20 µg/mL. This volume of beads can be scaled up as needed. Incubate the beads while rotating for 1 h at room temperature. Then spin down the beads at 14000 rpm for > 5 min and gently aspirate the supernatant using a vacuum. Then re-suspend the beads in 1000 µL of Block B buffer (Borate buffer containing 10 mM HEPES, 140 mM NaCl, 1 mM EDTA, 2% Dextran, 1% BSA, 0.1% v/v PEG compound, 0.1% NaN_3 pH 8.5) and continue incubating for 1 h while rotating. After this, spin down at 14000 rpm and was twice with PBSSB (1X PBS, 1% BSA, 0.1% NaN_3 pH 7.2 - 7.4) before re-suspending in 100 µL of same PBSSB pH 7.2 - 7.4. Sonicate beads for 5 m prior to labelling cells.

3.7.2.2. Cell culturing and labelling

Jurkat cells clone E6.1 was cultured in RPMI 1640 enriched with 10% FBS and 1% penicillin/streptomycin. Cells were harvested at mid – late log phase with a cell density of $1.5x10^6$ cells/mL. Wash cells two times with PBSSB buffer and re-suspend in same buffer containing 0.1% DMSO. Aliquot 500 µL into a 1.5 mL tube and add 50 µL of labelled beads (1:10 dilution of beads). Incubate cells with beads for 1 h at 37 ºC in a 95% air, 5% CO_2 incubator. Spin down cells at

1200 rpm for 4 m and carefully aspirate supernatant using a vacuum. At this speed, most unbound beads remain in suspension while cells form pellet. Wash cells with two volumes (1 mL) of PBSSB and fix with half volume (250 µL) of pre-chilled 0.25% PFA on ice for 30 m. Wash cells after fixing with two volumes of PBSSB and re-suspend in PBSSB for plating. Add 20 µL of re-suspended cells unto 200 µL of PBSSB in wells of a 96 well plate and re-suspend by pipetting up and down. Place plate in place holder on the Beckman Coulter Cell Lab Quanta SC cytometer and run using the programs 'Cairo Lab - NGE YG beads labelling' for the YG beads and/or 'Cairo lab- NGE Red beads labelling' in the case of red beads.

3.7.2.3. Activator/Inhibitor treatment and cell labelling with mAb against different LFA-1 epitope

Phorbol esters such as phorbol-12-myristate-13-acetate (PMA) have been shown to induce activation of LFA-1 receptors by clustering of LFA-1 receptors. Harvest cells at mid – late log phase at a density of $1.5x10^6$ cells/mL and was two times with PBSSP buffer at pH 7.2 – 7.4. Aliquot 500 µL of cells suspension (in PBSSB containing 0.1% DMSO) and add PMA to a final concentration of 100 ng/mL. In the case of cyto D, add to a final concentration of 5 µg/mL. Incubate cells for 30 m at 37 ºC following addition of the PMA or cyto D then add 50 µL of labelled beads. Continue incubation for 1 h at same temperature under 95% air and 5% CO_2. Spin cells at room temperature for 4 m at 1200 rpm to pellet cells. Carefully aspirate the suspension containing unbound beads using a vacuum

making sure the cell pellet is intact. Wash cells twice with one volume of PBSSB pH 7.2 each time. Washing the cells once with two volumes (1000 µL) of PBSSB equally works well. Then fix cells with 0.25% pre-chilled PMA on ice for 30 m. Following fixation, wash cells and re-suspend in PBSSB before plating 20 µL in 200 µL PBSSB on a 96 well plate.

As a negative control, pre-block LFA-1 receptors with TS2/4 mAb before labelling with beads. Pre-blocking was done by; adding 20 µg/mL TS2/4 mAb (total concentration) to washed and re-suspended cells. Incubate at 37 ºC for 30 m before adding labelled beads. Continue incubation for 1 h at same temperature. Then wash cells with PBSSB and fix with pre-chilled 0.25% PFA on ice for 30 m. Wash fixed cells and plate for FC analysis. Run FC under the program 'Cairo Lab-NGE YG beads labelling'

3.7.2.4. Glycosidase treatment and cell labelling with mAb against different LFA-1 epitope

Since most of the glycosidases used functions optimally at pH 4.5, unfortunately this pH environment is lower than physiological pH for Jurkat cells. Thus a pH of 5.5 was used at which most cells remain viable for up to 1 h 30 m while favouring the activity of the glycosidase. Harvest cells and re-suspend them in PBSSB pH 5.5. Add glycosidases to cells in separate tubes as follows: MBP–NEU3 (final concentration of 10 µg/mL), GST–NEU4 (10 µg/mL), bacterial NEUX (20 mU/mL), Endo H_f (10000 U/mL) and PNGase F (5000 U/mL). After addition of glycosidases, incubate cells for 1 h for glycosidases to act at 37 ºC in a

5% CO_2 incubator. Then spin down cells and was three times with two volumes of PBSSB pH 7.2. Re-suspend cells in same PBSSB pH 7.2 and add mAb labelled beads. Incubate cells with beads for 1 h before washing and fixing. Wash cells again with PBSSB buffer, pH 7.2 and fix cells with 0.25% PFA on ice for 30 m. Then re-suspend the cells in PBSSB after washing and plate on 96 well plate for sorting through the Beckman Coulter Cell Lab Quanta flow cytometer using the program 'Cairo Lab- NGE YG beads labelling'.

3.7.2.5. Fluorescently tagged proteins treatment and cell labelling with mAb against different LFA-1 epitope

Harvest cells at their mid–late log phase at a density of $1.5x10^6$ cells/mL. Wash cells with PBSSB and re-suspend cells in same buffer. Dialyze all proteins in a dialysis buffer containing 100 mM NaCl, 50 mM NaH_2PO_4 and 0.01% elugent in a 10 kDa MWC dialysis membrane. Remove all protein after dialysing for 4 h at 4 ºC and spin down to sediment all insoluble protein. Add proteins to washed cells at a final concentration of 20 µg/mL and incubate for 1 h at 37 ºC in a 5% CO_2 incubator. Spin down cells and wash two times with PBSSB before adding mAb labelled beads. Add 50 µL of labelled beads to 500 µL of cells suspension. Note that these volumes could be scaled down or up as required. Incubate cells with beads for an additional 1 h followed by spinning and washing. Spin down cells at 1200 rpm to pellet cells while unattached beads remain in suspension. Then wash the labelled cells with PBSSB and fix with 0.25% PFA. Add PFA to cells and incubate on ice for 30 m followed by washing with PBSSB.

Re-suspend cells in PBSSB and add cells unto PBSSB in wells of 96 well plate. Run the cells through the flow cytometer under the program 'Cairo lab – NGE Red beads/GFP labelling' at room temperature.

3.7.2.6. Data processing

All raw data was processed by transforming them or normalising them. All data obtained from the effects of agonist/antagonist treatment and from treatment with glycosidases was normalized to treatment under buffer condition (as control) or binding to pIgG beads (as control). The equations used were as follows:

Data normalized to binding of cells to pIgG beads

Normalized Avg. = (Avg. number of bound cells to a mAb beads under a given treatment) / (Avg. number of bound cells to pIgG beads under the same treatment condition)

Equation 3.1

Normalized SD = ((SD/Avg.)for each entry x (Normalized Ave for that entry))

Equation 3.2

Data normalized to binding of cells under buffer condition

Normalized Avg. = (Avg. number of bound cells to a mAb beads under a given treatment) / (Avg number of bound cells to the same mAb beads under buffer condition).

Equation 3.3

Normalized SD = (SD of cells bound to a mAb beads under a given treatment) x (SD of cells bound to the same mAb beads under buffer condition).

Equation 3.4

For treatments with recombinant proteins, we normalized the data to treatment under EGFP protein (as control). All data from the recombinant protein treatment were first transformed before normalized as follows:

Transformed Avg. = (Avg. number of bound cells to a mAb beads under a given treatment) – (Avg. number of bound cells to No mAb under the same treatment).

Equation 3.5

Fold = (%labelling from the different beads / (% labelling with pIgG beads).

Equation 3.6

3.8. REFERENCES

1. Zimmerman, T., and Blanco, F. J. (2008) Inhibitors targeting the LFA-1/ICAM-1 cell-adhesion interaction: design and mechanism of action, Curr Pharm Des 14, 2128-2139.
2. Evans, R., Patzak, I., Svensson, L., De Filippo, K., Jones, K., McDowall, A., and Hogg, N. (2009) Integrins in immunity, J Cell Sci 122, 215-225.
3. Norman, D. J. (1995) Mechanisms of action and overview of OKT3, Ther Drug Monit 17, 615-620.
4. Cosimi, A. B., Burton, R. C., Colvin, R. B., Goldstein, G., Delmonico, F. L., LaQuaglia, M. P., Tolkoff-Rubin, N., Rubin, R. H., Herrin, J. T., and Russell, P. S. (1981) Treatment of acute renal allograft rejection with OKT3 monoclonal antibody, Transplantation 32, 535-539.
5. Cosimi, A. B., Colvin, R. B., Burton, R. C., Rubin, R. H., Goldstein, G., Kung, P. C., Hansen, W. P., Delmonico, F. L., and Russell, P. S. (1981) Use of monoclonal antibodies to T-cell subsets for immunologic monitoring and treatment in recipients of renal allografts, N Engl J Med 305, 308-314.
6. Norman, D. J., Shield, C. F., 3rd, Barry, J., Bennett, W. M., Henell, K., Kimball, J., Funnell, B., and Hubert, B. (1988) Early use of OKT3 monoclonal antibody in renal transplantation to prevent rejection, Am J Kidney Dis 11, 107-110.
7. Bazil, V., Stefanova, I., Hilgert, I., Kristofova, H., Vanek, S., and Horejsi, V. (1990) Monoclonal antibodies against human leucocyte antigens. IV. Antibodies against subunits of the LFA-1 (CD11a/CD18) leucocyte-adhesion glycoprotein, Folia Biol (Praha) 36, 41-50.
8. Drbal, K., Angelisova, P., Cerny, J., Pavlistova, D., Cebecauer, M., Novak, P., and Horejsi. (2000) Human leukocytes contain a large pool of free forms of CD18, Biochem Biophys Res Commun 275, 295-299.
9. Drbal, K., Angelisova, P., Hilgert, I., Cerny, J., Novak, P., and Horejsi, V. (2001) A proteolytically truncated form of free CD18, the common chain of leukocyte integrins, as a novel marker of activated myeloid cells, Blood 98, 1561-1566.
10. Drbal, K., Angelisova, P., Cerny, J., Hilgert, I., and Horejsi, V. (2001) A novel anti-CD18 mAb recognizes an activation-related epitope and induces a high-affinity conformation in leukocyte integrins, Immunobiology 203, 687-698.
11. Van Epps, D. E., Potter, J., Vachula, M., Smith, C. W., and Anderson, D. C. (1989) Suppression of human lymphocyte chemotaxis and transendothelial migration by anti-LFA-1 antibody, J Immunol 143, 3207-3210.
12. Huang, C., and Springer, T. A. (1997) Folding of the beta-propeller domain of the integrin alphaL subunit is independent of the I domain and dependent on the beta2 subunit, Proc Natl Acad Sci U S A 94, 3162-3167.
13. Sanchez-Madrid, F., Nagy, J. A., Robbins, E., Simon, P., and Springer, T. A. (1983) A human leukocyte differentiation antigen family with distinct alpha-

subunits and a common beta-subunit: the lymphocyte function-associated antigen (LFA-1), the C3bi complement receptor (OKM1/Mac-1), and the p150,95 molecule, J Exp Med 158, 1785-1803.
14. Sanchez-Madrid, F., Krensky, A. M., Ware, C. F., Robbins, E., Strominger, J. L., Burakoff, S. J., and Springer, T. A. (1982) Three distinct antigens associated with human T-lymphocyte-mediated cytolysis: LFA-1, LFA-2, and LFA-3, Proc Natl Acad Sci U S A 79, 7489-7493.
15. Blumberg, P. M. (1980) In vitro studies on the mode of action of the phorbol esters, potent tumor promoters: part 1, Crit Rev Toxicol 8, 153-197.
16. Dustin, M. L., and Springer, T. A. (1989) T-cell receptor cross-linking transiently stimulates adhesiveness through LFA-1, Nature 341, 619-624.
17. Patarroyo, M., and Jondal, M. (1985) Phorbol ester-induced adhesion (binding) among human mononuclear leukocytes requires extracellular Mg++ and is sensitive to protein kinase C, lipoxygenase, and ATPase inhibitors, Immunobiology 170, 305-319.
18. Rothlein, R., and Springer, T. A. (1986) The requirement for lymphocyte function-associated antigen 1 in homotypic leukocyte adhesion stimulated by phorbol ester, J Exp Med 163, 1132-1149.
19. Casella, J. F., Flanagan, M. D., and Lin, S. (1981) Cytochalasin D inhibits actin polymerization and induces depolymerization of actin filaments formed during platelet shape change, Nature 293, 302-305.
20. Henrissat, B. (1991) A classification of glycosyl hydrolases based on amino acid sequence similarities, Biochem J 280 (Pt 2), 309-316.
21. Henrissat, B., and Bairoch, A. (1993) New families in the classification of glycosyl hydrolases based on amino acid sequence similarities, Biochem J 293 (Pt 3), 781-788.
22. Davies, G., and Henrissat, B. (1995) Structures and mechanisms of glycosyl hydrolases, Structure 3, 853-859.
23. Maley, F., Trimble, R. B., Tarentino, A. L., and Plummer, T. H., Jr. (1989) Characterization of glycoproteins and their associated oligosaccharides through the use of endoglycosidases, Anal Biochem 180, 195-204.
24. Plummer, T. H., Jr., and Tarentino, A. L. (1991) Purification of the oligosaccharide-cleaving enzymes of Flavobacterium meningosepticum, Glycobiology 1, 257-263.
25. Berrebi, G., Takayama, H., and Sitkovsky, M. V. (1987) Antigen-receptor interaction requirement for conjugate formation and lethal-hit triggering by cytotoxic T lymphocytes can be bypassed by protein kinase C activators and Ca2+ ionophores, Proc Natl Acad Sci U S A 84, 1364-1368.
26. Patarroyo, M., Beatty, P. G., Fabre, J. W., and Gahmberg, C. G. (1985) Identification of a cell surface protein complex mediating phorbol ester-induced adhesion (binding) among human mononuclear leukocytes, Scand J Immunol 22, 171-182.

27. Rothlein, R., Dustin, M. L., Marlin, S. D., and Springer, T. A. (1986) A human intercellular adhesion molecule (ICAM-1) distinct from LFA-1, J Immunol 137, 1270-1274.
28. Cairo, C. W., Mirchev, R., and Golan, D. E. (2006) Cytoskeletal regulation couples LFA-1 conformational changes to receptor lateral mobility and clustering, Immunity 25, 297-308.
29. Liu, S. J., Hahn, W. C., Bierer, B. E., and Golan, D. E. (1995) Intracellular mediators regulate CD2 lateral diffusion and cytoplasmic Ca2+ mobilization upon CD2-mediated T cell activation, Biophys J 68, 459-470.
30. Fox, J. E., and Phillips, D. R. (1981) Inhibition of actin polymerization in blood platelets by cytochalasins, Nature 292, 650-652.
31. Natori, S. (1986) Cytochalasins-actin filament modifiers as a group of mycotoxins, Dev Toxicol Environ Sci 12, 291-299.
32. Flanagan, M. D., and Lin, S. (1980) Cytochalasins block actin filament elongation by binding to high affinity sites associated with F-actin, J Biol Chem 255, 835-838.
33. Lin, D. C., Tobin, K. D., Grumet, M., and Lin, S. (1980) Cytochalasins inhibit nuclei-induced actin polymerization by blocking filament elongation, J Cell Biol 84, 455-460.
34. Morris, A., and Tannenbaum, J. (1980) Cytochalasin D does not produce net depolymerization of actin filaments in HEp-2 cells, Nature 287, 637-639.
35. Liu, Y., Pan, D., Bellis, S. L., and Song, Y. (2008) Effect of altered glycosylation on the structure of the I-like domain of beta1 integrin: a molecular dynamics study, Proteins 73, 989-1000.
36. Bellis, S. L., Newman, E., and Friedman, E. A. (1999) Steps in integrin beta1-chain glycosylation mediated by TGFbeta1 signaling through Ras, J Cell Physiol 181, 33-44.
37. Christie, D. R., Shaikh, F. M., Lucas, J. A. t., Lucas, J. A., 3rd, and Bellis, S. L. (2008) ST6Gal-I expression in ovarian cancer cells promotes an invasive phenotype by altering integrin glycosylation and function, J Ovarian Res 1, 3.
38. Seales, E. C., Jurado, G. A., Brunson, B. A., Wakefield, J. K., Frost, A. R., and Bellis, S. L. (2005) Hypersialylation of beta1 integrins, observed in colon adenocarcinoma, may contribute to cancer progression by up-regulating cell motility, Cancer Res 65, 4645-4652.
39. Seales, E. C., Jurado, G. A., Singhal, A., and Bellis, S. L. (2003) Ras oncogene directs expression of a differentially sialylated, functionally altered beta1 integrin, Oncogene 22, 7137-7145.
40. Seales, E. C., Shaikh, F. M., Woodard-Grice, A. V., Aggarwal, P., McBrayer, A. C., Hennessy, K. M., and Bellis, S. L. (2005) A protein kinase C/Ras/ERK signaling pathway activates myeloid fibronectin receptors by altering beta1 integrin sialylation, J Biol Chem 280, 37610-37615.
41. Woodard-Grice, A. V., McBrayer, A. C., Wakefield, J. K., Zhuo, Y., and Bellis, S. L. (2008) Proteolytic shedding of ST6Gal-I by BACE1 regulates the

glycosylation and function of alpha4beta1 integrins, J Biol Chem 283, 26364-26373.
42. Semel, A. C., Seales, E. C., Singhal, A., Eklund, E. A., Colley, K. J., and Bellis, S. L. (2002) Hyposialylation of integrins stimulates the activity of myeloid fibronectin receptors, J Biol Chem 277, 32830-32836.
43. Parker, R. B., and Kohler, J. J. (2010) Regulation of intracellular signaling by extracellular glycan remodeling, ACS Chem Biol 5, 35-46.
44. Albohy, A., Li, M. D., Zheng, R. B., Zou, C., and Cairo, C. W. (2010) Insight into substrate recognition and catalysis by the human neuraminidase 3 (NEU3) through molecular modeling and site-directed mutagenesis, Glycobiology 20, 1127-1138.
45. Tarasova, N. I., Rice, W. G., and Michejda, C. J. (1999) Inhibition of G-protein-coupled receptor function by disruption of transmembrane domain interactions, J Biol Chem 274, 34911-34915.
46. Tarasova, N. I., Seth, R., Tarasov, S. G., Kosakowska-Cholody, T., Hrycyna, C. A., Gottesman, M. M., and Michejda, C. J. (2005) Transmembrane inhibitors of P-glycoprotein, an ABC transporter, J Med Chem 48, 3768-3775.
47. Asada, M., Furukawa, K., Kantor, C., Gahmberg, C. G., and Kobata, A. (1991) Structural study of the sugar chains of human leukocyte cell adhesion molecules CD11/CD18, Biochemistry 30, 1561-1571.
48. Schroder, M., and Kaufman, R. J. (2005) The mammalian unfolded protein response, Annu Rev Biochem 74, 739-789.

CHAPTER FOUR: CONCLUSION AND FUTURE DIRECTIONS

4.1. GENERAL CONCLUSION

The goal of this project was to use molecular biology methods to make proteins that can be use to interfere with the function of the LFA-1 receptor on Jurkat cell clone E6.1. We realised this by making a chimeric gene containing EGFP as an *N*-terminal protein linked to β_2 TM as a *C*-terminal protein via a 9-mer linker. These genes were made using PCR of *egfp* and *ksi*β_2 (synthetic) genes with four primers to amplify the DNA. The chimeric genes were then ligated into the pBAD His vector and expressed in the DH10B *E coli*. Bacteria strain. The resulting proteins were designated EGFPβ_2TM+CD, EGFPβ_2TM-CD, EGFPβ_2TM-5B and EGFPβ_2TM-10B with EGFP as a control protein. The proteins were characterised by SDS-PAGE, CD spectroscopy, fluorescence spectroscopy, and mass spectroscopy. CD spectra confirmed the secondary structure of the proteins with the β_2-TM was predominantly α-helix.

These proteins were shown to bind to Jurkat cells in an *in vitro* binding assay where Jurkat cells (clone E6.1) were harvested at mid – late log phase and incubated with the recombinant proteins. Jurkat cells are T lymphocytes that express LFA-1 receptors on their surfaces. LFA-1 is a heterodimeric type I transmembrane protein made up of the α_L and β_2 integrins. LFA-1 binds to its counter receptors, the ICAM-1, 2 and 3 important in eliciting a number of cellular and physiological processes in the body include T cell recruitment, extravasation, cell adhesion, cell migration, apoptosis and have also been implicated in other diseases. LAD is a disease resulting from lack of the β_2 integrin in which the

individuals leukocytes lack the ability to firmly adhere to blood vessels with a subsequent persistent leukocytosis.

Jurkat cells were incubated with different concentrations of the β_2 TM proteins and analyzed for fluorescent cells using a Beckman Coulter Cell Lab flow cytometer. Only gated cells that had proteins bound to their surface, as detected by fluorescence of EGFP, were used to determine the percentage of labelled cells plotted against the protein concentration to obtain a binding curve with a K_d and an EC_{50} values for all proteins. Fitting these values to one-site competitive binding and saturation-binding equations (equations 2.1 and 2.2) we obtained the K_d and EC_{50} values. Relative to the control protein EGFP with an EC_{50} value > 100 µM, and a high $K_d > 100$ µM, the recombinant proteins showed a high preference for binding to the cells. The best K_d was obtained from the EGFPβ_2TM-5B protein with a K_d value of 280 ± 80 nM with a corresponding EC_{50} of 790 ± 50 nM. In general we observed a greater than 230-fold enhancement in binding by the β_2 TM proteins compared to EGFP alone.

We hypothesized that binding of these peptides to the cell may result in disruption of the LFA-1 receptor function. This could either have a stimulatory or inhibitory effect on the receptor function. Thus to study the effect, we utilised mAb-conjugated 1 µm fluosphere beads. We measured the binding of the receptor to ICAM-1 conjugated beads but were not successful in obtaining reproducible results. Thus we utilized different mAb specific to epitopes on the α_L and the β_2 integrins. MEM48 and MEM148 would bind to epitopes on the β_2 integrin while

TS1/22 and TS2/4 would bind to α_L integrin. We used pIgG as a negative control Ab and OKT3 a TCR binding Ab. Treating the cells with the recombinant proteins followed by incubating with the mAb conjugated beads (red 1 µm fluospheres) and sorting for both green (proteins) and red (fluorsphere) fluorescent cells, we could monitor the change in binding. In general, after treating cells with 20 µg/mL total protein concentration, we observed an increase in binding of the cells to MEM148 conjugated beads. In contrast, we observed a decrease in binding to MEM48 conjugated beads. We propose that these changes may be due to disruption of the LFA-1 heterodimeric association of the α_L and β_2 integrin in a way similar to the observed changes Tarasova *et al*. has previously reported for GPCR and the ABC transporters (45, 46). While the increase in binding of MEM148 may be due to exposure of the MEM148 epitope on β_2 integrin following disruption, decrease in the case of MEM48 may be due to homodimerisation association of the EGFPβ_2TM protein with the β_2 integrin which leads to a conformational change that instead buries the MEM48 epitope. There was a general increase in the case of the α_L epitope for TS1/22 conjugated beads whereas there was no change in the case of TS2/4. The observed increase with TS1/22 may be attributed to disruption of receptor by the β_2TM leading to exposure of the TS1/22 binding epitope which then binds to TS1/22 conjugated beads.

4.2. FUTURE DIRECTIONS

Since the system has shown that binding of the proteins to the cells can have an effect on the LFA-1 receptor, further insight into this work is important. Our model so far does not tell us anything about the association of the protein with the membrane; whether it is just binding or inserting or being internalized. Therefore further experiments that can rule out the pittfalls of our approach can be done to provide evidence of the effect of the proteins on LFA-1 receptor. A number of suggested experiments are outline below.

Firstly, the ICAM-1 system would give a better insight into the effect of the proteins to the LFA-1 receptor as ICAM-1 binds to whole and intact LFA-1. Therefore, having a functional adhesion assay using ICAM-1 would provide a better understanding of the biological effects of the recombinant proteins to the LFA-1 receptor. Secondly, we can design experiments that examine some of the downstream signalling pathway of LFA-1 following binding to its ligand, such as changes in IL-2 production. Thirdly, we can design plasmid that can express the different variants of the β_2TM proteins on Jurkat cells (or other LFA-1 expressing cell lines) and incorporate synthetic fluorophores on them if expressed on cell surfaces (although we are interested in exogeneous probes for our system). This approach can be very challenging due to the various proteins being expressed on cell surfaces which could be labelled too. Also, we can use FRET analysis to determine insertion of the proteins in the membrane in addition to microscopy experiments.

Due to the limitation of our method, further experiments should test the role of these proteins on different cells lines (both + and – LFA-1 cell lines) to determine specificity and selectivity of our proteins. We can further make scrambled sequences of the best proteins to rule out hydrophobic verses specific interactions. Deeper insight into understanding TM-TM interaction by targeting them with exogeneous probes is an active area for research that can create a new way for designing new chemotherapies.

4.3. APPENDIX

β_2 integrin protein region	Amino acid sequence
Integrin β_2 tail domain 622 - 700	CGKYISCAEC LKFEKGPFGK NCSAACPGLQ LSNNPVKGRT CKERDSEGCW VAYTLEQQDG MDRYLIYVDE SRECVAGPN
Transmembrane region 701- 723	IAAIVGGTVA GIVLIGILLL VIW
Cytoplasmic domain 724- 768	KALIHLSDLR EYRRFEKEKL KSQWNNDNPL FKSATTTVMN PKFAE
Target sequence	**ESRESVAGPN IAAIVGGTVA GIVLIGILLL VIWKALIHLS DLREY**

EGFP Protein: 5` to 3`frame.

```
atggtgagcaaaggcgaagaactgtttaccggcgtggtgccgattctggtggaactggatggcgatgtgaacggccataaatttagcgtgagcggcgaaggcgaaggcaatgcgacctatggcaaactgac
 M  V  S  K  G  E  E  L  F  T  G  V  V  P  I  L  V  E  L  D  G  D  V  N  G  H  K  F  V  S  G  E  G  E  G  D  A  T  Y  G  K  L  T  L
cctgaaatttatttgcaccaccggcaaactgccggtgccgtggccgaccctggtgaccaccctgacctatggcgtgcagtgctttagccgctatccggatcatatgaaacagcatgatttttttaaaagcg
 K  F  I  C  T  T  G  K  L  P  V  P  W  P  T  L  V  T  T  L  T  Y  G  V  Q  C  F  S  R  Y  P  D  H  M  K  Q  H  D  F  F  K  S  A  M
cgatgccggaaggctatgtgcaggaacgcaccatttttttttaaagatgatggcaactataaaaacccgcgcggaagtgaaatttgaaggcgataccctggtgaaccgcattgaactgaaaggcattgatttt
 P  E  G  Y  V  Q  E  R  T  I  F  F  K  D  D  G  N  Y  K  T  R  A  E  V  K  F  E  G  D  T  L  V  N  R  I  E  L  K  G  I  D  F  K  E
aaagaagatggcaacattctgggccataaactggaatataactataacagccataacgtgtatattatggcggataaacagaaaaacggcattaaagtgaactttaaaattcgccataacattgaagatgg
 D  G  N  I  L  G  H  K  L  E  Y  N  Y  N  S  H  N  V  Y  I  M  A  D  K  Q  K  N  G  I  K  V  N  F  K  I  R  H  N  I  E  D  G  S  V
cagcgtgcagctggcggatcattatcagcagaacaccccgattggcgatggcccggtgctgctgccggataaccattatctgagcacccagagcgcgctgagcaaagatccgaacgaaaaacgcgatcata
 Q  L  A  D  H  Y  Q  Q  N  T  P  I  G  D  G  P  V  L  L  P  D  N  H  Y  L  S  T  Q  S  A  L  S  K  D  P  N  E  K  R  D  H  M  V
tggtgctgctggaatttgtgaccgcggcgggcattaccctgggcatggatgaactgtat
R  L  L  E  F  V  T  A  A  G  I  T  L  G  M  D  E  L  Y  K
```

EGFPβ_2TM+CD Protein: 5` to 3`frame

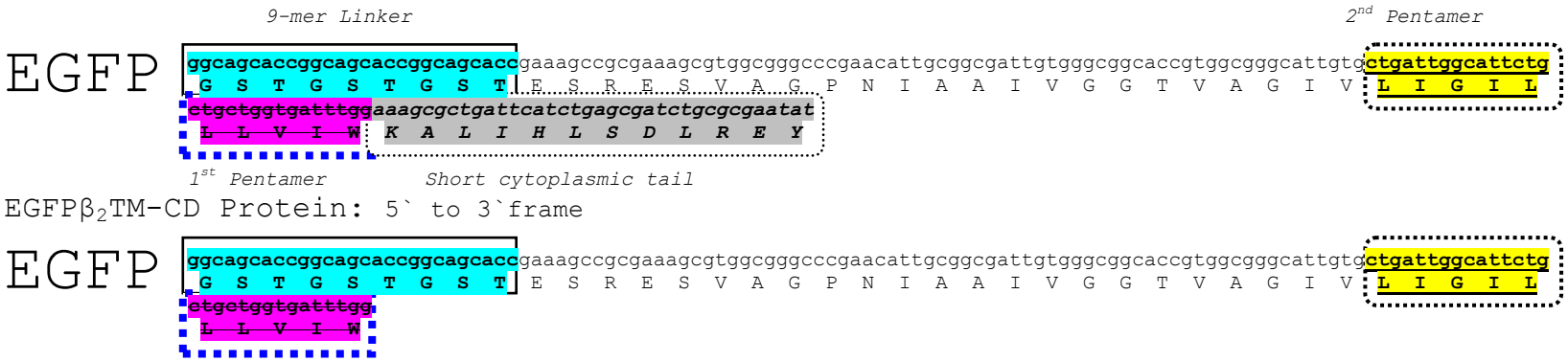

EGFPβ_2TM-CD Protein: 5` to 3`frame

EGFPβ_2TM-5B Protein: 5` to 3`frame

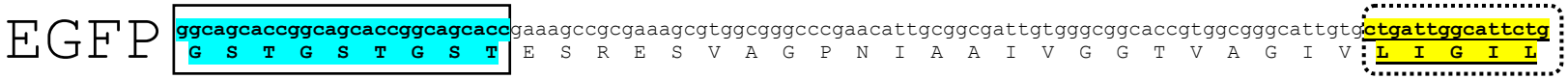

EGFPβ_2TM-10B Protein: 5` to 3` frame

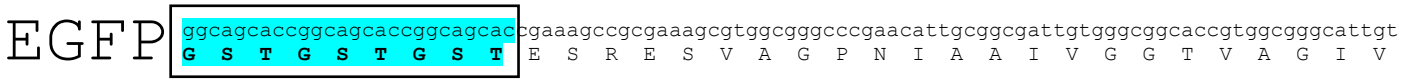

Figure A1. Targeted sequence of β_2 integrin for recombinant protein and the gene outline for the proteins.

Table shows the targeted sequence of the β_2 integrin for fusion at the C-terminus of EGFP protein. The outline shows the sequence of the recombinant β_2 constrructs. EGFP is fused to β_2 integrin transmembrane variant via a 9-mer shown in bold and enclosed in solid rectangle. EGFPβ_2TM+CD is distinguished with the presence of a short cytoplasmic tail represented in within a broken rectangle. The cytoplasmic tail is truncated in EGFPβ_2TM-CD. The first pentamer (bold broken rectangle) is truncated in EGFPβ_2TM-5B protein while the first and second pentamers (represented in broken oval rectangle) are truncated in the EGFPβ_2TM-10B protein.

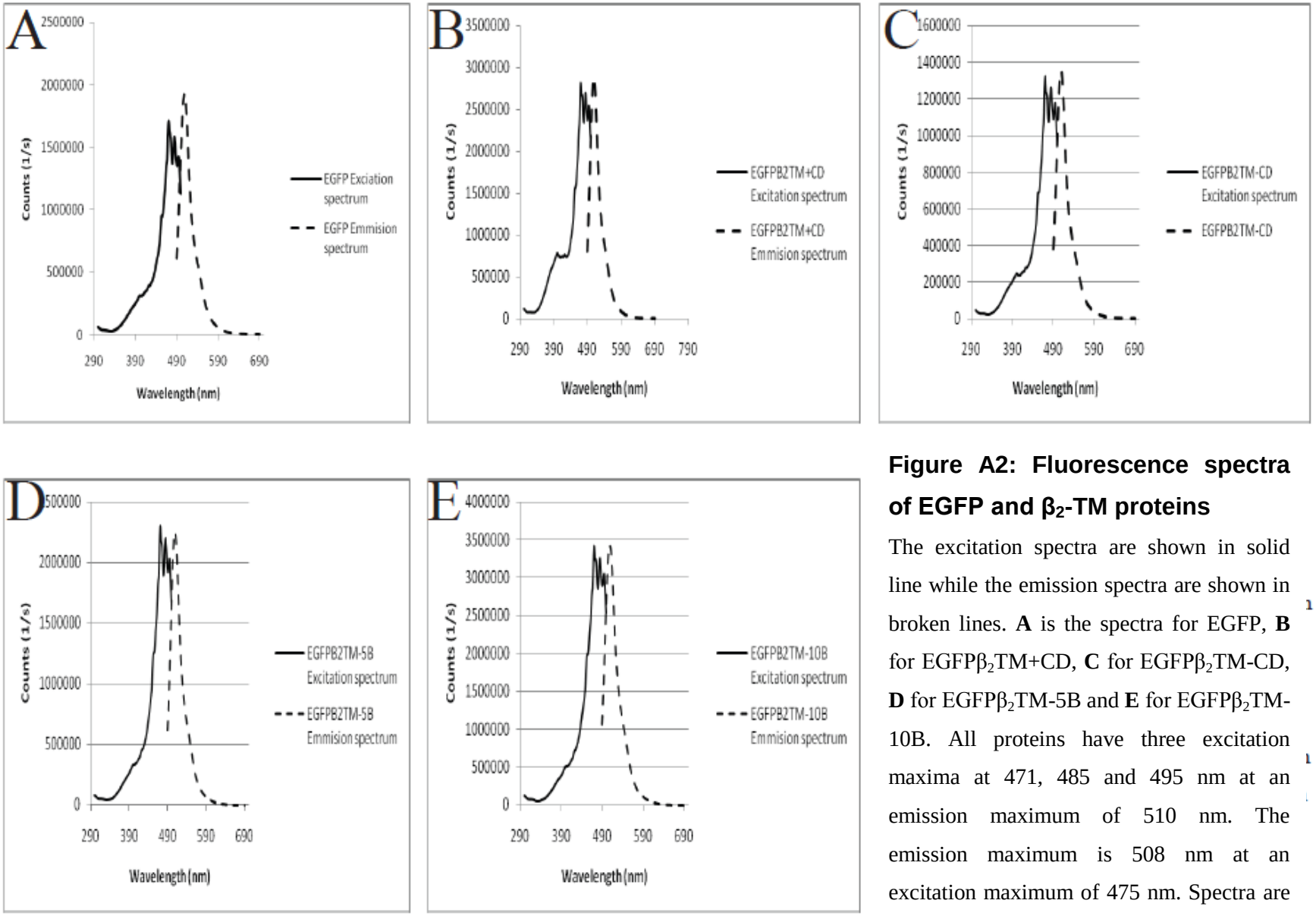

Figure A2: Fluorescence spectra of EGFP and β_2-TM proteins

The excitation spectra are shown in solid line while the emission spectra are shown in broken lines. **A** is the spectra for EGFP, **B** for EGFPβ_2TM+CD, **C** for EGFPβ_2TM-CD, **D** for EGFPβ_2TM-5B and **E** for EGFPβ_2TM-10B. All proteins have three excitation maxima at 471, 485 and 495 nm at an emission maximum of 510 nm. The emission maximum is 508 nm at an excitation maximum of 475 nm. Spectra are not corrected.

Protein concentration (µg/mL)	Log of Protein conc.	Transformed concentration (µg/mLx10^3)	Mean % of labelled cells.	Standard Deviation
0.0	0.000	0.000	3.113	0.567
2.0	0.301	0.002	3.713	0.552
4.0	0.602	0.004	3.646	0.631
6.0	0.778	0.006	4.313	0.952
8.0	0.903	0.008	4.666	0.360
10.0	1.000	0.010	4.340	1.052
20.0	1.301	0.020	5.333	1.250
30.0	1.477	0.030	6.740	0.499
40.0	1.602	0.040	7.080	1.330
50.0	1.698	0.050	9.206	1.283
100.0	2.000	0.100	14.880	0.720
200.0	2.301	0.200	28.673	1.392

Table A1: FC data for EGFP treated cells

The Jurkat cells clone E6-1 follows a Gaussian distribution with a mean cell diameter of 10 µm. The number of runs per sample was three (n = 3). The mean of the % of labelled cells and the sample SD (which represents the error) are shown.

Protein concentration (µg/mL)	Log of Protein conc.	Transformed concentration (µg/mL x10^3)	Mean % of labelled cells.	Standard Deviation
0.0	0.000	0.000	3.326	0.423
2.0	0.301	0.002	27.166	1.305
4.0	0.602	0.004	22.560	0.80721
6.0	0.778	0.006	25.673	0.570
8.0	0.903	0.008	28.400	1.314
10.0	1.000	0.010	34.675	4.948
20.0	1.301	0.020	57.560	0.757
30.0	1.477	0.030	59.630	2.182
40.0	1.602	0.040	65.655	0.902
50.0	1.698	0.050	68.350	3.240
100.0	2.000	0.100	86.603	1.248
200.0	2.301	0.200	97.186	4.527

Table A2: FC data for EGFPβ_2TM+CD treated cells

The Jurkat cells clone E6-1 follows a Gaussian distribution with mean cell diameter of 10 µm. The number of runs per sample was three (n = 3). The mean of the % of labelled cells and the sample SD (which represents the error) are shown.

Protein concentration (µg/mL)	Log of Protein conc.	Transformed concentration (µg/mL x10^3)	Mean % of labelled cells.	Standard Deviation
0.0	0.000	0.000	3.566	0.266
2.0	0.301	0.002	12.760	0.593
4.0	0.602	0.004	14.920	1.752
6.0	0.778	0.006	16.255	1.321
8.0	0.903	0.008	16.485	0.814
10.0	1.000	0.010	17.385	0.245
20.0	1.301	0.020	19.615	1.198
30.0	1.477	0.030	26.873	0.347
40.0	1.602	0.040	27.993	1.220
50.0	1.698	0.050	33.166	0.912
100.0	2.000	0.100	37.793	1.892
200.0	2.301	0.200	47.320	1.984

Table A3: FC data for EGFPβ_2TM-CD treated cells

The Jurkat cells clone E6.1 follows a Gaussian distribution with a mean cell diameter of 10 µm. The number of runs per sample was three (n = 3). The mean of the % of labeled cells and the sample SD (which represents the error) are shown.

Protein concentration (µg/mL)	Log of Protein conc.	Transformed concentration (µg/mL x10^3)	Mean % of labelled cells.	Standard Deviation
0.0	0.000	0.000	3.193	0.665
2.0	0.301	0.002	17.460	0.303
4.0	0.602	0.004	18.673	1.914
6.0	0.778	0.006	19.466	0.914
8.0	0.903	0.008	20.466	1.500
10.0	1.000	0.010	25.390	1.630
20.0	1.301	0.020	26.505	0.851
30.0	1.477	0.030	26.832	1.737
40.0	1.602	0.040	39.620	1.352
50.0	1.698	0.050	42.122	0.430
100.0	2.000	0.100	46.003	1.451
200.0	2.301	0.200	50.860	1.021

Table A4: FC data for EGFPβ_2TM-5B treated cells

The Jurkat cells clone E6.1 follows a Gaussian distribution with cell diameter of 10 µm. The number of runs per sample was three (n = 3). The mean of the % of labelled cells and the sample SD (which represents the error) are shown.

Protein concentration (µg/mL)	Log of Protein conc.	Transformed concentration (µg/mL x10^3)	Mean % of labelled cells.	Standard Deviation
0.0	0.000	0.000	3.480	0.950
2.0	0.301	0.002	19.226	0.513
4.0	0.602	0.004	20.153	1.420
6.0	0.778	0.006	18.446	1.220
8.0	0.903	0.008	21.013	0.541
10.0	1.000	0.010	28.560	0.924
20.0	1.301	0.020	50.520	1.558
30.0	1.477	0.030	53.145	1.357
40.0	1.602	0.040	59.555	1.240
50.0	1.698	0.050	67.350	1.468
100.0	2.000	0.100	68.890	1.605
200.0	2.301	0.200	71.659	1.931

Table A5: FC data for EGFPβ$_2$TM-10B treated cells

The Jurkat cells clone E6-1 follows a Gaussian distribution with a mean cell diameter of 10 µm. The number of runs per sample was three (n = 3). The mean of the % of labelled cells and the sample SD (which represents the error) are shown.

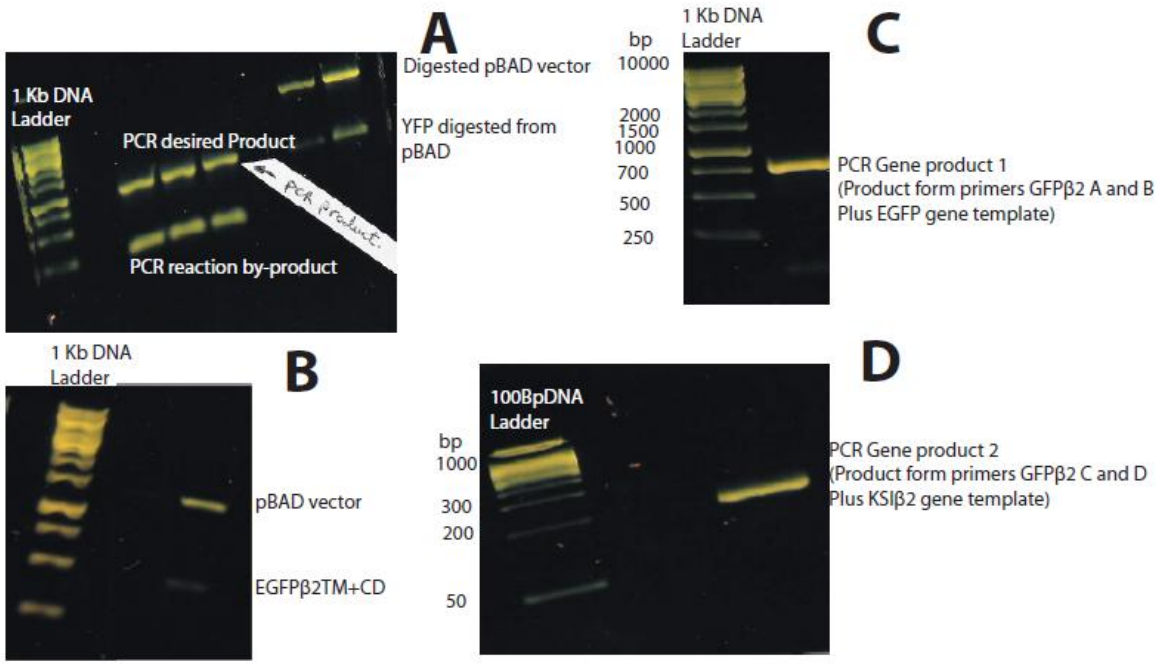

Figure A3: Agarose gels of PCR reaction products for *egfpβ$_2$tm+cd* gene

A: A 1% agarose gel on the digested pBAD-YFP vector to purify the pBAD vector. Digestion was done using EcoRI and XhoI restriction enzymes. **B:** A 1% gel for the digestion of pBAD-EGFPβ$_2$TM+CD vector to test for drop-outs of the *egfpβ$_2$tm+cd* genes. **C:** 1% gel of the clean-up of gene product 1from PCR amplification of *egfp* gene with primers GFPβ$_2$ A and B. **D**: 3% gel of the cleanu-up of gene product 2 from PCR amplification of the *ksiβ$_2$* gene with primers GFPβ$_2$ C and D. Any gene product less than 500 bp was purified by running the reaction product on a 3% gel while gene products above 500 bp were run on 1% agarose gel.

	Buffer		PMA treatment		Cyto D treatment		TS2/4 treatment	
mAb	AVE	SD	AVE	SD	AVE	SD	AVE	SD
pIgG	2.31	0.217	3.62	0.205	4.51	0.309	3.36	0.259
OKT3	23.32	0.600	28.47	0.782	8.22	0.714	5.42	0.325
MEM48	6.65	0.510	13.78	0.640	4.47	0.245	5.73	0.230
MEM148	12.68	0.373	29.88	0.763	8.68	0.498	12.90	0.574
TS1/22	67.82	0.480	70.68	0.442	40.24	0.977	61.72	0.493
TS2/4	88.68	1.846	83.53	3.303	82.86	0.213	18.06	0.988

Table A6: Raw FC data for effects of activators and inhibitors on LFA-1 binding to mAbs.

The cell population follows a normal distribution with a mean population cell diameter of about 10 µm. The number of repeats per sample was four (n=4). Error is computed as SD. The mAbsMEM48, MEM148 and TS1/22 were used at a final concentration of 20 µg/mL on fluospheres while TS2/4, pIgG and OKT3 were used at 10 µg/mL.

	Buffer		PMA treatment		Cyto D treatment		TS2/4 treatment	
mAb	AVE	SD	AVE	SD	AVE	SD	AVE	SD
pIgG	1.00	0.094	1.57	0.139	1.95	0.261	1.45	0.163
OKT3	1.00	0.026	1.22	0.041	0.35	0.011	0.23	0.003
MEM48	1.00	0.077	2.07	0.199	0.67	0.025	0.86	0.029
MEM148	1.00	0.029	2.36	0.142	0.68	0.027	1.02	0.046
TS1/22	1.00	0.007	1.04	0.007	0.59	0.009	0.91	0.007
TS2/4	1.00	0.021	0.94	0.035	0.93	0.002	0.20	0.002

Table A7: Raw FC data for effects of activators and inhibitors on LFA-1 binding to mAbs normalized, to binding of cells under buffer conditions.

All data was normalized to binding of cells under buffer condition which is PBSSB buffer at pH 7.2 (n=4)

	pIgG		OKT3		MEM48		MEM148		TS1/22		TS2/4	
Condition	AVE	SD	AVE	SD	AVE	SD	AVE	SD	AVE	SD	AV	SD
Buffer	1	0.047	10.10	0.130	2.88	0.110	05.49	0.081	29.34	0.104	38.39	0.401
PMA Treatment	1	0.042	7.86	0.160	3.80	0.131	8.25	0.156	19.52	0.091	23.08	0.677
Cyto D Treatment	1	0.095	1.82	0.221	0.99	0.076	1.92	0.154	8.912	0.302	18.35	0.066
TS2/4 Treatment	1	0.067	1.61	0.084	1.70	0.059	3.83	0.149	18.341	0.128	5.36	0.256

Table A8: Raw FC data for effects of activators and inhibitors on LFA-1 binding to mAbs, normalized to cells bound to pIgG Ab beads.

Data was equally normalized to results obtained from binding to pIgG beads to show that cells bound to mAb compared to pIgG (n=4).

	Buffer		NEU3 Treatment		NEU4 Treatment		NEUX Treatment		Endo H_f Treatment		PNGase F Treatment	
mAbs	AVE	SD	AVE	SD	AVE	SD	AVE	SD	AVE	SD	AVE	SD
pIgG	14.89	0.71	13.79	1.24	10.5	0.32	18.1	0.35	10.5	0.35	14.67	0.23
OKT3	23.76	0.16	44.28	1.79	23.4	0.74	52.02	0.46	23.4	0.46	36.32	0.88
MEM48	16.04	0.24	18.445	0.365	15.91	0.01	24.8	0.22	15.91	0.22	18.4	0.22
MEM148	16.855	0.385	20.54	0.08	14.83	0.89	28.59	0.05	14.83	0.05	21.07	0.57
TS1/22	30.03	0.53	46.7	0.39	19.36	2.04	37.87	0.23	19.36	0.23	34.75	0.71
TS2/4	87.02	0.4	97.905	0.005	86.41	0.77	93.90	0.715	86.41	0.715	87.5	0.52

Table A9: Raw FC data on the effect of glycosidases treatment on binding of mAbs to LFA-1 epitopes.

The number of runs per sample is four (n=4). SD was computed for the errors as the sample population follows a normal distribution in average cell diameter.

	Buffer		NEU3 Treatment		NEU4 Treatment		NEUX Treatment		Endo Hf Treatment		PNGase F Treatment	
mAbs	AVE	SD	AVE	SD	AVE	SD	AVE	SD	AVE	SD	AVE	SD
pIgG	1.00	0.048	0.93	0.083	0.71	0.021	1.22	0.024	0.71	0.024	0.99	0.015
OKT3	1.00	0.007	1.86	0.075	0.98	0.031	2.19	0.019	0.98	0.019	1.53	0.037
MEM48	1.00	0.015	1.15	0.023	0.99	0.001	1.55	0.014	0.99	0.014	1.15	0.014
MEM148	1.00	0.023	1.22	0.005	0.88	0.053	1.70	0.003	0.88	0.003	1.25	0.034
TS1/22	1.00	0.018	1.56	0.013	0.64	0.068	1.26	0.008	0.64	0.008	1.16	0.024
TS2/4	1.00	0.005	1.13	0.000	0.99	0.009	1.08	0.008	0.99	0.008	1.01	0.006

Table A10: Raw FC data on the effect of glycosidases treatment on binding of mAbs to LFA-1 epitopes, normalized to binding of cells under buffer condition.

The data was normalized by dividing the number of bound cells under each treatment by the corresponding number of bound cells for the buffer condition using the same mAb. All treatments were done in PBSSB pH 5.5 (buffer) at 37 ºC for 1 hr (n=4).

	pIgG		OKT3		MEM48		MEM148		TS1/22		TS2/4	
Conditions	AVE	SD	AVE	SD	AVE	SD	AVE	SD	AVE	SD	AVE	SD
PBSSB pH 5.5	1.00	0.504	1.59	0.113	1.07	0.170	1.13	0.273	2.02	0.376	5.84	0.284
NEU3 Treatment	1.00	1.537	3.21	2.219	1.34	0.452	1.49	0.099	3.38	0.484	7.10	0.006
NEU4 Treatment	1.00	0.102	1.86	0.086	0.83	0.003	1.04	0.034	2.57	0.275	8.11	0.515
NEUX Treatment	1.00	0.122	2.87	0.161	1.37	0.077	1.57	0.018	2.09	0.081	5.19	0.250
Endo H_f Treatment	1.00	0.102	2.22	0.236	1.51	0.003	1.41	0.285	1.84	0.653	8.23	0.246
PNGase F Treatment	1.00	0.052	2.47	0.202	1.25	0.050	1.44	0.131	2.37	0.163	5.96	0.120

Table A11: Raw FC data on the effect of glycosidases treatment on binding of mAbs to LFA-1 epitopes, normalized to binding to pIgG beads.

The data was normalized by dividing the number of bound cells under each mAb by the corresponding number of bound cells to pIgG Ab under the same condition (n=4).

	No treatment		EGFP treatment		EGFPβ_2TM+CD treatment		EGFPβ_2TM-CD treatment		EGFPβ_2TM-5B treatment		EGFPβ_2TM-10B treatment	
Mab	AVE	SD	AVE	SD	AVE	SD	AVE	SD	AVE	SD	AVE	SD
No Ab	0.65	0.134	0.62	0.304	2.24	0.028	3.22	0.162	2	0.113	1.19	0.049
pIgG	4.47	0.127	5.65	0.240	6.73	0.049	8.77	0.169	6.38	0.085	5.13	0.183
OKT3	58.39	1.202	57.05	1.972	54.98	1.456	59.49	0.169	46.62	1.640	60.35	0.813
MEM48	9.29	0.014	11.17	0.007	11.79	0.183	9.35	0.431	8.18	0.028	10.83	0.480
MEM148	7.54	1.930	3.87	0.261	6.125	0.134	7.58	0.261	5.71	0.219	5.65	0.459
TS1/22	9.41	1.173	7.67	0.091	12.23	0.438	11.46	0.099	8.04	0.113	9.35	0.883
TS2/4	88.48	1.025	86.7	0.494	88.84	0.431	87.38	0.516	79.48	0.148	87.75	1.223

Table A12: Raw FC data from the number of labelled cells following protein treatments.

The number of runs per sample was three (n=3) and the error was computed as the SD since the cell population followed a normal distribution with mean cell diameter of 12 µm.

	No treatment		EGFP treatment		EGFPβ_2TM+CD treatment		EGFPβ_2TM-CD treatment		EGFPβ_2TM-5B treatment		EGFPβ_2TM-10B treatment	
mAb	AVE	SD	AVE	SD	AVE	SD	AVE	SD	AVE	SD	AVE	SD
pIgG	3.82	0.127	5.04	0.240	4.49	0.049	5.56	0.169	4.38	0.085	3.94	0.184
OKT3	57.74	1.202	56.43	1.972	52.74	1.456	56.28	0.169	44.62	1.640	59.15	0.814
MEM48	8.64	0.014	10.56	0.007	9.55	0.184	6.14	0.431	6.18	0.028	9.64	0.481
MEM148	6.89	1.930	3.26	0.261	3.89	0.134	4.37	0.261	3.705	0.219	4.46	0.460
TS1/22	8.76	1.173	7.06	0.092	9.99	0.438	8.25	0.099	6.04	0.113	8.15	0.883
TS2/4	87.83	1.025	86.09	0.495	86.6	0.431	84.17	0.516	77.48	0.113	86.54	1.223

Table A13: Transformed data obtained from the number of labelled cells following protein treatment.

The number of runs per sample was three (n=3) and the error was computed as the SD since the cell population followed a normal distribution with mean cell diameter of 12 µm.

	EGFP treatment		EGFPβ_2TM+CD treatment		EGFPβ_2TM-CD treatment		EGFPβ_2TM-5B treatment		EGFPβ_2TM-10B treatment	
mAb	AVE	SD	AVE	SD	AVE	SD	AVE	SD	AVE	SD
pIgG	1.00	0.048	0.89	0.010	1.10	0.034	0.87	0.017	0.78	0.037
OKT3	1.00	0.035	0.93	0.026	1.00	0.003	0.79	0.029	1.05	0.014
MEM48	1.00	0.001	0.90	0.017	0.58	0.041	0.59	0.003	0.91	0.046
MEM148	1.00	0.080	1.19	0.041	1.34	0.080	1.14	0.067	1.37	0.141
TS1/22	1.00	0.013	1.42	0.062	1.17	0.014	0.86	0.016	1.15	0.125
TS2/4	1.00	0.006	1.01	0.005	0.98	0.006	0.90	0.001	1.01	0.014

Table A14: Raw FC data from the number of labelled cells following protein treatments, normalized to EGFP treatment of cells.

The data was normalized by dividing the number of bound cells under each treatment by the corresponding number of bound cells for the EGFP condition using the same mAb. All treatments were done in PBSSB pH 5.5 (buffer) at 37 ºC (n=3).

	pIgG		OKT3		MEM48		MEM148		TS1/22		TS2/4	
	AVE	SD	AVE	SD	AVE	SD	AVE	SD	AVE	SD	AVE	SD
EGFP treatment	1.00	0.058	11.20	0.474	2.10	0.001	0.65	0.063	1.40	0.022	17.10	0.120
EGFPβ_2TM+CD treatment	1.00	0.002	11.76	0.07	2.13	0.009	0.87	0.007	2.23	0.022	19.31	0.021
EGFPβ_2TM-CD treatment	1.00	0.029	10.13	0.029	1.11	0.073	0.79	0.044	1.48	0.017	15.15	0.088
EGFPβ_2TM-5B treatment	1.00	0.007	10.19	0.139	1.41	0.002	0.85	0.019	1.38	0.010	17.69	0.010
EGFPβ_2TM-10B treatment	1.00	0.034	15.03	0.150	2.45	0.088	1.13	0.084	2.07	0.162	21.99	0.225

Table A15: Raw FC data from the number of labelled cells following protein treatments, normalized to binding of cells to pIgG beads.

The data was normalized by dividing the number of bound cells under each mAb by the corresponding number of bound to pIgG Ab beads under the same treatment condition. The table shows the number of folds by which the population of cells labelled with the various Ab was shifted relative to those labelled with pIgG (n=3).

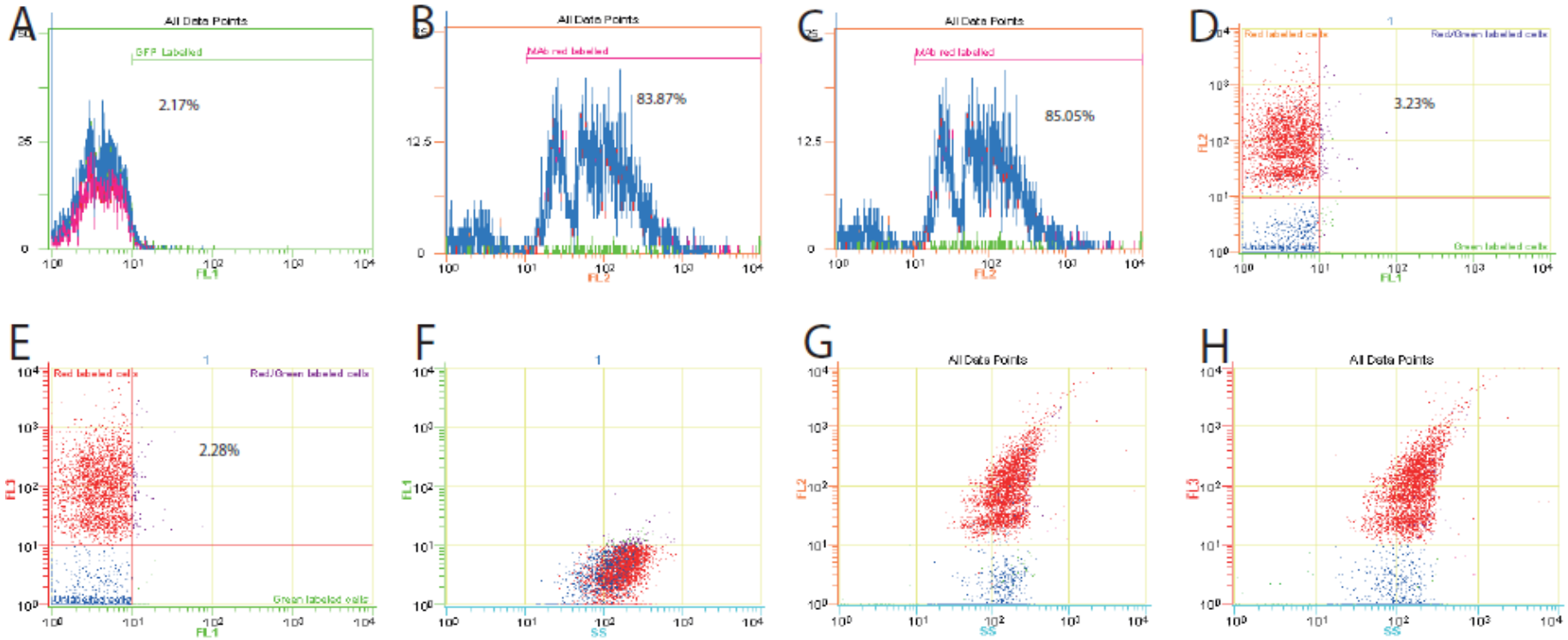

Figure A4: Flow cytometry histograms showing cells treated with EGFP and labeled with TS2/4 mAb conjugated beads.

Cells were incubated in PBSSB buffer for 1 h at 37 ºC, and then washed with the same buffer before adding mAb labelled fluosphere beads. The beads were incubated with cells for additional 1 h at 37 ºC before washed. Washed cells were fixed with 0.25% PFA on ice for 30 min, washed and re-suspended in same buffer for FC analysis. **A**: FL1 channel showing population of green fluorescent cells (2.17%). **B**: FL2 channel plot showing the population of red fluorescent cells (83.87%). **C**: FL3 channel plot showing the population of red fluorescent cells (85.05%). **D**: FL2 vs FL1 plot showing the population of cells which are both red and green (3.23%). **E**: FL3 vs FL1 plot still showing the population of cells that are both red and green fluorescent (2.28%). **F**: FL1 vs SS plot showing the cells that are green fluorescent as a function of their side scattering. **G**: FL2 vs SS plot showing the cells that are green fluorescent as a function of their side scattering. **H**: FL3 vs SS plot showing the cells that are red fluorescent as a function of their side scattering.

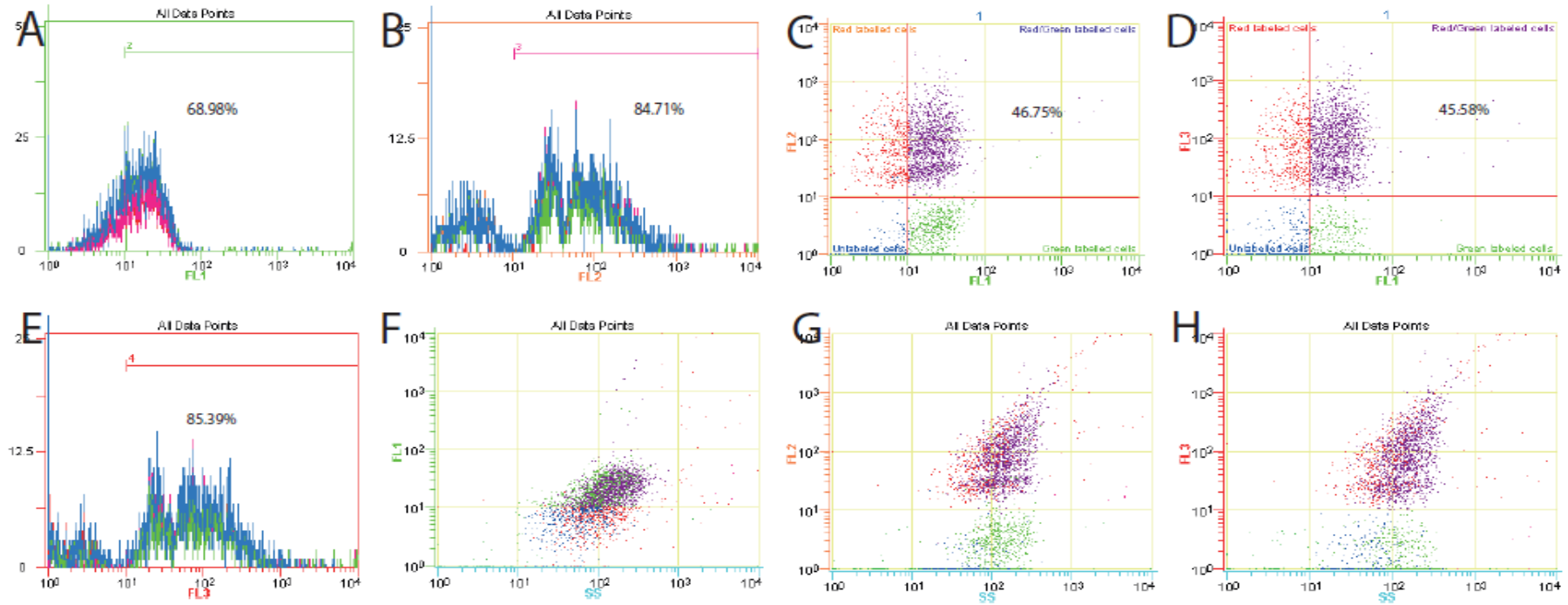

Figure A5: Flow cytometry histograms showing cells treated with EGFPβ2TM+CD protein and labeled with TS2/4 mAb conjugated beads.

Cells were incubated with 20 µg/mL total protein concentration in PBSSB buffer for 1 h at 37 ºC, and then washed with the same buffer before adding mAb labelled fluosphere beads. The beads were incubated with cells for additional 1 h at 37 ºC before washed. Washed cells were fixed with 0.25% PFA on ice for 30 min, washed and re-suspended in same buffer for FC analysis. **A**: FL1 channel showing population of green fluorescent cells (68.03%). **B**: FL2 channel plot showing the population of red fluorescent cells (84.71%). **C**: FL2 vs FL1 plot showing the population of cells which are both red and green (46.75%). **D**: FL3 vs FL1 plot still showing the population of cells that are both red and green fluorescent (45.58%). **E**: FL3 channel plot showing the population of red fluorescent cells (85.39%). **F**: FL1 vs SS plot showing the cells that are green fluorescent as a function of their side scattering. **G**: FL2 vs SS plot showing the cells that are green fluorescent as a function of their side scattering. **H**: FL3 vs SS plot showing the cells that are red fluorescent as a function of their side scattering.